Expression of Genes Involving Disease Resistance in Citrus Fruit Induced by *Bacillus subtilis* Lipopeptides Elicitors and Fungal Pathogen

Paiboon Tunsagool

A Thesis Submitted in Partial Fulfillment of the Requirements for the Degree of Doctor of Philosophy in Biochemistry

Prince of Songkla University

2018

Expression of Genes Involving Disease Resistance in Citrus Fruit Induced by *Bacillus subtilis* Lipopeptides Elicitors and Fungal Pathogen

Paiboon Tunsagool

A Thesis Submitted in Partial Fulfillment of the Requirements for the Degree
of Doctor of Philosophy in Biochemistry
Prince of Songkla University
2018

Thesis Title	Expression of genes involving disease resistance in citrus fruit induced by *Bacillus subtilis* lipopeptides elicitors and fungal pathogen
Author	Mr. Paiboon Tunsagool
Major Program	Biochemistry

Major Advisor

…….....

(Assoc. Prof. Dr. Wichitra Leelasuphakul)

Co-advisor

……

(Dr. Sittiruk Roytrakul)

Examining Committee :

……..……Chairperson

(Prof. Dr. Liang Li)

……..……..…Committee

(Assoc. Prof. Dr. Wichitra Leelasuphakul)

……..……..…Committee

(Dr. Sittiruk Roytrakul)

……..……..…Committee

(Asst. Prof. Dr. Ladda Leelawatwattana)

The Graduate School, Prince of Songkla University, has approved this thesis as partial fulfillment of the requirements for the Doctor of Philosophy Degree in Biochemistry

…….……..……..

(Prof. Dr.Damrongsak Faroongsarng)

Dean of Graduate School

This is to certify that the work here submitted is the result of the candidate's own investigations. Due acknowledgement has been made of any assistance received.

…….. Signature

(Assoc. Prof. Dr. Wichitra Leelasuphakul)

Major Advisor

…….. Signature

(Mr. Paiboon Tunsagool)

Candidate

I hereby certify that this work has not been accepted in substance for any degree, and is not being currently submitted in candidature for any degree.

…….. Signature

(Mr. Paiboon Tunsagool)

Candidate

ชื่อวิทยานิพนธ์ การแสดงออกของยีนที่เกี่ยวข้องกับการต้านทานโรคในผลส้มเหนี่ยวนำโดยสารไลโปเปปไทด์จากเชื้อแบซิลลัส ซับทิลลิส อิลิซิเตอร์และเชื้อรา-ก่อโรค

ผู้เขียน นายไพบูลย์ ตั่นสกูล

สาขาวิชา ชีวเคมี

ปีการศึกษา 2561

บทคัดย่อ

สารไลโปเปปไทด์จากเชื้อแบคทีเรียแบซิลัส ซับทิลลิสมีประสิทธิภาพในการกระตุ้นการแสดงออกของยีน โปรตีน และสารเมแทบอไลท์ที่เกี่ยวข้องกับระบบภูมิต้านทานโรคพืช เพื่อตอบสนองต่อสภาวะเครียดและการติดเชื้อราเขียวในผลส้มโชกุน โดยสารสกัดไลโปเปปไทด์ รวมถึง fengycin iturin A และ surface สามารถกระตุ้นการแสดงออกของยีนที่เกี่ยวข้องกับการต้านทานโรคพืชได้ เช่น ยีน *PAL LOX ACS1 ACO CHI GLU POD* และ *PR1* เป็นต้น ทั้งนี้สารสกัดไลโปเปปไทด์ยังสามารถเพิ่มปริมาณของโปรตีนที่เกี่ยวข้องกับวิถีแคลเซียม กรดแอบไซซิก อนุพันธ์ออกซิเจนที่ว่องไว ระบบยูบิควิติน-โปรติเอโซม รวมไปถึงผลผลิตของสารที่ให้พลังงานเพื่อการต้านทานโรคพืช อีกทั้ง fengycin ยังเพิ่มปริมาณของโปรตีนที่เกี่ยวข้องกับการพัฒนาของพืช และการสังเคราะห์ยูบิควิโนนในกลุ่มที่ไม่มีการติดเชื้อราเขียว ในขณะที่โปรตีนที่เกี่ยวข้องกับฮอร์โมนพืช เช่น ออกซินและกรดแอบไซซิกนั้นถูกเพิ่มปริมาณโดยการกระตุ้นจาก iturin A และ surfactin การทดสอบการจับระหว่างสารไลโปเปปไทด์กับโปรตีนที่เกี่ยวข้องกับการต้านทานโรคพืชสะท้อนให้เห็นว่า iturin A สามารถจับกับโปรตีน 12-oxophytodienoate reductase 2 ซึ่งเกี่ยวข้องกับกระบวนการสังเคราะห์ oxylipin ที่นำไปสู่การกระตุ้นระบบการต้านทานโรคพืช induced systemic resistance (ISR) การวิเคราะห์ทางด้านเมแทโบโลมิกส์โดยวิธี dansylation isotope labeling LC-MS ชี้ชัดว่า สารกลุ่มไลโปเปปไทด์สามารถกระตุ้นการเพิ่มปริมาณของกรดอะมิโนบางชนิดได้ เช่นกรดแอสพาร์ติก โฮโมเซอรีน ทรีโอนีน เซอรีน ไกลซีน และ ทริปโตเฟน ซึ่งถือเป็นเมแทโบไลท์ชนิดปฐมภูมิ รวมทั้ง เซโรโทนิน และทริปตามีน ซึ่งถือเป็นสารเมแทโบไลท์ชนิดทุติยภูมิที่เกี่ยวข้องกับกระบวนการเมแทบิลิซึมของทริปโตเฟนและไทโรซีน ตามลำดับ ในผลส้มโชกุนหลังการเก็บเกี่ยวเพื่อตอบสนองต่อสภาะเครียด

Thesis Title	Expression of genes involving disease resistance in citrus fruit induced by *Bacillus subtilis* lipopeptides elicitors and fungal pathogen
Author	Mr. Paiboon Tunsagool
Major Program	Biochemistry
Academic Year	2018

ABSTRACT

Cyclic lipopeptides (CLPs) obtained from *Bacillus subtilis* ABS-S14 had ability to activate some important genes, proteins, and metabolites which are involved in plant defensive pathways to stress responses and infection caused by *Penicillium digitatum* in mandarin fruit. The effects of CLP extract, fengycin, iturin A and surfactin in enhancement of the expression of *PAL*, *LOX*, *ACS1*, *ACO*, *CHI*, *GLU*, *POD* and *PR1* genes in postharvest mandarin fruit were revealed. Also the proteins relating to Ca^{2+} pathway, ABA signaling pathway, reactive oxygen species pathway, and ubiquitin-proteasome system including energy production for plant resistance were significantly accumulated. During stress responses (non-fungal infection), fengycin activated plant production of a protein that is involved in plant development and the ubiquinone biosynthetic process while iturin A and surfactin were shown to be involved in auxin and abscisic acid modulating signaling pathways. In addition, a comparative elicitor-protein binding assay of each CLP illustrated that iturin A attached to 12-oxophytodienoate reductase 2 that plays role in oxylipin biosynthetic process required for jasmonic acid production led to inducing systemic resistance (ISR). Furthermore, metabolomic analysis revealed that CLPs elicited a high accumulation of some amino acids; aspartic acid, homoserine, threonine, serine, glycine and tryptophan, which are primary metabolites via the metabolism of glycine, serine and threonine, and the secondary metabolites; serotonin and tyramine, which are active in the metabolism of tryptophan and tyrosine, respectively in postharvest mandarin fruit.

ACKNOWLEDGEMENT

I would like to express my deepest gratitude to my advisor, Assoc. Prof. Wichitra Leelasuphakul, and my co-advisor, Dr. Sittiruk Roytrakul, for their excellent advices to solve to problems including their expert suggestion to perform the experiments and for their patient correcting my writing in this thesis.

I would like to express my sincere appreciation to Prof. Liang Li to give me a chance to learn the new things in his laboratory and Xiaohang Wang for his assistance in metabolomics, as well as, Miss Janthima Jaresitthikunchai, Miss Narumon Phaonakrop, and Miss Suthathip Kittisenachai for their assistances in Proteomic Research Laboratory.

I am grateful to the TRF Royal Golden Jubilee Ph.D. Program student scholarship and the Prince of Songkla University Graduate Fund for financial support.

I thank all members and staffs of ST. 416 laboratory in Department of Biochemistry, Faculty of Science, Prince of Songkla University including Proteomic Research Laboratory and Microbe Interaction Laboratory, BIOTEC, NSTDA, as well as, W3-44 Laboratory, Department of Chemistry, Faculty of Science, University of Alberta for all laboratory facilities.

Finally, I would like to thank each person to support me in everything such as my family, especially, Mr. Naphatheep Phatthanukit including all my friends; Miss Vilailak Tiyao, Miss Wassamon Moyadee, Miss Rarinthorn Samrid, Mr. Sekkarin Ploypetch, Miss Kisana Bhinija, Mr. Chaiporn Kongpun, Miss Petchploy Rungkamoltip and the members in SAMALA'HO group. This accomplishment would be quite impossible without the mentioned people.

Paiboon Tunsagool

CONTENTS

LIST OF TABLES

LIST OF FIGURES

LIST OF FIGURES (Continued)

LIST OF FIGURES (Continued)

LIST OF FIGURES (Continued)

LIST OF ABBREVIATIONS AND SYMBOLS

%	=	percentage
°C	=	degree Celsius
µg	=	microgram
µL	=	microliter
µm	=	micrometer
µmol	=	micromole
Å	=	angstrom
ABA	=	abscisic acid
ACN	=	acetonitrile
ACO	=	1-aminocyclopropane-1-carboxylate oxidase
ACS1	=	1-aminocyclopropane-1-carboxylate synthase 1
avg	=	average
^{12}C	=	carbon-12
^{13}C	=	carbon-13
Ca^{2+}	=	calcium (II) ion
cDNA	=	complementary deoxyribonucleic acid
CHI	=	chitinase
CLPs	=	cyclic lipopeptides
cm	=	centimeter
Ct	=	cycle Threshold
DNA	=	deoxyribonucleic acid
DTT	=	dithiothreitol
EF-1α	=	elongation factor-1-alpha
ESI	=	electrospray ionization
ET	=	ethylene
Et	=	ethephon
Fig	=	figure

LIST OF ABBREVIATIONS AND SYMBOLS (Continued)

FT-ICR	=	Fourier-transform ion cyclotron resonance
g	=	gram
GC-MS	=	gas chromatography mass spectrometry
GLU	=	glucanase
h	=	hour
H_2O_2	=	hydrogen peroxide
HPLC	=	high-performance liquid chromatography
IAA	=	iodoacetamide
ISR	=	induced systemic resistance
JA	=	jasmonic acid
LA	=	Luria-Bertani agar
LB	=	Luria-Bertani broth
LC	=	liquid chromatography
LC-MS	=	liquid chromatography mass spectrometry
LC-MS/MS	=	liquid chromatography tandem-mass spectrometry
LOX	=	lipoxygenase
M	=	molar
MALDI-TOF	=	matrix assisted laser desorption ionization-time of flight
MAMP	=	microbe-associated molecular patterns
MeJA	=	methyl jasmonate
mg	=	milligram
min	=	minute
mL	=	milliliter
mM	=	milimolar
mm	=	millimeter
mm^3	=	cubic millimeter
mRNA	=	messenger ribonucleic acid

LIST OF ABBREVIATIONS AND SYMBOLS (Continued)

N	=	normal
NA	=	nutrient agar
NAD+	=	nicotinamide adenine dinucleotide
PAGE	=	polyacrylamide gel electrophoresis
PAL	=	phenylalanine ammonia-lyase
PDA	=	potato dextrose agar
PDF1.2	=	plant defensin 1.2
PGPR	=	plant growth promoting bacterium
PR	=	pathogenesis-related
PR1	=	pathogenesis-related protein 1
PTLC	=	preparative thin-layer chromatography
POX	=	peroxidase
qRT-PCR	=	quantitative-real time polymerase chain reaction
RNA	=	ribonucleic acid
ROS	=	reactive oxygen species
rpm	=	revolution per minute
RP-HPLC	=	reverse phase high pressure liquid chromatography
SA	=	salicylic acid
SDS	=	sodium dodecyl sulfate
sec	=	second
SPE	=	solid phase extraction
TFA	=	trifluoroacetic acid
TLC	=	thin-layer chromatography
Trp	=	tryptophan
Tyr	=	tyrosine
UV	=	ultraviolet
v/v/v	=	volume/volume/volume

CHAPTER 1

INTRODUCTION

1.1 Background and Rationale

Citrus fruit plays an important role in world economy because of being the export product of many countries. Sweet mandarin orange (*Citrus reticulata*) is the favorite citrus fruit with sweet taste and easy peeling. Unfortunately, citrus fruit are susceptible to postharvest fungi such as *Penicillium digitatum, P. itaticum* and *Colletotrichium gloeosporioides* since they have low pH, high moisture content and many essential nutrients which are necessary for the growth of postharvest fungi. *P. digitatum* is one of the most destructive agents of the citrus green mold rot of postharvest disease (Eckert, 1978). The infected citrus crops often occur during postharvest handling, as a consequent this causes economic losses. *P. digitatum* is necrotrophic fungi that enter the fruit via wounding (Eckert and Eaks, 1989). The application of fungicides after harvesting has been shown to be the most effective control method for reduction of postharvest loss caused by the fungal diseases (Smilanick et al., 2005, 2006). Nevertheless, the continuous use of the certain chemical fungicides in long term of postharvest crops has led to the fungal pathogenic development of resistant strains against the certain chemical fungicides (Kinay et al., 2007). Moreover, contamination of hazardous fungicides in the fruits, also in the environmental system caused a serious health problem and water contamination.

In recent year, one of the green strategy methods is biological control or biocontrol which is friendly to environment and human health because it mostly exploits natural cycles with reduced environmental impact. The biological method that depends on antagonistic microorganisms which plays several modes of action to prevent crops from the certain pathogen infections. Principles of biocontrol mechanisms which have been suggested as being effective against the pathogens in postharvest fruits were

reviewed in Droby et al. (2009). Induction of natural resistance in host plant to control the plant diseases is one of alternative approaches. Systemic Acquired Resistance (SAR) and Induced Systemic Resistance (ISR) are two forms of induced resistance when the host plants is challenged by a pathogen or parasite (reviewed in Pieterse et al., 2014). In addition, ISR is suggested to be involved in plant resistant to pathogens elicited by specific environmental stimuli, whereby the plant's innate defenses are potentiated against a broad spectrum of attackers. ISR is conducted by *Bacillus* spp. antagonistic microorganism was demonstrated by Ongena et al. (2005). Fengycin obtained from *B. subtilis* strain M4 showed a strong antifungal activity and could protect bean seedlings and apple fruit from *Pythium ultimum* and gray mold infections. Its action exerts through plant defense mechanism by induced-activation of plant phenolic compound synthesis. *B. subtilis* provides the categories of secondary metabolites such as enzymes, volatile organic compounds and cyclic lipopeptides (CLPs). Leelasuphakul et al. (2008) showed the effectiveness of *B. subtilis* 155 through its secondary metabolites in the growth inhibition of *P. digitatum in vitro*. Moreover, *B. subtilis* ABS-S14 endospores and CLP extract showed strong antagonistic activities against *P. digitatum*. Families of CLPs, i.e., iturin A, fengycin, and surfactin isolated from *B. subtilis* ABS-S14 showed a significant reduction of fruit decay and induced the activities of POX and PAL enzymes in the infected flavedo tissues of mandarin fruit caused by *P. digitatum* (Waewthongrak et al., 2015).

Synthetic fungicides have been used to control the plant diseases during postharvest period. Recently, groups of phytohormones as well as *Bacillus* CLPs, have become part of the effective agents showed the promising inhibitory effect to control fruit decay during postharvest period to replace utilization of synthetic fungicides. This study aimed to monitor the efficacy of the *B. subtilis* ABS-S14 agents in biological control approaches to inhibit *P. digitatum* infection during postharvest period in mandarin fruit in comparison to exogenous plant hormones' action. Exogenous plant hormones; salicylic acid (SA), methyl jasmonate (MeJA), and ethephon (Et) were applied in the same manner as the *B. subtilis* ABS-S14 CLPs on the wounded fruit to determine an induction of gene expression, accumulation of proteins, and metabolites involving in the signal transduction

pathway which enhanced defensive response of mandarin fruit with and without *P. digitatum* challenging.

1.2 Review of Literature

1.2.1 Citrus fruit

Citrus is classified as Rutaceae family. Mandarin orange has aromatic flowers and glossy leaves, and it is a globose fruit with sweet aromatic pulp including light yellow-orange to flame-orange peel, which is loose and easily removed (Nogata et al., 2003). Because of the types with red-orange skin, *C. reticulata* fruit is referred to as a tangerine, a mandarin, or Kamala lebu in Bengali (Mandal and Mandal, 2016). Mandarin fruit is one kind of citrus fruits which contain a lot of flavonoids, high amounts of vitamins and minerals, and antioxidant chemicals (Tripoli et al., 2007). Citrus fruit consists of three layers. The first layer is an outer peel (pericarp) with oil glands producing the odor of orange. The second is a whitish, thread-like mesocarp. The last layer is an endocarp containing juice sacs (Mandal and Mandal, 2016). The pericarp can divide into two parts; the outer peel (flavedo), or epicarp largely made of parenchymatous cells and cuticle. The second part is albedo (mesocarp lying beneath the flavedo) which contains tubular-like cells (Fig. 1.1). A plethora of microflora such as fungus and bacteria are present on the skin of the citrus fruit (Etebu and Nwauzoma, 2014).

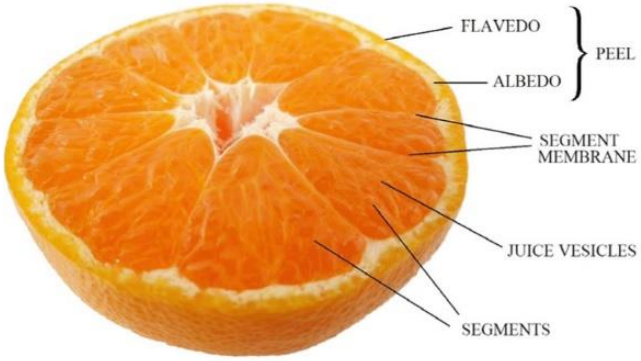

Fig. 1.1 Structure of citrus fruit. (Putnik et al., 2017)

1.2.2 ***Penicillium digitatum*** Sacc.

P. digitatum is a necrotrophic fungus causing green mold which is one of major postharvest pathologic diseases in citrus fruit (Eckert, 1978). Pores or wounds which are occurred during storage period are the vital factor for the growth of *P. digitatum* in citrus fruit. The water spot of fungal hyphal growth with characteristic powdery olive-colored conidia commonly known as green-mold appears will happen on the surface of the wounded citrus peel (Fig. 1.2), if suitable temperature and moisture conditions are available. *P. digitatum* produces a large number of spores on the surface of infected citrus fruit. Spores of *P. digitatum* are airborne, thereby these can easily overspread and contaminate into the packinghouse and its equipment, storage room, transit container and marketplace. Moreover, its spores can be survived over season to season after contaminating into the orchard leading to serious damages in commerce.

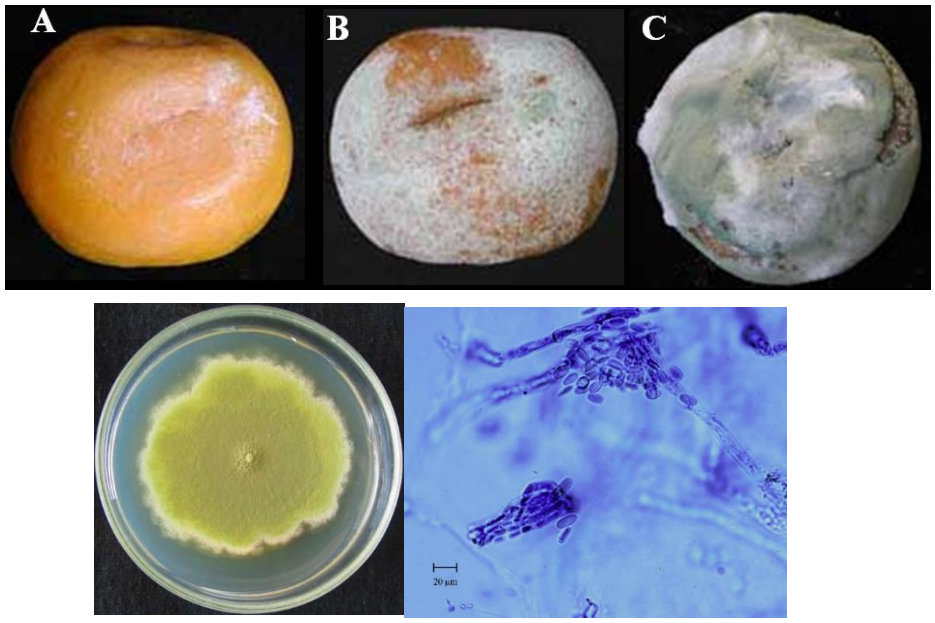

Fig. 1.2 Growth of *Penicillium digitatum* on citrus peel and its colony grown on potato dextrose agar. (Up) (A), (B), and (C): 2, 4 and 6 days after infection, respectively. (Down) The conidiospores stained with lactophenol cotton blue under light microscope with magnification of 400X.

1.2.3 Biological control

Biological control is a method of controlling disease in plants using other living organisms such as yeasts, bacteria and fungi (Cook, 1993). Biological control has become an approach to control postharvest pathogens instead of synthetic fungicide (Barkai-Golan, 2001; Janisiewicz et al., 2000). There are many types of mechanisms contributing to biological control such as competition, antibiosis, and parasitism. Induction of host resistance is one of the biological control methods by activating the signal molecules in plant defensive pathways against pathogens (Pal and McSpadden Gardener, 2006). SAR and ISR are an important system to induce host plant resistance (Choudhary et al., 2007).

1.2.4 Systemic acquired resistance (SAR)

SAR is a distinct signal transduction pathway which is long-lasting and broad-spectrum protection with no specificity to the initial infection. After a necrotic lesion was made on the host plants, hypersensitive response which considered as a symptom of disease is occurred resulting in SAR induction (Ryals et al., 1996). When SAR is activated in plant, contribution of mobile signals, accumulation of the defense hormone (SA), and secretion of the antimicrobial PR (pathogenesis-related) proteins are happened for plant immunity (Fu and Dong, 2013) as shown in Fig. 1.3. Mobile signals in SAR are created very fast (within 4–6 h) in the condition of primary infection. The accomplishment of SAR induction depends on the perception of mobile signals in the distal tissues especially, SA (Shine et al., 2018).

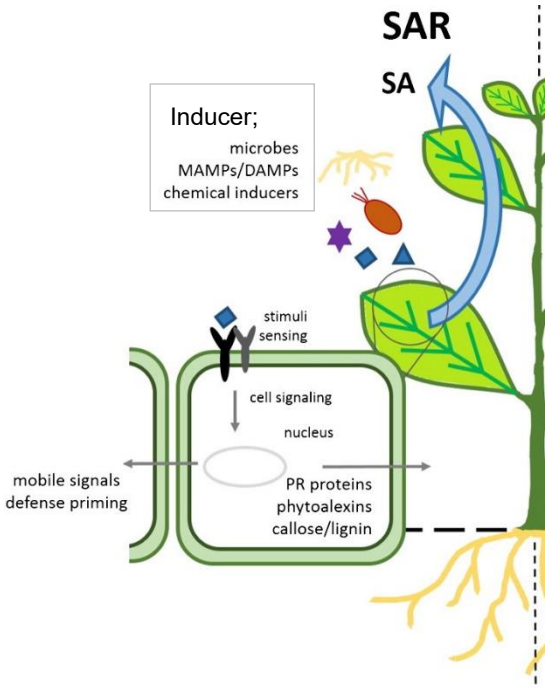

Fig. 1.3 Scheme of systemic acquired resistance (SAR). Inducers activate SAR resulting in elicitation of complex signaling and defense responses in the plant cell such as production of pathogenesis-related (PR) proteins, antimicrobial phytoalexins or cell wall fortification with callose or lignin. The other parts of plant prepare for defense system by transportation of mobile signals via xylem and prime distal plant parts. (Burketova et al., 2015).

1.2.5 Salicylic acid (SA)

SA is a phytohormone in plant providing the immune system during pathogen attack. Biosynthesis of SA is occurred by shikimic acid pathway in plastid of the cell. There are two routes with different key enzymes (phenylalanine ammonia-lyase (PAL) and isochorismate synthase (ICS)) in shikimic acid pathway for SA biosynthesis. Chorismic acid is an important precursor to produce SA for both routes (Kumar, 2014; Wildermuth et al., 2001). Methyl salicylate (MeSA) is the biologically inactive derivative of SA serving SA accumulation to distal tissues. To act as a defensive signal, MeSA must be converted to SA in the distal tissue during SAR (Kumar, 2014; Shine et al., 2018). In addition, SAR is required for many SA signaling components such as nonexpresser of PR

protein 1 (NPR1) which is the central regulator of SA signaling pathway (Shine et al., 2018). Furthermore, SA-dependent signaling pathway affects production of *PR* genes which encoded to PR proteins against pathogen invasion (Fig. 1.4). The production of PR-1, PR-2, and PR-5 are partially controlled by SA signaling pathway during SAR for plant defense (Ali et al., 2018). Exogenous SA was reported to inhibit green mold disease which was caused by *P. digitatum* in citrus fruit (Moscoso-Ramírez and Palou, 2013), by enhancing the gene expression involved in the phenylpropanoid pathway (Zhou et al., 2018).

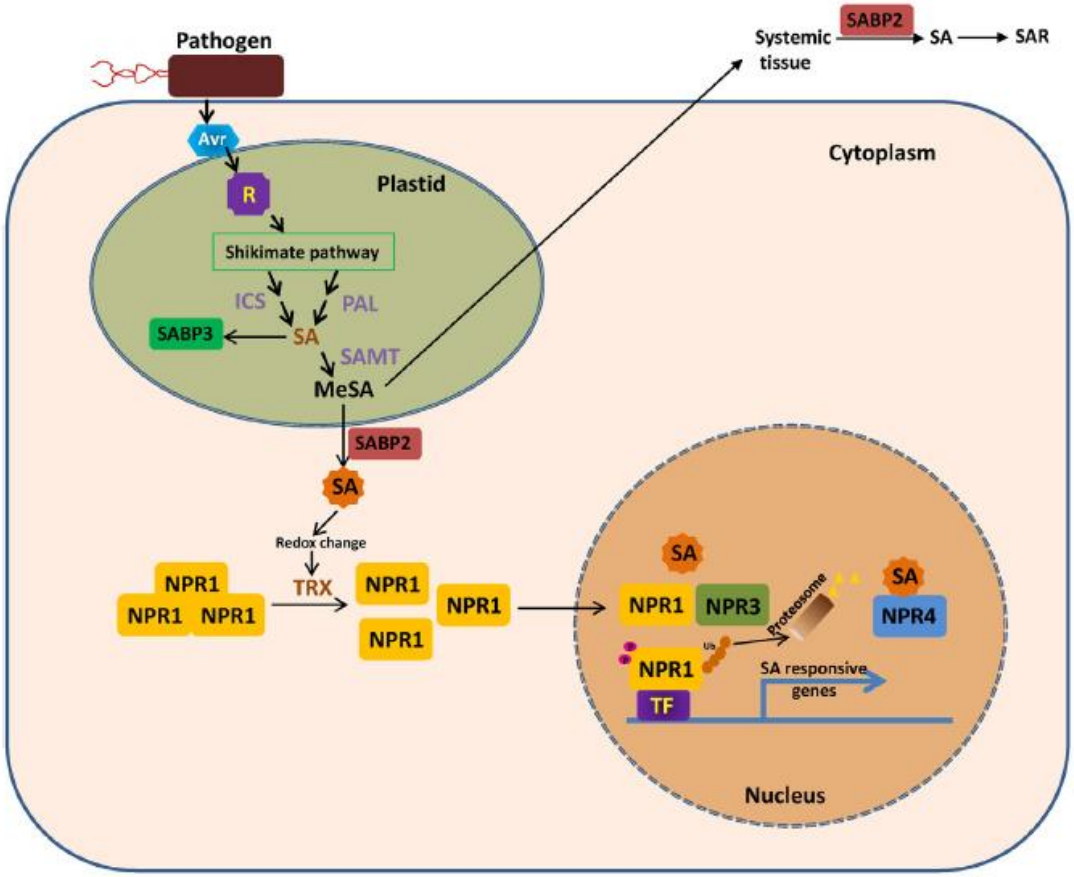

Fig. 1.4 Activation of salicylic acid (SA) signaling model in a plant cell. An increase of SA biosynthesis via shikimic acid pathway is activated by pathogen attack. Increased SA levels in the cytoplasm affects the induction of SAR and the formation of nonexpresser of pathogenesis-related protein 1 (NPR1) resulting in stimulation of SA responsive defense genes in nucleus such as *PR* genes for plant immunity. (Kumar, 2014)

1.2.6 Induced systemic resistance (ISR)

ISR is an important mechanism of plant growth-promoting rhizobacteria (PGPR) to activate defensive system in host plant against a broad range of pathogens. *Pseudomonas*, *Bacillus*, *Trichoderma*, and mycorrhiza species are root-associated mutualists which elicit an immune system in plant without directly activating costly defenses (reviewed in Pieterse et al., 2014). The effects of ISR-triggering rhizobacteria are different from the effects of pathogen elicitors because of no damage result of beneficial rhizobacteria to their host plants (Choudhary et al., 2007). Defensive mechanism of elicitation which generate to induced resistance by beneficial microbes is microbe-associated molecular patterns (MAMPs) (Van Wees et al., 2008). Successful stimulation of ISR relies on JA and ET signaling to produce additive resistance effects (reviewed in Pieterse et al., 2014). ISR signaling pathway was shown in Fig. 1.5.

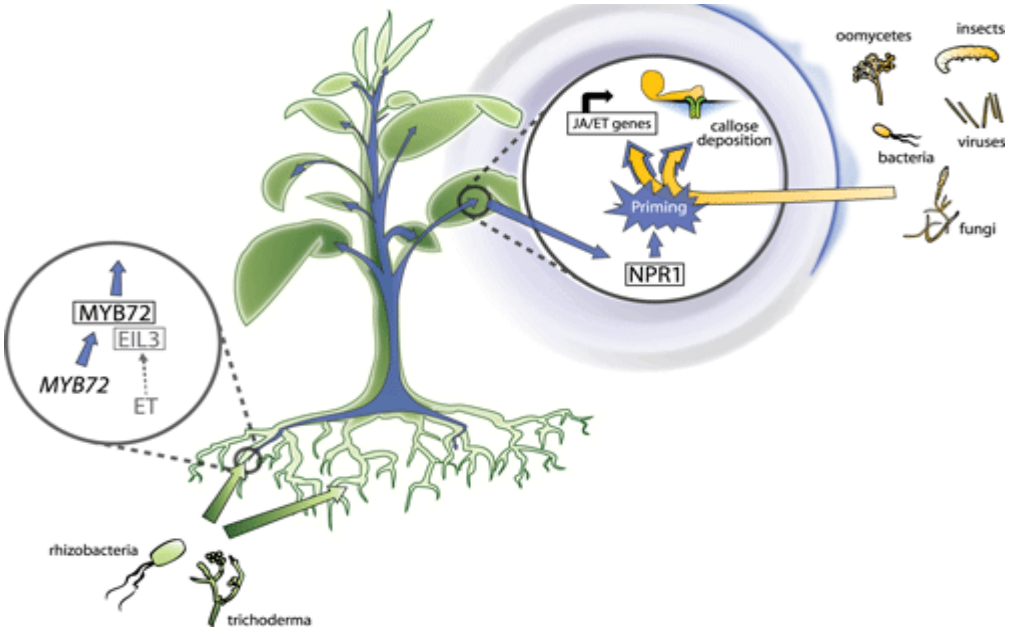

Fig. 1.5 Scheme of induced systemic resistance (ISR). Exposure of inducers such as rhizobacteria and *Trichoderma* species to roots of host plant leading to activation of plant growth promoting rhizobacteria (PGPR). Resulting in elicitation of transcription factors (MYB72 and MYC2) and dependent on jasmonic acid (JA) and ethylene (ET) signaling including stimulating e.g. callose formation. (http://web.science.uu.nl/pmi/)

1.2.7 Jasmonic acid (JA)

JA is an alpha-linolenic acid derivative which is an important regulator of plant defenses against pathogens in ISR pathway (reviewed in Pieterse et al., 2014). To synthesize JA, conversion of alpha-linolenic acid is performed in many steps by the key enzymes such as lipoxygenase (LOX), allene oxide synthase (AOS), and allene oxide cyclase (AOC) (Wasternack, 2007). Various JA derivatives were modified from JA in cytosol. JA methyl transferase is an important enzyme to produce MeJA which is one of JA derivatives. Conjugation of JA with amino acid is one of JA modification such as JA-Ile by an amino acid synthetase encoded from *jasmonate resistant1* (*JAR1*) gene which is an important in activation of JA signaling pathway (Fig. 1.6) (Kazan and Manners, 2008). JA and its derivatives induce the expression of genes which encode defense-related proteins with antimicrobial and antifungal activity such as plant defensin protein 1.2 (PDF1.2) (Rojo et al., 2003) including *PR* gene which express to PR protein such as chitinase (PR3) (Ali et al., 2018). Moreover, JA regulator has ability to trigger genes and proteins involved in phytoalexin biosynthesis (Kazan and Manners, 2008; reviewed in Pieterse et al., 2014). Exogenous MeJA has the ability to inhibit postharvest disease and to enhance the enzyme activity of polyphenol oxidase, and peroxidase in citrus fruit, and catalase for plant immunity in mandarins (Guo et al., 2014).

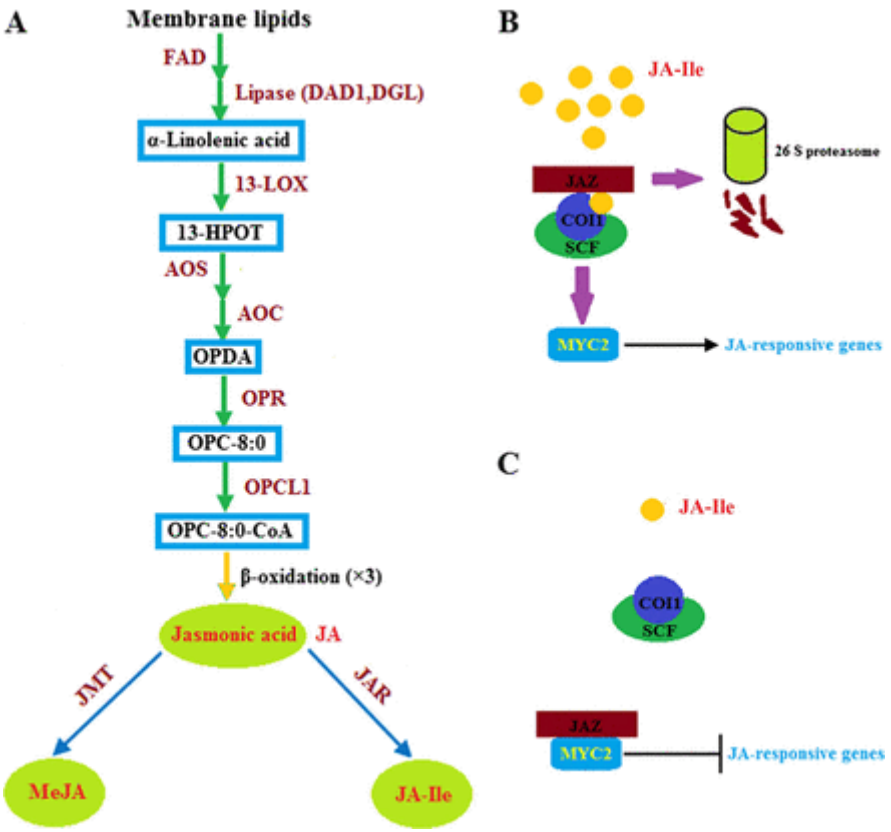

Fig. 1.6 Jasmonic acid (JA) biosynthesis and signaling pathway. (A) JA biosynthetic pathway using many enzymes for these reactions; fatty acid desaturase (FAD), defective anther dehiscence 1 (DAD1) and dongle (DGL), 13-lipoxygenase (13-LOX), allene oxide synthase (AOS), allene oxide cyclase (AOC), OPDA reductase (OPR), OPC-8:0 CoA ligase (OPCL), jasmonic acid-conjugating enzyme (JAR1), and jasmonic acid carboxyl methyltransferase (JMT). (B) When JA-Ile levels are high, coronatine insensitive 1 (COI1), which is a receptor, functions as an F-box protein in the Skp-Cullin-F-box (SCF) complex. Jasmonate ZIM-domain proteins (JAZs) are required by COI1, ubiquitinated, and subsequently subject to degradation by proteasome. Resulting in release of MYC2 for elicitation of JA-responsive gene expression. (C) When JA-Ile levels are low, JAZs interact with MYC2 to prevent MYC2 for activation of JA-responsive gene expression. (Wang et al., 2016)

1.2.8 Ethylene (ET)

ET is a member of plant hormones which involves in many roles in plant such as plant development and response to environmental stimuli from biotic and abiotic stresses (Wang et al., 2002). *S*-adenosyl-l-methionine (SAM) and 1-aminocyclopropane-1-carboxylic acid (ACC) are vital components in ET biosynthesis (Fig. 1.7A). There are two key enzymes to synthesize ET production. The first key enzyme is ACC synthase (ACS), which catalyzes the conversion of SAM into ACC. The second key enzyme is ACC oxidase (ACO), which converts ACC into ethylene (Yang and Hoffman, 1984). ET signaling pathway for induction of plant defensive system is shown in Fig. 1.7B. ET can trigger the different classes of PR protein production responding to stress such as PR3 (chitinases) and PR12 (PDFs). Moreover, ET can also induce expression of *PDF1.2* gene like JA induction for plant resistance (Adie et al., 2007). Ethephon (Et) is a chemical which can release ET. Et was applied to sweet orange trees to investigate the changes of genes related to the ET signaling pathway and was shown to be potent in inducing the expression of ACO and ACS1 which are the key genes expressing enzymes in ET production (John-Karuppiah and Burns, 2010) resulting in the activation of the plant's defense mechanism.

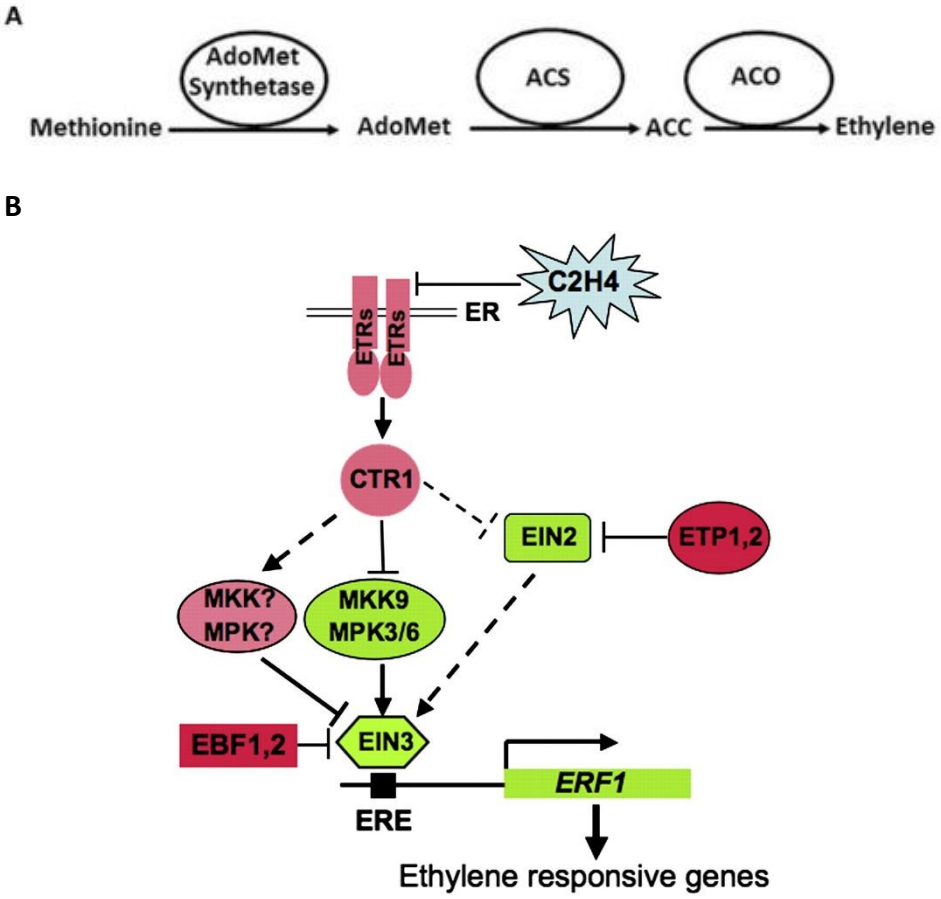

Fig. 1.7 Ethylene (ET) biosynthesis and signaling pathway. (A) ET biosynthesis. (Song and Liu, 2015) (B) ET signaling pathway. ETRs, ETR1 and ERS1 are ET ethylene receptors. When absence of ET, the receptors of ET stimulate the RAF-like MAPKK kinase CTR1, which represses ET signaling by inhibiting the function of MKK9–MPK3/6 and EIN2. CTR1 may activate another unknown MAPK and phosphorylate the T592 site of EIN3, resulting in EIN3degradation through the two F-box proteins EBF1 and EBF2. When ET presents, it binds to the receptors to inhibit the action of receptors and CTR1 generating to elicitation of the MKK9–MPK3/6 module, which phosphorylates EIN3 on T174. Then, EIN3 enhances the expression of ERF1 resulting in expression of ethylene-responsive genes. ET-induced responses is promoted by EIN2 through EIN3. ETP1 and ETP2 which are F-box proteins are negative regulator of EIN2. (Wang et al., 2009)

1.2.9 *Bacillus subtilis*

B. subtilis is a gram-positive bacterium. Antagonistic strains of *B. subtilis* were discovered to reduce the disease incidence of fungal disease in many studies. *B. subtilis* isolates F1, L2, and L2-5 significantly controlled citrus green and blue molds caused by *P. digitatum* and *P. italicum*, respectively (Obagwu and Korsten, 2003). *B. subtilis* 155 showed ability to suppress the growth of *P. digitatum* in mandarin fruit (Leelasuphakul et al., 2008). *B. subtilis* CCTCC M 207209 was used to inhibit the growth of *Aspergillus carbonarius* CCTCC AF 2011004 in grapes (Jiang et al., 2014). *B. subtilis* CCMI 355 revealed the resistance effect against wood surface contaminant fungi (Moita et al., 2005). Moreover, *B. subtilis* ABS-S14 was reported to produce CLPs with antimicrobial activity particularly iturin A, fengycin, and surfactin which were reported to control green mold decay in sweet oranges by the enhancement of *LOX*, *POD*, *GLU*, *CHI* expression which plays a defensive role in plants (Waewthongrak et al., 2014).

1.2.10 Cyclic lipopeptides (CLPs)

CLPs are biosynthesized via production of the peptide ring using nonribosomal peptide synthetases as an enzyme. The fatty acyl chain is filled to the peptide ring through lipoinitiation during synthesis. CLPs are contained a fatty acid tail linked to a short oligopeptide cyclizing to a lactone ring formation between two amino acids in the peptide chain (Raaijmakers et al., 2006) (Fig. 1.8). There have been many reports which have demonstrated the mode of antibiotic action of individual CLP on pathogens and how they function through sterol and phospholipid molecules which stimulate pore formation, thus affecting the permeability of the fungal cell membrane (Deleu et al., 2005), and by aggregating and disturbing the sequence of the lipid bilayer (Horn et al., 2013; Sur et al., 2018). In addition, CLPs have been revealed to inhibit the synthesis of fungal DNA (Tao et al., 2011).

The CLPs generated by *Bacillus* species comprising, fengycin, iturin A, and surfactin, have also been found to function by inducing defensive gene transcription

as a plant defensive response (Kawagoe et al., 2015; Ongena et al., 2007) such as the transcription of *plant defensin 1.2* (*PDF1.2*) (Chandler et al., 2015). CLPs isolated from *B. subtilis* ABS-S14 has shown strong elicitation of defense–related gene transcription leading to PR protein production and an increase in the enzyme activities of glucanase (GLU), chitinase (CHI), peroxidase (POD) and lipoxygenase (LOX) in Valencia fruit (Waewthongrak et al., 2014).

Fengycin showed the greatest induction of *GLU* gene expression. The expression levels of *GLU* and *CHI* genes were incresed by the synergystic actions of fengycin-iturin A and fengycin-surfactin, respectively (Waewthongrak et al., 2014). Moreover, fengycin has the potential to control rot disease in apple (Fan et al., 2017). The iturin family stimulates the salicylic acid (SA) and jasmonic acid (JA) signaling pathways (Farace et al., 2015) and iturin A activates the expression of *PR1* and *PDF1.2* genes which are important genes in the SA and JA signaling pathways, respectively (Kawagoe et al., 2015). Surfactin was shown to be involved in the resistance process by triggering the transcriptional levels of *LOX* and *POD* gene expression (Waewthongrak et al., 2014). The effectiveness of surfactin on ISR elicitation in disease protection in tobacco leaves has also been confirmed (Cawoy et al., 2014). The potential of *Bacillus* CLPs to trigger ISR in part, at least, by reinforcing basal plant defense responses was shown in rice against *Rhizoctonia solani* (Chandler et al., 2015).

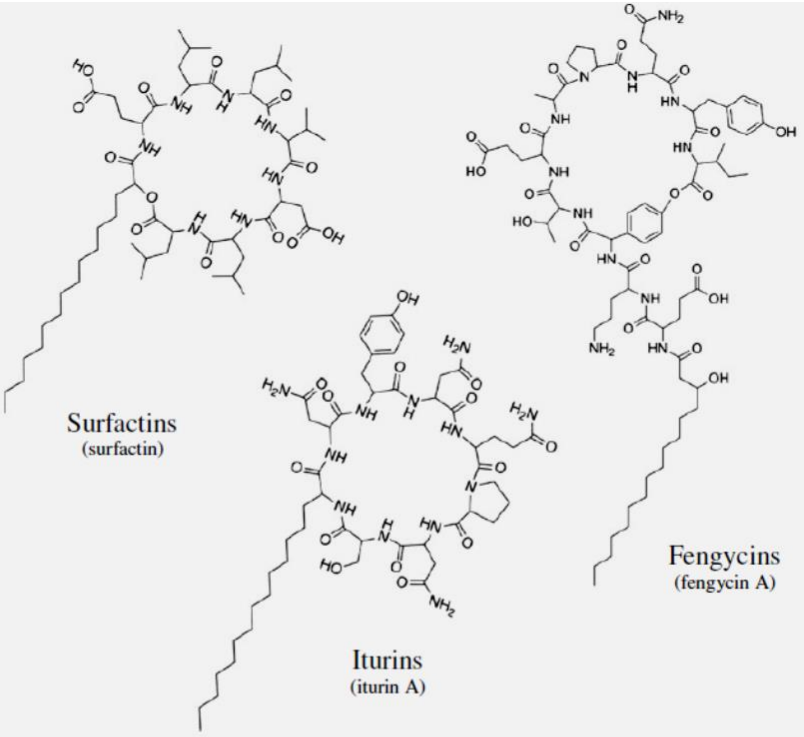

Family	Variant	Amino Acid Sequence	Acyl Chain Length
Surfactin	Esperin[1]	L-Glu - L-Leu - **D-Leu** - L-Val - **L-Asp** - **D-Leu** - L-Leu - COOH	C_{13} - C_{15}
	Halobacillin	L-Gln[2] - L-Lue[3] - **D-Leu** - L-Val[3] - **L-Asp** - **D-Leu** - L-Val[3]	
	Pumilacidin	L-Glu - L-Leu - **D-Leu** - L-Leu - **L-Asp** - **D-Leu** - L-Val[3]	
	Surfactin	L-Glu - L-Val[4] - **D-Leu** - L-Ala[5] - **L-Asp** - **D-Leu** - L-Val[4]	
Fengycin	Fengycin A	**L-Glu** - **D-Orn** - D-Tyr - D-**a**Thr - **L-Glu** - D-Ala - **L-Pro** - **L-Gln** - **L-Tyr** - **L-Ile**	C_{14} - C_{18}
	Fengycin B	**L-Glu** - **D-Orn** - D-Tyr - D-**a**Thr - **L-Glu** - D-Val - **L-Pro** - **L-Gln** - **L-Tyr** - **L-Ile**	
	Plipastatin A	**L-Glu** - **D-Orn** - L-Tyr - D-**a**Thr - **L-Glu** - D-Ala - **L-Pro** - **L-Gln** - **L-Tyr** - **L-Ile**	
	Plipastatin B	**L-Glu** - **D-Orn** - L-Tyr - D-**a**Thr - **L-Glu** - D-Val - **L-Pro** - **L-Gln** - **L-Tyr** - **L-Ile**	
Iturin	Bacillomycin D	L-Asn - **D-Tyr** - **D-Asn** - L-Pro - L-Glu - D-Ser - L-Thr	C_{14} - C_{17}
	Bacillomycin F	L-Asn - **D-Tyr** - **D-Asn** - L-Gln - L-Pro - D-Asn - L-Thr	
	Bacillomycin L	L-Asp - **D-Tyr** - **D-Asn** - L-Ser - L-Gln - D-Ser - L-Thr	
	Bacillopeptin	L-Asn - **D-Tyr** - **D-Asn** - L-Ser - L-Glu - D-Ser - L-Thr	
	Iturin A	L-Asn - **D-Tyr** - **D-Asn** - L-Gln - L-Pro - D-Asn - L-Ser	
	Iturin C	L-Asp - **D-Tyr** - **D-Asn** - L-Gln - L-Pro - D-Asn - L-Ser	
	Mycosubtilin	L-Asn - **D-Tyr** - **D-Asn** - L-Gln - L-Pro - D-Ser - L-Asn	

[1]Asp at position 5 forms the lactone ring
[2]May also be L-Glu
[3]May also be L-Ile
[4]May also be L-Leu or L-Ile
[5]May also be L-Val, L-Leu, or L-Ile

Fig. 1.8 Structure of cyclic lipopeptides. (Falardeau et al., 2013)

1.2.11 Proteomics

Proteomics has become one of the main methods of exploring and better understanding protein changes during stress responses (Yun et al., 2010). Liquid chromatography mass spectrometry (LC-MS)-based techniques were used as the major approach to increase the knowledge of orange proteomes (Lerma-Garcia et al., 2016). LC-MS was also employed to study the differential proteomic pattern of sweet oranges during ripening, with proteins being classified based on known biosynthetic pathways, secondary metabolism and oxidative process proteins (Muccilli et al., 2009). Moreover, the investigation of changes in amino acid, sugar, and organic acid profiles by gas chromatography mass spectrometry (GC-MS), when SA and JA were applied to citrus leaves, to induce wound stress showed that tryptophan (Trp) and serine were significant biomarkers of wound stress (Asai et al., 2017). Furthermore, the proteome study of anaerobic stress in mandarins by Shi et al. (2008) using two-dimensional polyacrylamide gel electrophoresis (2D-PAGE) combined with MS provided a better understanding of citrus-specific anaerobic-response mechanisms (Shi et al., 2008). Many studies identified a broad range of plant proteins generated during responses to abiotic and biotic stresses (Tan et al., 2017), and changes in the protein contents in the epicarp of orange fruit after heat treatment (Perotti et al., 2015) by proteomic approaches.

1.2.12 Metabolomics

Metabolomics is a powerful modern approach to expand the knowledge of plant defense mechanism through signaling pathways by determination of the metabolites which occurred in specific metabolic networks and stress responses of plant (Hall et al., 2002). Metabolomics has been used to investigate primary and secondary metabolites to monitor and assess gene function (Asai et al., 2017; Hall et al., 2002; Sampaio et al., 2016). It has also been used to characterize post-genomic processes from a broad perspective (Tugizimana et al., 2013), and to find biomarker candidates during defense responses in citrus leaves (Asai et al., 2017). Stresses in citrus leaves after wounding and exposure to MeJA and SA involving Trp and serine regulation were recently reported, based on GC-MS and statistical analysis (Asai et al., 2017).

The conventional MS techniques were used to perform metabolomic analysis with the recent development of high-performance chemical isotope labeling (CIL) coupled with LC-MS (Guo and Li, 2009; Han et al., 2017; Hooton et al., 2016). It is now possible to quantify the metabolomic changes of biological systems with high metabolic coverage and high accuracy including precision, thereby allowing the possibility of revealing up- and down-regulated metabolites in many metabolic pathways. For example, the dansylation labeling method was used to profile the amine-/phenol-containing metabolites or the amine/phenol submetabolome with high coverage (Guo and Li, 2009). Dansylation LC-MS uses ^{12}C- and ^{13}C-dansyl chloride to label an individual sample and a pooled sample, respectively. The ^{13}C-labeled pooled sample is spiked into each ^{12}C-labeled sample, so that the ^{13}C-labeled pool is employed as a reference. The result of mass spectra which detect the labeled metabolites as peak pairs and the intensity ratio of the ^{12}C-labeled and ^{13}C-labeled peaks could be used for relative quantification of metabolite concentrations in comparative samples (Luo et al., 2016).

1.3 Objectives

1. To compare the efficacy of enhancement in host plant resistance by *B. subtilis* ABS-S14 CLP and exogenous plant hormones of biological control approaches to inhibit *P. digitatum* infection during postharvest period in mandarin fruit.

2. To determine the effect of *B. subtilis* ABS-S14 CLP extract compared with exogenous plant hormones with and without *P. digitatum* infection on the transcript pattern of genes involved in the signal transduction pathway. Based on the proteomic study analysis of PR protein abundance changes in treated mandarin fruit was carried out.

3. To indicate the effect of fengycin, iturin A, surfactin obtained from *B. subtilis* ABS-S14 with and without *P. digitatum* infection on the transcriptional changes of defense related genes and proteomic profiling in mandarin fruit.

4. To explore capability of fengycin, iturin A, surfactin obtained from *B. subtilis* ABS-S14 binding interaction to plant derived proteins following *P. digitatum* infection involving ISR activation.

5. To investigate the regulation of primary and secondary metabolite productions in the defense responses of mandarin fruit to wound stress among treatments of *B. subtilis* ABS-S14 CLPs, exogenous plant hormones and *P. digitatum* infection by dansylation LC-MS analysis.

CHAPTER 2

MATERIALS AND METHODS

2.1 Materials

2.1.1 Instruments

Instruments	Model	Company
Autoclave	ES-315	Tomy
Analytical Balance		Mettler Toledo
Benchtop pH meter	Orion 2 strar	Thermo
Benchtop centrifuge	5415D	Eppendorf
Bioharzard carbinet	BSB 3A	Gelaire
Concentrator	Vacufuge	Eppendorf
Electrophoresis	AE-6530	Atto
FT-ICR mass spectrometer	9.4 T Apex-Qe	Bruker Daltonics
Gel documentation system	Bio chemi system	UVP
	System 120	Kodak DC
Haemacytometer		Boeco
Heat block		VWR Scientific
Hot plate	KIKA	Labortechnik
	PC-101	Corning
Homogenizer		Kinematica
HPLC column	Chromolite RP-18e	Merck
HPLC system	1200	Agilent
Incubator		Memmert
Laminar flow hood	BSB 3A	Gelaire
MALDI-TOF	Ultraflex III TOF/TOF	Bruker Daltonics
Micropipette	P2	BioPette

Instruments	Model	Company
Micropipette	P10	BioPette
	P20	BioPette
	P200	BioPette
	P1000	BioPette
Micropipette tip-C18		Merck
Microscope	Compound	Nikon
	Stereo	Meiji
NanoDrop spectrophotometer	NanoDrop 1000	Thermo Fisher Scientific
Orbital shaker	PB4002-s/FACT PG5002-s	Mettler
Orbital shaker		Gallenkamp
PTLC plate	Silica gel 60 F_{254}	Merck
Refrigerated Centrifuge	J2-21	Beckman
	J-30I	Beckman
	EBA 12R	Hettichzentrifugen
	RC5C	Sorvall
Rotary evaporator	R-210	Buchi
Regular PCR	Veriti Thermal Cyclers	Thermo Fisher Scientific
Realtime PCR	Exicycler™ 96	Bioneer
Scales (2 digits)		
Scales (4 digits)		
Sonicator		Delta
Spectrophotometer	UV-Vis 8435	Hewlett-Packard
	UV-160A	Shimudzu
SPE cartridge	Ziptip® Pipette Tips	Merck
TLC plate	Silica gel 60 F_{254}	Merck
UPLC system	AQUALITY	Waters
UV transilluminator	ECX-15M	Vilber Lourmat
Water bath		Memmert

2.1.2 Chemicals

Chemicals	Grade	Company
Absolute ethanol	AR	J.T. Baker
Acetic acid	AR	J.T. Baker
Acetone	AR	J.T. Baker
Acetonitrile	HPLC	Fisher
Acrylamide monomer (40%)	Molecular biology	GE Healthcare
Ammonium bicarbonate	Molecular biology	Sigma-Aldrich
Ammonium persulfate	Molecular biology	Bio basic
β-mercaptoethanol	Molecular biology	Sigma
Bovine serum albumin	Molecular biology	Sigma-Aldrich
Bromophenol blue	Molecular biology	GE Healthcare
Chloroform	Molecular biology	Sigma
Coomassie brilliant blue G-250	AR	Fluka
Coomassie brilliant blue R-250	AR	Sigma
Copper (II) sulphate	AR	Fisher scientific
Dimethyl sulfoxide	Molecular biology	Fisher Scientific
Disodium hydrogen phosphate	Molecular biology	Merck
Dithiothreitol	Molecular biology	SB corporation
DNase I	Molecular biology	Amercham
Ethylenediaminetetraacetate	AR	USB Products
Ethephon	AR	Sigma-Aldrich
Ethidium bromide	Molecular biology	Bio-rad
Fengycin	HTLC standard	Sigma-Aldrich
Folin-ciocalteuphenol reagent	AR	Merck

Chemicals	Grade	Company
Formadehyde (37%)	AR	Sigma-Aldrich
Formic acid	AR	Fluka
Glycerol	AR	GE Healthcare
Glycine	AR	Fisher Scientific
Guanidine thiocyanate	Molecular biology	Amresco
Hydrochloric acid	AR	RCI Labscan
Iodoacetamide	Molecular biology	GE Healthcare
Improm-II™ Reverse Transcription System	Molecular biology	Promega
Iturin A	HPLC standard	Sigma
Methanol	AR	J.T.Baker
	HPLC	Thermo Fisher Scientific
Methyl jasmonate	AR	Sigma-Aldrich
Monopotassium phosphate	Molecular biology	Sigma-Aldrich
Low Molecular Weight SDS marker kit	Molecular biology	GE Healthcare
Lithium carbonate	Molecular biology	Sigma-Aldrich
Phosphoric acid	AR	BDH
PCR master mix kit	Molecular biology	Bioneer
Potassium chloride	Molecular biology	Merck
RNase H	Molecular biology	Invitrogen
Salicylic acid	AR	Sigma-Aldrich
Silver nitrate	Molecular biology	Applichem GMbH
Sodium acetate	Molecular biology	Sigma
Sodium carbonate	AR	Panreac Applichem
Sodium chloride	AR	Lab-Scan
Sodium citrate	Molecular biology	Sigma
Sodium dodecyl sulfate (SDS)	AR	Sigma

Chemicals	Grade	Company
Surfactin	TLC standard	Sigma
SYBR Green	Molecular biology	Kapa Biosystems
Tatalic acid	Molecular biology	Carlo Erba
Trifluoroacetic acid	HPLC	Merck
Tris base	AR	Fisher Scientific
Trypsin	Molecular biology	Promega
6X loading dye	Molecular biology	Promega

2.1.3 Medium

Agar	Grade	Company
Agar	Microbiology	Merck
Nutrient agar	Microbiology	Merck
Luria -Bertani broth	Microbiology	Merck
Malt extract agar	Microbiology	Merck
Potato dextrose agar	Microbiology	Merck
Potato dextrose broth	Microbiology	Merck

2.2 Methods

2.2.1 Plant materials

Mandarin fruit (*Citrus reticulata* Blanco cv. Shogun) of uniform size and color without physical injuries or infections were selected from a commercial market located in Bangkok, Thailand. The fruit were surface-sterilized with 1% sodium hypochlorite solution for 5 min, wiped thoroughly with 70% ethanol, and then allowed to air dry at 25 °C and the artificial wound sites were made following the described methods in previous study (Waewthongrak et al., 2014).

2.2.2 Microorganisms

P. digitatum was isolated from decayed mandarin fruit and identified (Leelasuphakul et al., 2008). A pure culture was placed on a potato dextrose agar (PDA) plate and incubated at 24 °C for 7 days. To maintain their pathogenicity, the fungal spores were routinely inoculated back into mandarin fruit. The *P. digitatum* spore suspension was prepared from a 7-day-old culture and a haemacytometer was used to adjust it to the desired concentration (10^7 spores L^{-1}).

B. subtilis ABS-S14 was isolated from soil collected from citrus groves around the south of Thailand (Narawitsaree et al., 2009). It was identified by Gram staining, cell shape and the presence of spores, and bio-chemical analysis. The screening test of its antagonistic properties against a fungal colony of *P. digitatum in vitro* was performed prior to use (Leelasuphakul et al., 2008).

2.2.3 Preparation of exogenous plant hormone solution

SA, MeJA and Et used as exogenous plant hormones were purchased from Sigma-Aldrich and the hormone solutions were prepared ~~in 80% ethanol~~ prior to fruit treatment. The concentration of SA (250 µmol L^{-1}), MeJA (100 µmol L^{-1}) and Et (450 µL L^{-1}) solution was prepared in 80 % ethanol according to the previous studies (Guo et al., 2014; John-Karuppiah and Burns, 2010; Moscoso-Ramírez and Palou, 2013).

2.2.4 Preparation of *B. subtilis* ABS-S14 CLP extract

The *B. subtilis* ABS-S14 strain was grown in Luria-Bertani (LB) medium (Waewthongrak et al., 2014) following the method reported (McKeen et al., 1986). A CLP extract was prepared from culture-free filtrates obtained after drying in a rotary vacuum evaporator at 65 °C. It was weighed and re-dissolved in 80% ethanol, then adjusted to a 50 g L^{-1} stock solution (Leelasuphakul et al., 2006). The three families of CLPs obtained from CLP extract were basically confirmed by thin-layer chromatography (TLC) analysis (silica gel 60 F_{254}, Merck, Germany).

2.2.5 Separation and purification of CLPs

Fengycin, iturin A and surfactin, that belongs to CLP members were prepared from *B. subtilis* ABS-S14 CLP extract using preparative thin-layer chromatography (PTLC) following the reported method (Waewthongrak et al., 2014). They were recovered by ethanol extraction from silica gel on a PTLC plate and further separated using a C18 solid phase extraction (SPE) cartridge (Sep-Pak®, Vac 12 cc (2 g), silica, 15-105 µm, 125 Å pore size, Waters, U.S.A.) to increase the purity. A sorbent matrix was eluted by step gradients of acetonitrile in 0.1% trifluoroacetic acid: 40% to 55%, 25% to 35% and 60% to 80% for fengycin, iturin A and surfactin, respectively. The fractions were dried by rotary evaporator and re-dissolved in 80% ethanol.

2.2.6 Identification of CLPs

Identification of the CLPs was performed at the Proteomics Research Laboratory, National Center for Genetic Engineering and Biotechnology (BIOTEC), National Science and Technology Development Agency (NSTDA), Thailand by HPLC (Agilent 1200, Agilent Technologies Inc., U.S.A.) and matrix-assisted laser desorption ionization time-of-flight (MALDI-TOF) MS (Bruker Daltonic Ultraflex III TOF/TOF, Bruker Daltonics Ltd., Germany) following the previous study (Waewthongrak et al., 2014). The matrix was α-cyano-4-hydroxycinnamic acid. The bacterial CLPs were detected in the range of molecular ion peaks from m/z 600 to 1,800.

2.2.7 *In vitro* inhibitory effect of CLPs against *P. digitatum* growth

2.2.7.1 *B. subtilis* endospores

The ability of *B. subtilis* endospores to inhibit the growth of *P. digitatum* was explored using the dual-culture assay. An actively growing mycelial plug of fungus with the diameter size of 0.1 cm were placed in the center of a 9 cm of PDA-Petri dish and then incubated at 25 °C for 24 h prior to the test. The *B. subtilis* cells, which were collected

from overnight bacterial cultures in LB broth by centrifugation at 8,000 rpm for 20 min, were streaked approximately 1 cm away from the growing edge of the mycelium on the PDA plate, and further incubated at 25 °C. The percentage of mycelial growth inhibition was calculated using the formula in a previous work (Gamliel et al., 1989) after being incubated at 25 °C for 48 h.

$$\text{Percentage of inhibition} = 100\text{-}[(R^2/r^2) \times 100]$$

R = Radial growth of fungal colony on treatment plate

r = Radial growth of fungal colony on control plate

2.2.7.2 *B. subtilis* cell-free supernatant

The ability of *B. subtilis* cell-free culture supernatant to inhibit the growth of *P. digitatum* was explored using the agar well diffusion assay. The *B. subtilis* cell-free supernatant was harvested by centrifugation of a 3 day-old bacterial culture in LB broth. The sterilization was performed by autoclaving at 121 °C for 15 min. An actively growing mycelial plug with the diameter size of 0.1 cm was placed in the center of a PDA-Petri dish and incubated at 25 °C for 24 h prior to the test. Aliquots of 45 µL of supernatant were added to the two cavities (0.5 cm diameter) which were made at approximately 1 cm away from the growing edge of the fungal colony, and further incubated at 25 °C. The percentage of mycelial growth inhibition was calculated using the formula as described in 2.2.7.1 after being incubated at 25°C for 48 h.

2.2.7.3 *B. subtilis* CLP extract

The ability of CLP extract to inhibit the growth of *P. digitatum* was explored using the half maximal efficient concentration (EC_{50}) assay which was tested on two well concave slides. Four two-well concave slides (8 replications) were set over a semicircle filter paper placed in Petri dish (15 cm diameter) plate to keep moist as presented in Fig. 2.1. The plates were sterilized by autoclaving. The 900 µL of the pre-warmed PDA were

mixed with 100 µL of CLP extract at different concentrations (two fold serial dilution) (10, 5, 2.5, 1.25, 0.625, 0.313 and 0.156 mg mL^{-1}), mixed well and set aside to allow solidification after transferring into each well of concavity slides. Finally, actively growing mycelial plug (0.1 cm diameter) was placed on the center of each well. Sterile distilled water was added to filter paper to maintain the humidity system in the plate and then incubated at 25 °C for 48 h. The plates were kept in a sealed plastic box. The radial extension of the mycelium was measured by ocular micrometer under a stereo-microscope, and the percentage of mycelial growth of inhibition was calculated as described in 2.2.7.1. The EC_{50} value was analyzed using the linear regression equation with the Microsoft Excel 365 program .

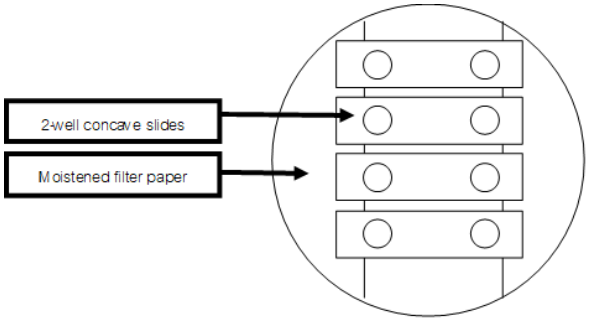

Fig. 2.1 Plate of EC_{50} assay.

2.2.8 Transcription and proteome analysis of defense-related genes in mandarins triggered by *B. subtilis* CLPs and exogenous plant hormones upon *P. digitatum* infection

2.2.8.1 Inoculation of mandarin fruit

Two experiments were conducted to determine the effects of CLP extract obtained from *B. subtilis* ABS-S14 and exogenous plant hormones on the production of plant defensive proteins in mandarin oranges with and without pathogen inoculation. They consisted of eight treatments (five fruit per treatment with three replicates) and the experiment was performed twice. The aliquots of 20 µL of solution was dropped onto the wound sites. The first experiment utilized comprising SA, MeJA, Et, and CLP extract (10 g L^{-1}) (Table 2.1). The second experiment was performed in the same manner as the first treatment experiments with the exception that they were followed by the inoculation of 10^7

spores L^{-1} of *P. digitatum* (Table 2.2). Sterile distilled water was used as a control for both experiments. All the treatments were placed in sealed plastic boxes containing a cup of water to maintain a high humidity at 25 ^{o}C and further incubated for 0, 24, 48, and 72 h. Tissues from the mandarin peel (flavedo) obtained from the various treatments was collected approximately 1 cm away from the wound site. The flavedo tissues were pooled and ground to a fine powder under liquid nitrogen and kept at -80 ^{o}C prior to use.

Table 2.1 Induction of defense responses in citrus fruit without *P. digitatum* infection by exogenous plant hormones and *Bacillus* CLP extract.

Treatment	Treatment agents (20 µL each)
T 1	sterile distilled water (control)
T 2	salicylic acid
T 3	methyl jasmonate
T 4	Ethephon
T 5	*Bacillus* CLP extract

Salicylic acid; 250 µmol L^{-1}, methyl jasmonate; 100 µmol L^{-1}, ethephon; 450 µL L^{-1}, *Bacillus* CLP extract; 10 g L^{-1}

Table 2.2 Induction of defense responses in citrus fruit with *P. digitatum* infection by exogenous plant hormones and *Bacillus* CLP extract.

Treatment	Treatment agents (20 µL each)
T 1	sterile distilled water (control)
T 2	*P. digitatum*
T 3	salicylic acid + *P. digitatum*
T 4	methyl jasmonate + *P. digitatum*
T 5	Ethephon + *P. digitatum*
T 6	*Bacillus* CLP extract + *P. digitatum*

P. digitatum spore suspension; 10^{8} spores L^{-1}, salicylic acid; 250 µmol L^{-1}, methyl jasmonate; 100 µmol L^{-1}, ethephon; 450 µL L^{-1}, *Bacillus* CLP extract; 10 g L^{-1}

2.2.8.2 Transcription analysis

The total RNA content was extracted from a fine powder using TRI Reagent® following the protocol recommended by the manufacturer (Molecular Research Center, Ohio, USA). DNase I-treated total RNA was reverse-transcribed using an Improm-II™ Reverse Transcription System (Promega) to cDNA. qRT-PCR (*Exicycler*™ 96, Bioneer, Republic of Korea) was performed (40 cycles of amplification; denature template at 95 °C for 30 sec, anneal primer at 60 °C for 30 sec, extension at 72 °C for 30 sec) with a KAPA SYBR® FAST qPCR kit (Kapa Biosystems, USA) to quantify the transcriptional levels. Primers were designed using the sequences of the target genes following methods outlined in previous studies (Table 2.3); elongation factor 1 alpha (*EF-1α*) (a housekeeping gene), *LOX, CHI, GLU*, *POD* (Waewthongrak et al., 2014), *PAL* (Jiwanit et al., 2018), *ACS1* (John-Karuppiah and Burns, 2010) and *PR1* (Dutt et al., 2015). The endogenous control was performed by the expression of *EF-1α* gene (Waewthongrak et al., 2014). The transcriptional fold-relative expression of each gene was calculated; $(E_{target})^{\Delta Ct,\ target\ (calibrator\ -\ test)}/(E_{ref})^{\Delta Ct,\ ref\ (calibrator\ -\ test)}$, where E is amplification efficiency and Ct is cycle threshold (Pfaffl, 2001). For each gene, the value of lowest sample in the sterile water (control treatment) was defined as the expression level, and results were expressed as fold increases of the mRNA over the control sample.

2.2.8.3 Proteomic profiling analysis

(1) Extraction of proteins and preparation of peptide samples

Flavedo tissues were ground to a fine powder under liquid nitrogen in a mortar and pestle, and then transferred to -20 ºC acetone. The homogenates were filtered through a filter paper (Whatman No.1) using vacuum suction pump and washed with 20 mL of cold acetone. The resulting acetone powder was air-dried at room temperature and kept in the refrigerator at -80 ºC. The proteins were extracted from the treated flavedo in acetone powder form using 0.5 % SDS. The protein precipitation was performed

according to a previous research (Peterson, 1977), then washed with cold acetone and re-dissolved in 0.5 % SDS. The proteins in each treatment and a low molecular weight protein standard marker (Amersham Biosciences, UK) were fractionated on 12.5 % SDS-PAGE (Atto, Tokyo, Japan). The gels were silver stained according to the method detailed in a previously published study (Blum et al., 1987) and were excised into 1 mm^3 pieces. In-gel digestion was performed to proteins in the gel plugs according to a previous study (Pisamai et al., 2018). The pooled peptides extracted were kept at -80 ^{o}C for mass spectrometric analysis.

Table 2.3 Gene-specific primer sequences of defense-related gene and reference genes.

Gene name	Accession No.	Primer	Sequence (5'→3')
Elongation Factor-1-alpha (*EF-1α*)	AY498567.1	-F	ACATGATTACCGGTGCCTCACA
		-R	ACACCAAGGGTGAAAGCAAGCA
Glucanase (*GLU*)	AJ000081.1	-F	ACCTCCGAAGAATCGCTTCCAA
		-R	TGTTTCTCATGGCGGGAACA
Chitinase (*CHI*)	Z70032.1	-F	AATGATGAACGATGCCCTGCCA
		-R	CCACTTGATGCTGTCTCCAA
Phenylalanine ammonia-lyase (*PAL*)	DQ088064.1	-F	TAGCCTCAAACAGAACCATAGAAG
		-R	GGGCCTAATGGAGAGATCATTG
Peroxidase (*POX*)	EF122403.1	-F	AGCCAGGAGACAATGAACAG
		-R	TAGTTTCATGGCCAGTTTGGGC
Lipoxygenase (*LOX*)	XM_006465842.3	-F	GTCGTTCTGGAACTTGTCGGCACT
		-R	CTGTGATTGCACCAGGCGTCCC
1-aminocyclopropane-1-carboxylate synthase 1(*ACS1*)	AJ871088.1	-F	TTCGAATCCACTAGGCACAACTT
		-R	CAACGCTCGTGAACTTAGGAGA
1-aminocyclopropane-1-carboxylate oxidase (*ACO*)	AJ871090.1	-F	AAGATGGCCAGTGGATTGATG
		-R	TCACCGAGGTTGACAACAATG
Pathogenesis-related protein 1 (*PR-1*)	XM_006486769.3	-F	AACTCGCCTCAAGACTACCT
		-R	TGCAACTGTGTCGTTCCATA

(2) LC-MS/MS analysis, quantitation, and identification

The peptide solutions were analyzed using an HCTultra PTM Discovery System (Bruker Daltonics Ltd., U.K.) coupled to an UltiMate 3000 LC System (Dionex Ltd., U.K on a nanocolumn (PepSwift monolithic column 100 µm i.d. x 50 mm). The running system for LC-MS/MS was conducted following the previous report (Pisamai et al., 2018). To perform protein quantitation, DeCyder MS Differential Analysis software (DeCyderMS, GE Healthcare) (Johansson et al., 2006; Thorsell et al., 2007) was used. The raw LC-MS data acquired were converted and the PepDetect module was used for automated peptide detection, charge state assignments, and quantitation based on the peptide ion signal intensities in MS mode. The analyzed MS/MS data from DeCyderMS were submitted to a database search using the Mascot software (Matrix Science, London, UK) (Perkins et al., 1999) against the NCBI database (Viridiplantae) for protein identification. Data normalization and quantification of the changes in protein abundance between the control and treated samples were performed and visualized using *Multi-Figure Experiment Viewer* (Mev) software version 4.6.1 (Howe et al., 2010) and the result was analyzed and presented in the form of the heatmap.

2.2.8.4 Statistical analysis

A statistical test of variance of differences (ANOVA) was performed for the data sets to identify statistically significant proteins ($P < 0.05$) and identical proteins were compared in Venn diagrams. Tukey's range test was used to establish the significant differences in mean values which were reported as the mean ± standard error (n = 3).

2.2.9 Transcriptional analysis and targeted proteomics derived from CLP-protein binding assay

2.2.9.1 Inoculation of mandarin fruit

(1) Gene expression and proteomic profiling analysis

This experiment was designed to study the transcriptional change in the desired genes under treatment with individual CLP in stress condition in mandarins, with and without the co-applying of *P. digitatum*. In the first treatment group, aliquots of 20 µL each of fengycin, iturin A, and surfactin solution were dropped onto the wound sites at the same concentration (1 g L^{-1}) (Table 2.4). In the second group the previous treatment was followed by fungal inoculation, with an aliquot of 20 µL of 10^7 spores L^{-1} of *P. digitatum* conidial suspension being added to the CLP-treated groups (Table 2.5). The treated fruit were incubated and collected as described in 2.2.8.1.

Table 2.4 Induction of defense responses in citrus fruit without *P. digitatum* infection by the individual *Bacillus* CLPs.

Treatment	Treatment agents (20 µL each)
T 1	sterile distilled water (control)
T 2	fengycin
T 3	iturin A
T 4	surfactin

Fengycin, itirin A, surfactin; 1 g L^{-1}

Table 2.5 Induction of defense responses in citrus fruit with *P. digitatum* infection by the individual *Bacillus* CLPs.

Treatment	Treatment agents (20 µL each)
T 1	sterile distilled water (control)
T 2	*P. digitatum*
T 3	fengycin + *P. digitatum*
T 4	iturin A+ *P. digitatum*
T 5	surfactin + *P. digitatum*

P. digitatum spore suspension; 10^8 spores L^{-1}, fengycin, itirin A, surfactin; 1 g L^{-1}

(2) CLP-protein binding assay

The experiment was conducted to investigate the associated flavedo proteins that bound to individual CLP in the saturated C18 pipette tip columns, derived from the various treatments, with and without fungal inoculation. Equal volumes of 20 µL of the conidial suspension of *P. digitatum* (10^7 spores L^{-1}) or sterile distilled water (control) were dropped onto wound sites of the fruit in each treatment group. These treatments were incubated as described in 2.2.8.1 for 48 h. The collection of treated flavedo tissues was conducted as described in 2.2.8.1.

2.2.9.2 Transcription analysis

The total RNA was extracted from the experiment described in 2.2.9.1. Transcription analysis including *ACO* gene was performed following 2.2.8.2.

2.2.9.3 Proteomic profiling analysis

The fine-powder samples in 2.2.9.1 were performed as describe in 2.2.8.3.

2.2.9.4 CLP–protein binding assay

This experiment was performed to investigate the binding interaction of the individual CLP with flavedo tissue protein extract obtained after pathogen infection. The interaction between CLP molecules and plant defensive proteins may offer a means of identifying the specific intermediates in host plants that may be involved in the priming process and signal transduction pathways leading to activation of the plant immunity system in responding to stress in mandarin fruit.

(1) CLP-saturated C18 preparation

The preparation of individual saturated CLP C18-pipette tip was carried out by employing C18 pipette tips (Ziptip® Pipette Tips, 10 µL spherical silica, 15 µm, 200 Å pore size, 31 mm, Merck, Germany) as the SPE columns. The activation of the C18 was performed three times by up-and down pipetting of 100 % ACN (10 µL) and 0.1 % TFA (10 µL). To ensure that the individual CLP was entirely bound to the C18 in a saturated manner, concentrations of 5, 6, and 7 µg CLP solution were primarily applied and eluted with unbound CLP solution and the left-over unbound CLP was monitored using a NanoDrop® spectrophotometer.

A binding experiment was conducted as shown in the flow chart (Fig. 2.2) by separating the individual saturated CLP C18-pipette tip into two sets; five replications in the first set were loaded with 5 µg of *P. digitatum*-treated protein extracts and the other with sterile distilled water-treated proteins in 2.2.9.1 and the extraction method was performed as described in 2.2.8.3, they were then subjected to up and down pipetting three times. The unbound proteins were removed from the individual saturated CLP C18-pipette tip by the same means with a micropipette, using ACN in a 0.1 % TFA solution with concentrations of 40 %, 25 %, and 65 % for the fengycin, iturin A, and surfactin saturated C18-pipette tip, respectively. Finally, 100 % ACN was applied in the individual saturated CLP C18-pipette tip to elute all the attached proteins for the collection of bound proteins.

To monitor binding ability of extracted proteins obtained from *P. digitatum* and sterile distilled water-treated flavedo with C18 molecules and to CLP in the C18-pipette tip those protein extracts were loaded into C18-pipette tips by pipetting up and down for three times. The unbound proteins were removed from the C18-pipette tip by the same means with a micropipette. The solution of 100 % ACN was applied in the C18-pipette tip to elute all the attached proteins which bound to C18 molecules in the pipette tip. The bound proteins which were found in both CLP C18-pipette tips and C18-pipette tips without CLP binding were subtracted to endorse the binding ability of extracted proteins to CLP molecules.

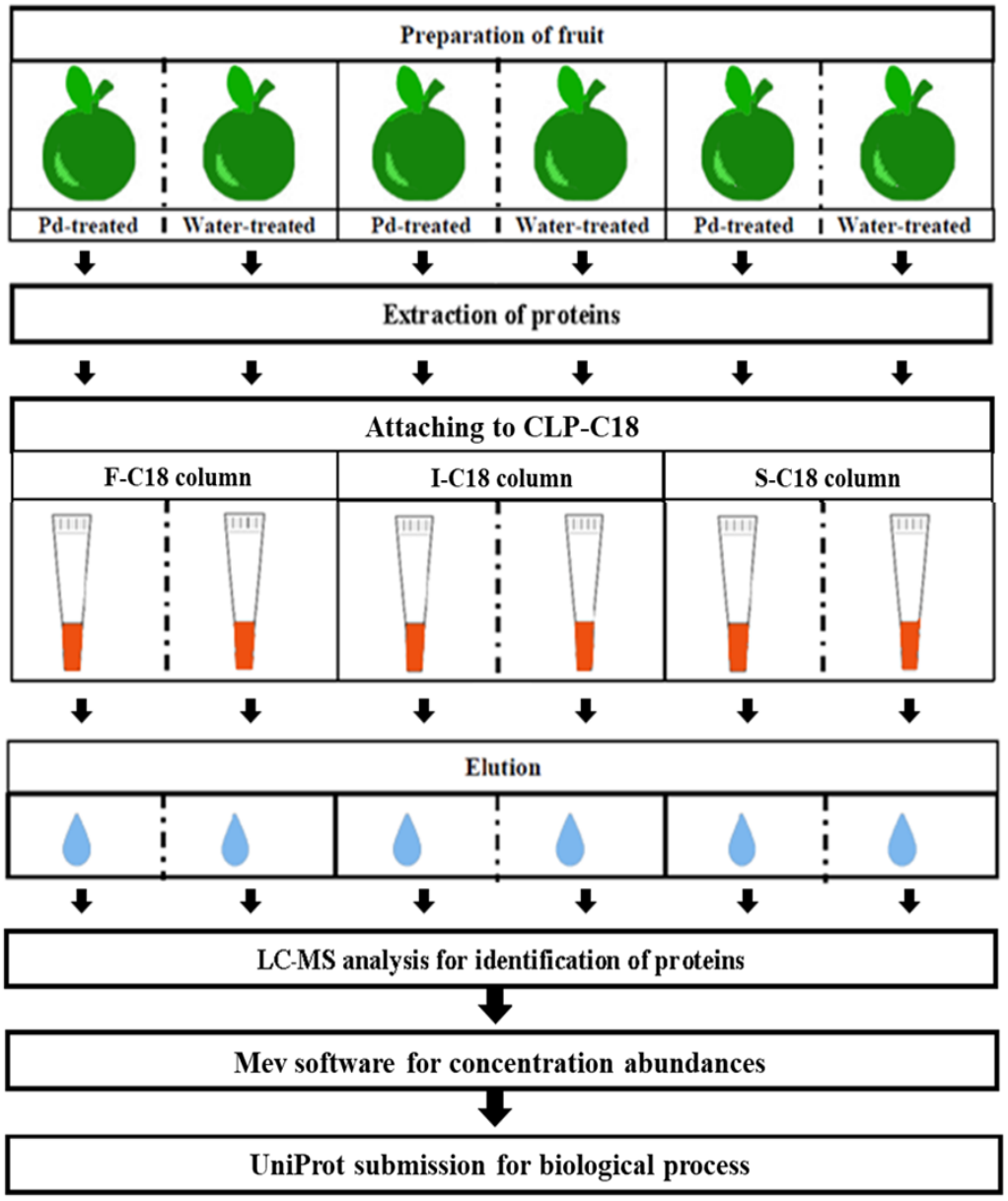

Fig. 2.2 An overview of the CLP-protein association workflow. (Pd: *Penicillium digitatum*, F: fengycin, I: iturin A, S: surfactin).

(2) In-solution digestion

The bound protein eluting solution derived from the same treatment was pooled, dried, and re-dissolved in 5 mM ammonium bicarbonate. Aliquots of 5 µL of 10 mM DTT in 10 mM ammonium bicarbonate and 20 µL of 100 mM IAA in 10 mM ammonium bicarbonate were added to the bound proteins. Then, a trypsin digestion process was carried out in 10 µL of 0.01 g L^{-1} trypsin solution (Promega, U.S.A.) which was incubated overnight prior to use for mass spectrometric analysis.

(3) LC-MS/MS analysis, quantitation, and identification

The bound proteins in each treatment were performed following the method described in 2.2.8.3 against NCBI database (Viridiplantae and Fungi). The proteins identified were displayed in Venn diagrams and were submitted to UniProt (https://www.uniprot.org/) for biological processing (Chen et al., 2017). The statistical analysis was performed as described in 2.2.8.4.

2.2.10 Metabolomic study of postharvest mandarin defense responses upon applications of *B. subtilis* CLPs in comparison to plant hormones, and *P. digitatum* infection

2.2.10.1 Inoculation of mandarin fruit

The mandarin oranges were divided into ten treatment groups. An aliquot of 20 µL at the same concentration as described in 2.2.8.1 and 2.2.9.1 without co-applied with fungal infection of sterile distilled water, *P. digitatum* conidial suspension, 80% ethanol SA, MeJA, Et, CLP extract, fengycin, iturin A and surfactin was dropped into wound sites (Table 2.6) and then incubated and collected as described in 2.2.8.1. The workflow of this experimental section was shown in Fig. 2.3.

2.2.10.2 Extraction of metabolites

The metabolites from the fine powder of treated flavedo tissues (15 mg) were extracted, based on a method previously reported (Asai et al., 2017), by dissolution in 1 mL of a mixture of methanol/water/chloroform (2.5:1:1 v/v/v), incubation at 40 ^{o}C for 5 min, and then centrifugation at 12,000 rpm for 10 min. The supernatant (950 µL) was transferred to a new tube and 400 µL of water was added. The mixture was centrifuged at 12,000 rpm for 10 min to obtain a polar phase solution. Each sample was transferred to a new tube and stored at -80 ^{o}C.

Table 2.6 Induction of stress responses in citrus fruit by the induction of *P. digitatum*, exogenous plant hormones, and *Bacillus* CLPs.

Treatment	Treatment agents (20 µL each)
T 1	sterile distilled water (control)
T 2	*P. digitatum*
T 3	ethanol
	(control for exogenous plant hormone and *Bacillus* CLPs treatments)
T 4	salicylic acid
T 5	methyl jasmonate
T 6	Ethephon
T 7	CLP extract
T 8	Fengycin
T 9	iturin A
T 10	Surfactin

P. digitatum spore suspension; 10^{8} spores L^{-1}, salicylic acid; 250 µmol L^{-1}, methyl jasmonate; 100 µmol L^{-1}, ethephon; 450 µL L^{-1}, *Bacillus* CLP extract; 10 g L^{-1}, fengycin, itirin A, surfactin; 1 g L^{-1}

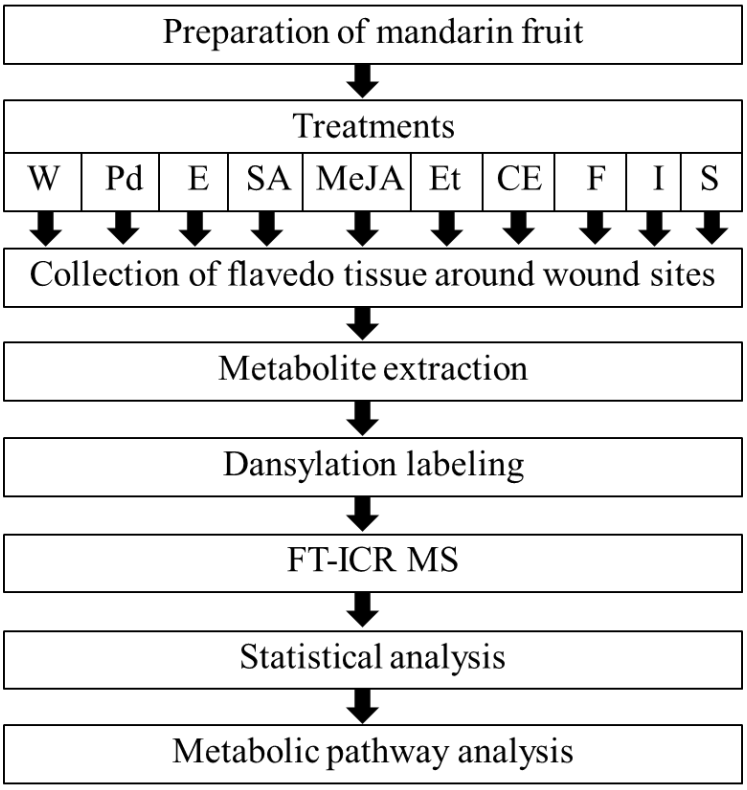

Fig. 2.3 Workflow of the metabolomic study.

2.2.10.3 Dansylation LC-MS metabolomic profiling assay

To prepare the samples for dansyl labeling, an individual sample was prepared from 25 µL of the polar phase solution in each replicate. A pooled sample was obtained by mixing small aliquots of all the samples. Methanol was evaporated by a SpeedVac concentrator and 25 µL of water was added just prior to labeling. An individual sample was labeled with ^{12}C-dansyl chloride and the pooled sample was labeled with ^{13}C-dansyl chloride following a reported method (Han et al., 2017). The labeled sample was injected into LC-UV for measuring the total concentration of labeled metabolites for sample amount normalization. For LC-UV, a Waters ACQUITY UPLC system with a photodiode array detector operating with a Phenomenex Kinetex C18 column (50 mm x 2.1 mm, 1.7 µm particle size, 100 Å pore size) was used. The total peak areas were detected under 338 nm for the quantification of each sample (Hooton et al., 2016). An equal mole amount of ^{12}C-labeled sample and ^{13}C-labeled pool was mixed. The mixture

was then injected to an HPLC system interfaced to an electrospray ionization (ESI) source in a Bruker 9.4 T Apex-Qe Fourier-transform ion cyclotron resonance (FT-ICR) mass spectrometer (Bruker, Billerica, MA). The ESI mass spectra were acquired in the positive ion mode. The setup of FTICR-MS was following a previous report: nitrogen nebulizer gas, 2.3 L min^{-1}; dry gas flow, 7.0 L min^{-1}; dry temperature, 195 ^{o}C; capillary voltage, 4200 V; spray shield, 3700 V; acquisition size, 256 k; mass scan range, *m*/z 200 - 1000; ion accumulation time, 1 s; TOF (AQS), 0.007 s; DC extract bias, 0.7 V (Peng et al., 2014). The HPLC flow rate used was 180 µL min^{-1} and the sample injection volume was 13 µL. The samples were randomly injected in no particular order. Quality control sample (^{12}C-/^{13}C-labeled pool) was injected every ten sample-runs.

2.2.10.4 Data processing

To analyze the ^{12}C-/^{13}C-peak pairs from each LC-MS run, the IsoMS, IsoMS-Align, Zero-fill and IsoMS-Quant programs were used. Metabolite identification was done by using the DnsID standards library for positive metabolite identification (Huan et al., 2015). A search for putative metabolite identification was performed using MyCompoundID MS software (Huan et al., 2015), against the Human Metabolome Database (HMDB) library and the Evidence-based Metabolome Library (EML) database following the methods described in previous reports (Han et al., 2017; Huan et al., 2015; Shen et al., 2016).

2.2.10.5 Statistical analysis

MetaboAnalyst 4.0 was used for principal components analysis (PCA) and pathway analysis of the LC-MS data (Chong et al., 2018). Microsoft Excel was used to calculate the fold change and *P*-value between groups. Venn diagram was built following in-house R program. Volcano plots (binary comparison) were performed using OriginPro 8.0 (OriginLab). The q-value, multiple-testing-corrected p-value, was calculated using R and BioConductor (www.bioconductor.org).

CHAPTER 3

RESULTS

3.1 Identification of *B. subtilis* ABS-S14 CLPs

3.1.1 Separation of *B. subtilis* ABS-S14 CLPs by TLC

The *B. subtilis* ABS-S14 CLP extract 2.299 g was obtained from the shaken bacterial culture 29 L in LB medium with 7.92 % yield. TLC analysis was performed to determine the existence of fengycin, iturin A, and surfactin in CLP extract as they were shown in TLC plate with three spots. The relative retardation factor (R_f) of the first, second, and third spot was 0.28, 0.1, and 0.6, respectively. The first, second, and third spots had the corresponded R_f values to fengycin (SMB00292, Sigma-Aldrich, USA), iturin A (I1774, Sigma-Aldrich, USA), and surfactin (S3523, Sigma-Aldrich, USA), respectively (Fig. 3.1).

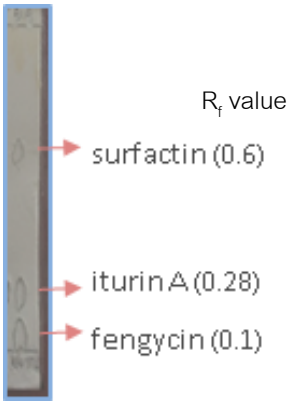

Fig. 3.1 TLC pattern of *B. subtilis* ABS-S14 CLP extract.

3.1.2 Separation of *B. subtilis* ABS-S14 CLPs by PTLC and SPE

The solution of 1 mL-CLP extract (50 g L^{-1}) was each loaded to each PTLC plate for six plates. After running system with the mobile phase (chloroform-methanol-water; 65:25:4), the silica gel on each PTLC plate was divided into 25 horizontal lines according to the R_f value of commercial standards of fengycin, iturin A, and surfactin

(Sigma-Aldrich, USA) as shown in Fig. 3.2. The number of the same lines in each PTLC plate was collected and pooled together and, then labeled as 1 to 25 fractions. The three main families of CLPs were divided into three bands on PTLC plate. The first band covered the fractions from line no. 3 to 5 (R_f = 0.1). The second band covered the fractions from line no. 8 to 10 (R_f = 0.26). The third band covered the fractions from line no. 15 to 17 (R_f = 0.6). Each fraction in the same band was pooled together. The values of % yield of fraction no. 3, 4, 5, 8, 9, 10, 15, 16 and 17 were 5.19, 5.17, 5.34, 2.82, 1.65, 1.18, 2.31, 5.64 and 3.39, respectively. To increase the purity of fengycin, iturin A, and surfactin, the solution of pooled sample from each band number was loaded into C18 SPE cartridge. The step gradients of ACN in 0.1% TFA concentrations were used as a mobile phase. The fractions of ACN in 0.1% TFA at 40% to 55%, 25% to 35% and 60% to 80% were collected from C18 SPE cartridge and were pooled together for gathering of fengycin, iturin A and surfactin, respectively, prior to identification by mass spectrometric approaches.

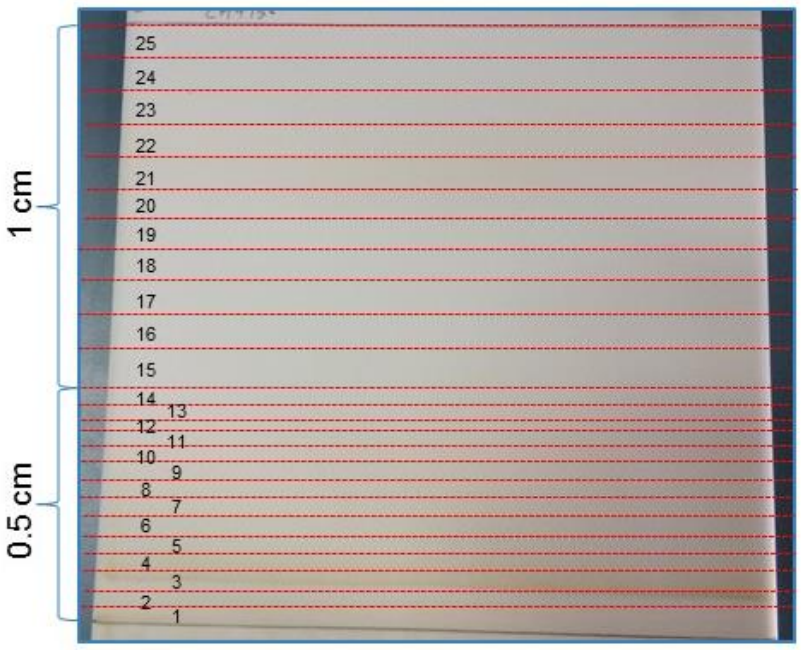

Fig. 3.2 Purification of *B. subtilis* ABS-S14 CLPs by PTLC. The lines on PTLC plate were divided into 25 horizontal lines. The width of band space no. 1-14 and 15-25 were 0.5 and 1 cm, respectively. The solvent front was line no. 25.

3.1.3 HPLC analysis

The eluting fractions of three bands obtained from C18 SPE cartridge and CLP extract were injected to reverse phase (RP)-HPLC system for CLP identification as shown in Fig. 3.3. The eluting fractions obtained from the C18 SPE cartridge at intervals of 19-32, 5-18, and 41-57 min retention time (RT) of RP-HPLC chromatograms are fengycin, iturin A and surfactin, respectively based on their corresponding retention times comparing with the commercial standards of fengycin, iturin A, and surfactin (Sigma-Aldrich, USA).

3.1.4 MALDI-TOF MS analysis

The eluting fractions of three bands obtained from C18 SPE cartridge and CLP extract were analyzed by MALDI-TOF MS for CLP identification as shown in Fig. 3.4-3.6. The MALDI-TOF MS spectra displayed three intervals of m/z values in the ranges of 1,449.74-1,547.82 (fengycin), 1,058.61-1,110.60 (iturin A) and 1,044.61-1,074.62 (surfactin) with % yields of 11.03, 14.45, and 5.94, respectively based on the comparing ranges of corresponding peak areas with the commercial standards of fengycin, iturin A, and surfactin (Sigma-Aldrich, USA). The purity of fengycin, iturin A, and surfactin were 93.79, 96.78, and 96.5 %, respectively.

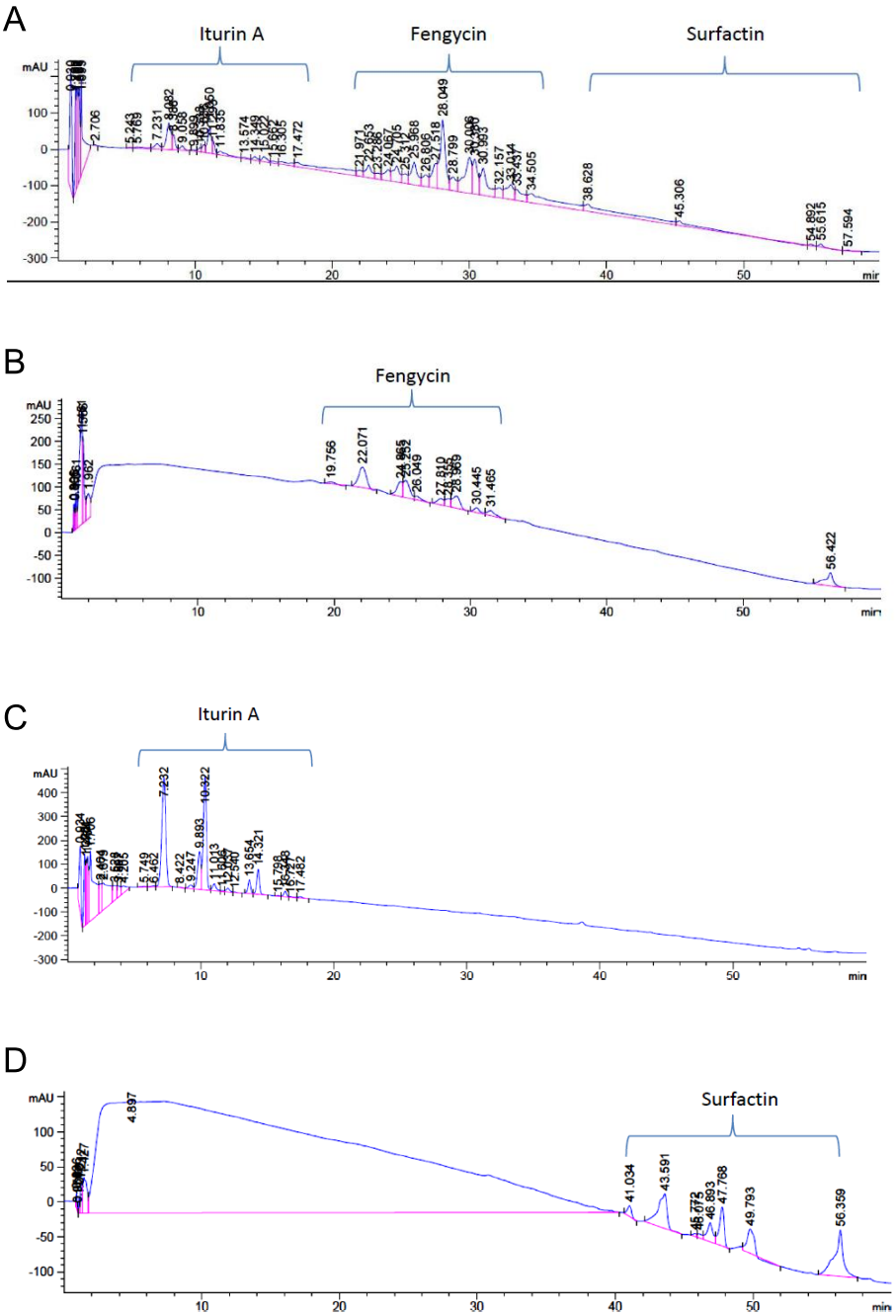

Fig. 3.3 RP-HPLC chromatogram of *B. subtilis* ABS-S14 CLPs. (A) CLP extract, (B) PTLC fraction no. 3-5, (C) PTLC fraction no. 8-10, and (D) PTLC fraction no. 15-17 obtained from *B. subtilis* ABS-S14.

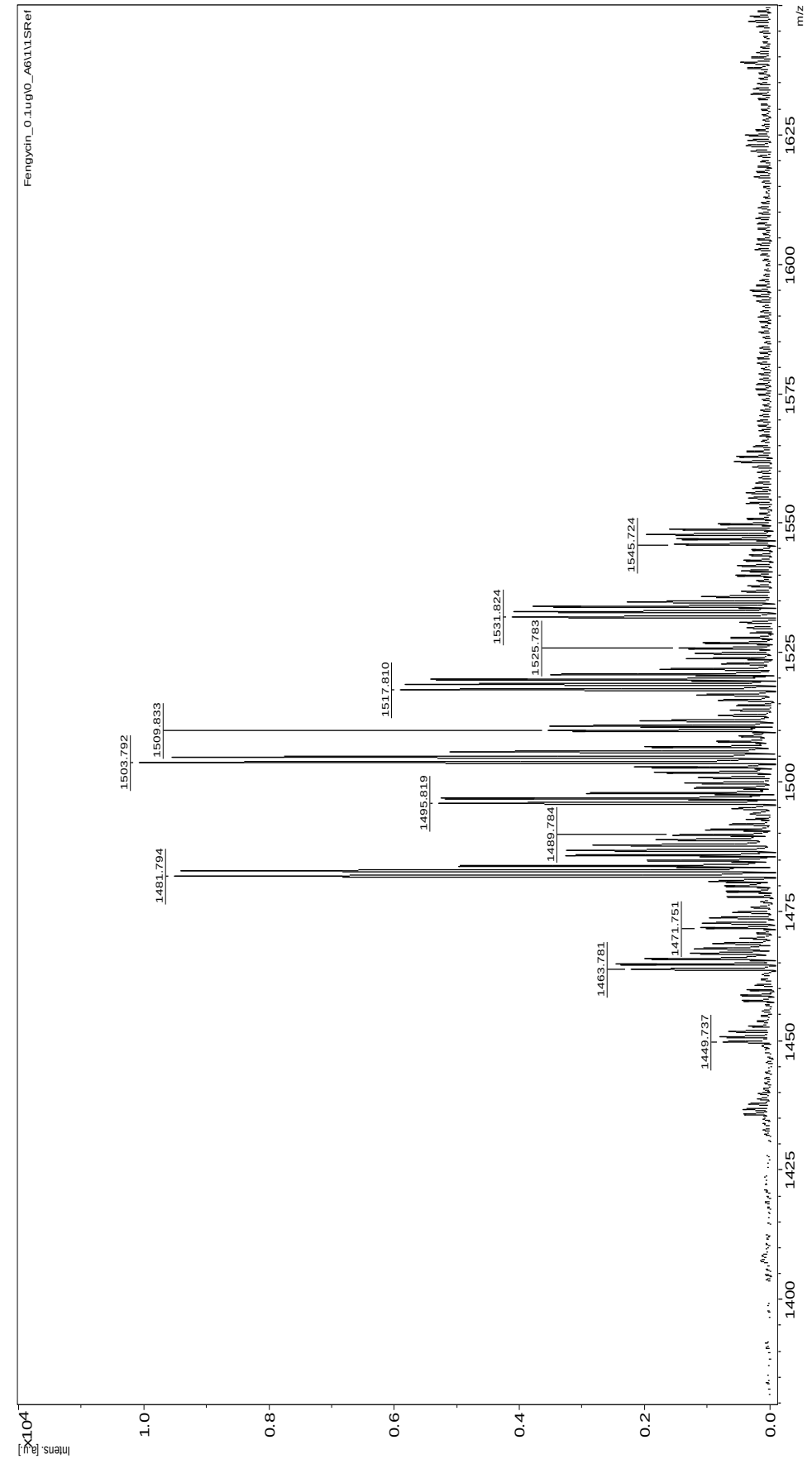

Fig. 3.4 MALDI-TOF MS chromatogram of *B. subtilis* ABS-S14 fengycin.

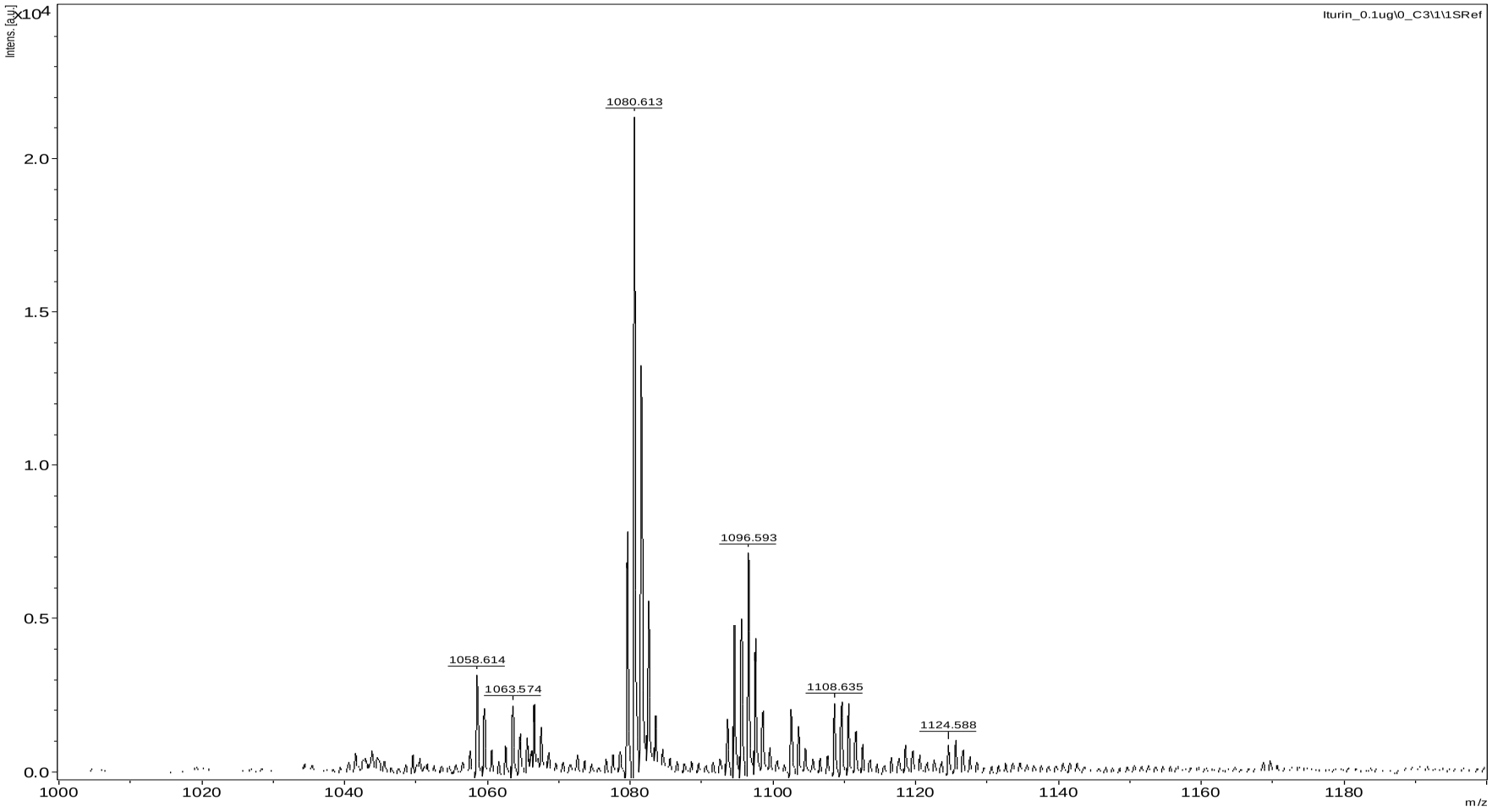

Fig. 3.5 MALDI-TOF MS chromatogram of *B. subtilis* ABS-S14 iturin A.

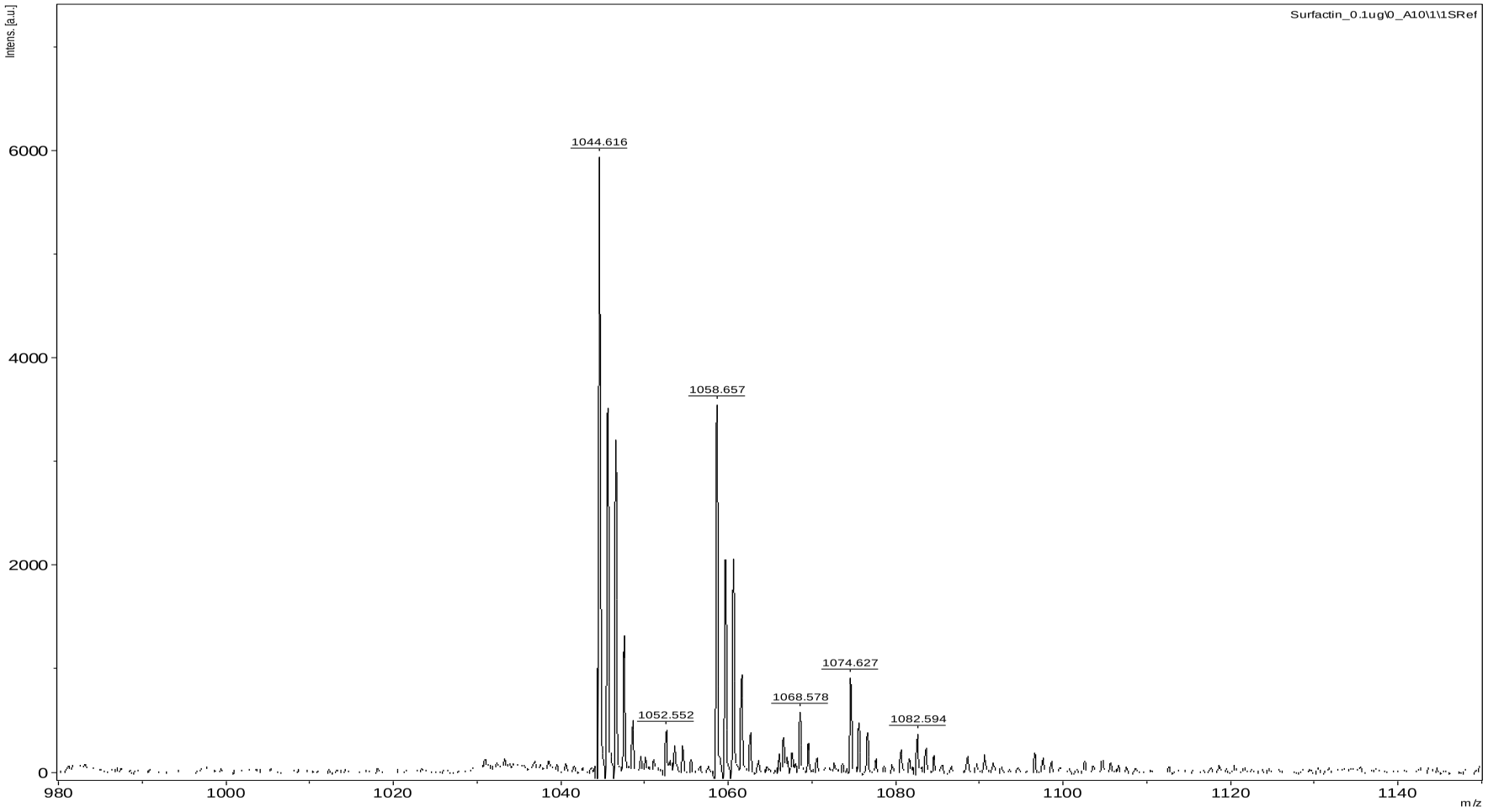

Fig. 3.5 MALDI-TOF MS chromatogram of *B. subtilis* ABS-S14 surfactin.

3.2 Inhibitory effect of *B. subtilis* CLPs against *P. digitatum* mycelial growth *in vitro*

3.2.1 Inhibitory effect of *B. subtilis* endospores and cell-free supernatant on mycelial growth of *P. digitatum*

Dual culture assay was performed to investigate the ability of *B. subtilis* endospores to inhibit the green mold growth. After 48 h incubation at 25 °C, the growth of fungal mycelium was observed. The diameter of *P. digitatum* mycelium on PDA medium which contains the *B. subtilis* endospores and the control group were 0.7 and 1.25 cm, respectively (Fig. 3.7A and B). The percent inhibition of *B. subtilis* endospores was 68.64.

Agar well diffusion assay was performed to investigate the ability of *B. subtilis* cell-free culture supernatant to inhibit the green mold. After 48 h incubating at 25 °C, the growth of fungal mycelium was observed. The diameter of *P. digitatum* mycelium on PDA medium amended with the *B. subtilis* cell-free culture supernatant and the control group were 0.58 and 0.95 cm, respectively (Fig. 3.7C and D). The percent inhibition of *B. subtilis* sterilized cell-free culture supernatant was 63.37.

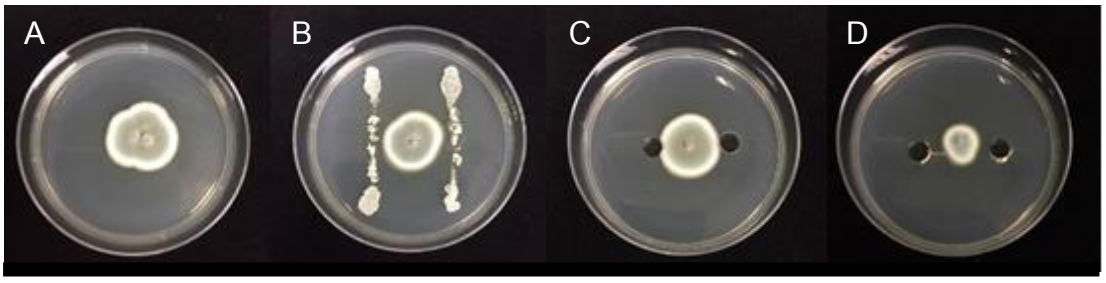

Fig. 3.7 Inhibitory effect of *B. subtilis* endospores and cell-free supernatant on *P. digitatum* mycelial growth after 4-day incubation at 25 °C on PDA plate. (A) control of dual culture assay. (B) *B. subtilis* endospores of dual culture assay. (C) control of agar well diffusion assay. (D) *B. subtilis* cell-free supernatant of agar well diffusion assay.

3.2.2 Inhibitory effect of CLP extract on *P. digitatum* mycelial growth

EC_{50} assay was performed to investigate the ability of CLP extract of *B. subtilis* to inhibit the green mold growth. After 48 h of incubation at 25 °C, the radial extension of the mycelium was measured by ocular micrometer under a stereo-microscope. The percentage of inhibition of CLP extract at the concentration of 1, 0.5, 0.25, 0.125, 0.0625, 0.0313, 0.0156, and 0 mg mL^{-1} were 100, 72.68, 63.53, 58.67, 45.20, 32.56, 27.64, and 0, respectively (Fig. 3.8). The percentage of mycelial growth inhibition using the linear regression equation with the Microsoft Excel 365 or EC_{50} value was 75.38 µg $µL^{-1}$.

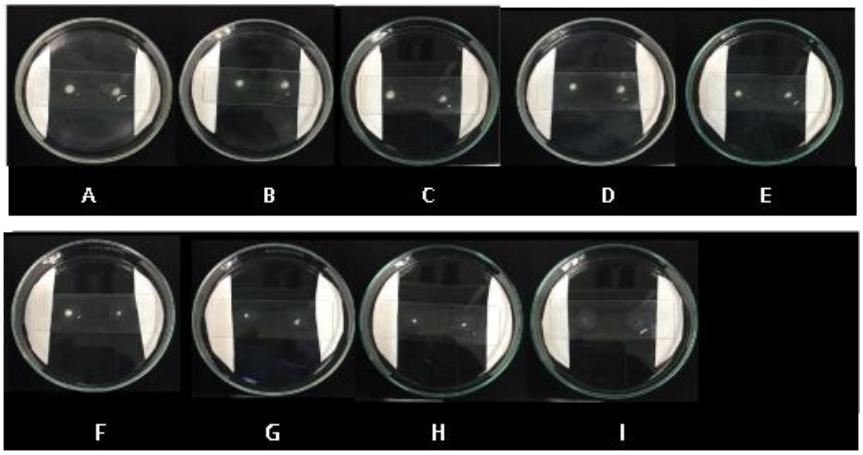

Fig. 3.8 Inhibitory effect of CLP extract on *P. digitatum* mycelial growth. (A) control (H_2O). (B) 80% ethanol. (C-I) CLPs at concentration of 0.0156, 0.0313, 0.0625, 0.125, 0.25, 0.50, and 1 µg $µL^{-1}$, respectively.

3.3 Transcription and proteome analysis of defense-related genes in mandarins triggered by *B. subtilis* CLP extract and exogenous plant hormones upon *P. digitatum* infection

3.3.1 Expression of plant genes involving in SA, JA, and ET signal transduction pathways

To determine the ability of the *B. subtilis* CLP extract to activate plant defensive proteins, determination of the transcript abundance of *PAL*, *LOX*, and *ACS1* genes (the key genes known to be involved in SA, JA, and ET signaling pathways, respectively) was carried out. The patterns of change in the transcript abundances of the three genes in the flavedo tissues elicited by the *Bacillus* CLP extract compared with exogenous plant hormones, with and without pathogen attack are shown in Fig. 3.9 The greatest amount of *PAL* transcripts induced by the CLP extract was detected at 24 h post-treatment in both the with and without infection conditions (Fig. 3.9A and B), but without infection it had decreased by half at 48 h. Interestingly, a remarkable 5 fold *PAL* transcript change during infection was found for both the SA and CLP extract treatments as early as 24 h and there was a further small increase up to 48 h (5.5 fold) although only in the CLP extract-treated tissues when co-applied with fungal infection. However, a rapid decline was later noted in all treatments (Fig. 3.9B). In contrast, the CLP extract had a minor effect on *LOX* gene expression compared to exogenous plant hormones at 24 h without fungal infection (Fig. 3.9C). In particular, at 48 h post-treatment, the level of *LOX* transcripts in the flavedo tissues with CLP extract was half of those induced by exogenous plant hormones, which reached the highest level. Fig. 3.9D shows that the *LOX* gene expression reached the highest level (3.5 fold) with the difference being significant ($P \leq 0.05$) in the treatment with Et co-applied with the pathogen, and the pathogen itself was highly increased at 24 h then declined by half at both 48 and 72 h post-treatment. Induction of *ACS1* expression was consistently highest in the presence of CLP extract at all-time points without *P. digitatum* (Fig. 3.9E). However, the *ACS1* expression elicited by all the exogenous plant hormones was higher than that elicited by the CLP extract except at 72 h with pathogen infection (Fig. 3.9F).

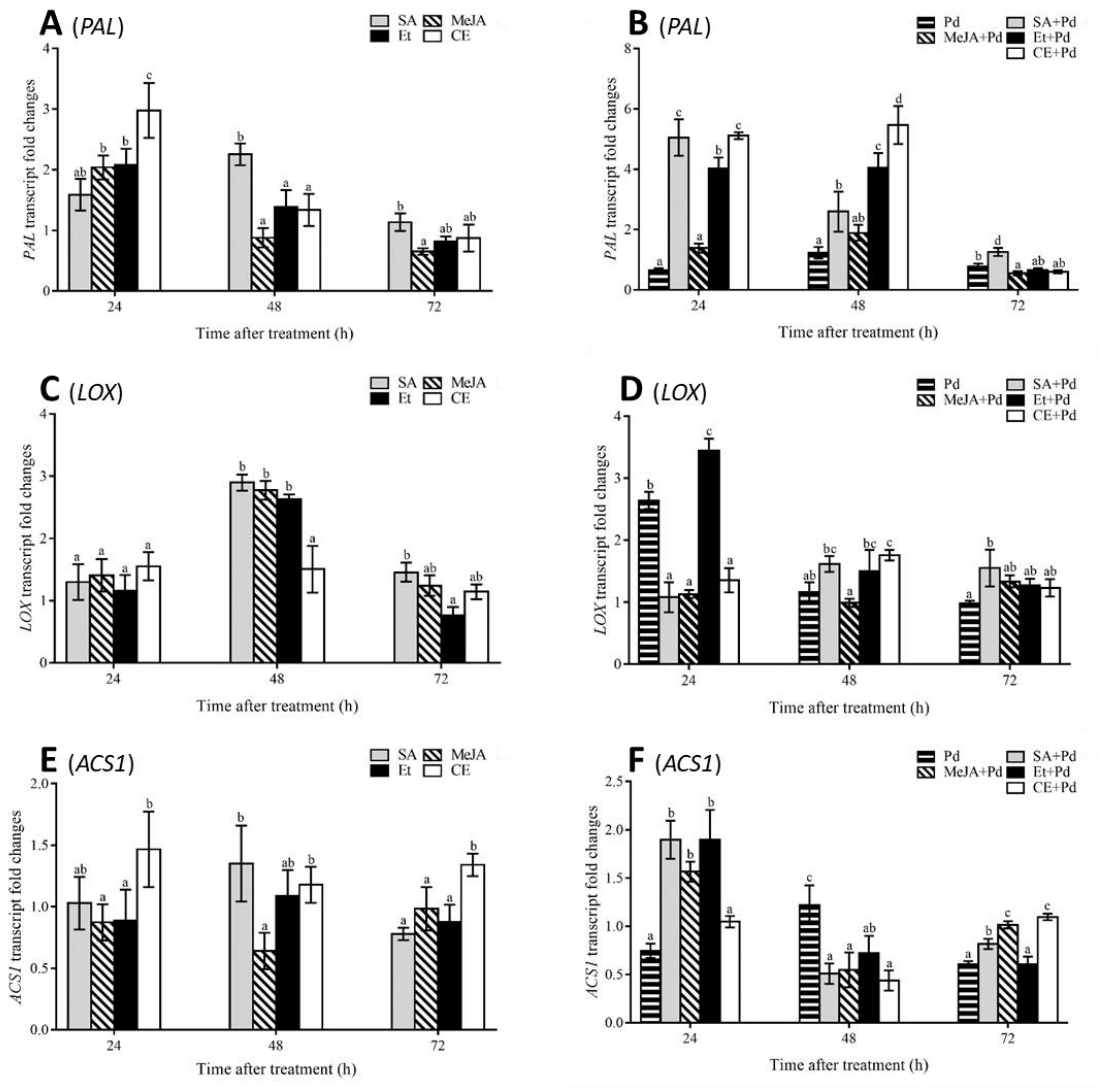

Fig. 3.9 Transcriptional fold changes of key genes in plant hormone signaling pathway in mandarin fruit by activation of exogenous plant hormones and CLP extract with and without fungal infection. Salicylic acid (SA), methyl jasmonate (MeJA), ethephon (Et), CLP extract (CE), *P. digitatum* (Pd) and *P. digitatum* co-applied with salicylic acid (SA+Pd), methyl jasmonate (MeJA+Pd), ethephon (Et+Pd), and CLP extract (CE+Pd). The treatments with non-fungal infection (A), (C), and (E), and with fungal infection (B), (D), and (F). Transcript abundances of *PAL* (A), (B), *LOX* (C), (D), and *ACS1* (E), (F). Vertical bars represent standard errors of the mean value of three trials; columns with the same letter above them show no significant difference to each other at $P \leq 0.05$ according to Tukey's range test.

3.3.2 Expression of plant defensive genes relating to PR proteins

The differential expression of the plant defensive genes; *CHI*, *GLU*, *POD*, and *PR1* induced by exogenous plant hormones and CLP extract was investigated both with and without pathogen infection. The accumulation of *CHI* transcripts in the CLP extract treatment without fungal infection was significantly lower than that of the exogenous plant hormones at all-time points except at 72 h post-treatment ($P \leq 0.05$) (Fig. 3.10A). On the other hand, the most elevated level of *CHI* transcripts in the CLP extract co-applied with infection treatment was only seen at 72 h, but was not as strong as that induced by MeJA co-applied with *P. digitatum* at 48 h post-infection as shown in Fig. 3.10B.

Differences in changes of *GLU* expression in the flavedo tissues treated with various exogenous plant hormones and CLP extract with and without fungal infection were investigated. The flavedo tissues treated with SA and CLP extract presented an equal level of change in abundance in the *GLU* transcript-induction effects at 24 and 48 h post-treatment without fungal attack, but the level was then reduced at 72 h (Fig. 3.10C). Interestingly, during fungal attack the *GLU* gene was fully expressed in all treatments, especially in those with CLP extract-treated tissues (8 fold) at 48 h with a sudden decline at 72 h (Fig. 3.10D). Obviously, the change in the level of *GLU* transcription in the non-fungal infected tissues was much less than those found in the fungal-infected treatments.

Similar patterns of changes in the *POD* transcription level in all the non-pathogen treated flavedo tissues was demonstrated at all-time points except in the treatments with SA, and MeJA at 72 h (Fig. 3.10E). Upon pathogen infection at 48 h post-treatment a distinctly high increase in the abundance of *POD* transcripts (5.7 fold) was found in the tissues treated with CLP extract and these higher abundances were also found in the exogenous plant hormone treatments with the exception of the MeJA treatment and pathogen infection (Fig. 3.10F).

The strongest induction of *PR1* gene expression in fruit tissues by SA among the treated elicitors was noted at 48 h post-treatment in non-fungal infected treatments (Fig. 3.10G). On the other hand, Et co-applied with the pathogen showed the

highest change (7 fold) in gene induction of *PR1* as early as 24 h. During green mold attack, the CLP extract treatment showed lower activation of *PR1* transcripts than those were found in the exogenous plant hormone treatments at 24 and 48 h, but later, at 72 h post-treatment it presented the 7 fold change in *PR1* transcript abundance (Fig. 3.10H). It was noticeable that the transcription level of *PR1* in the presence of fungal infection was more highly triggered by the elicitors tested than in the non-fungal infection treatments.

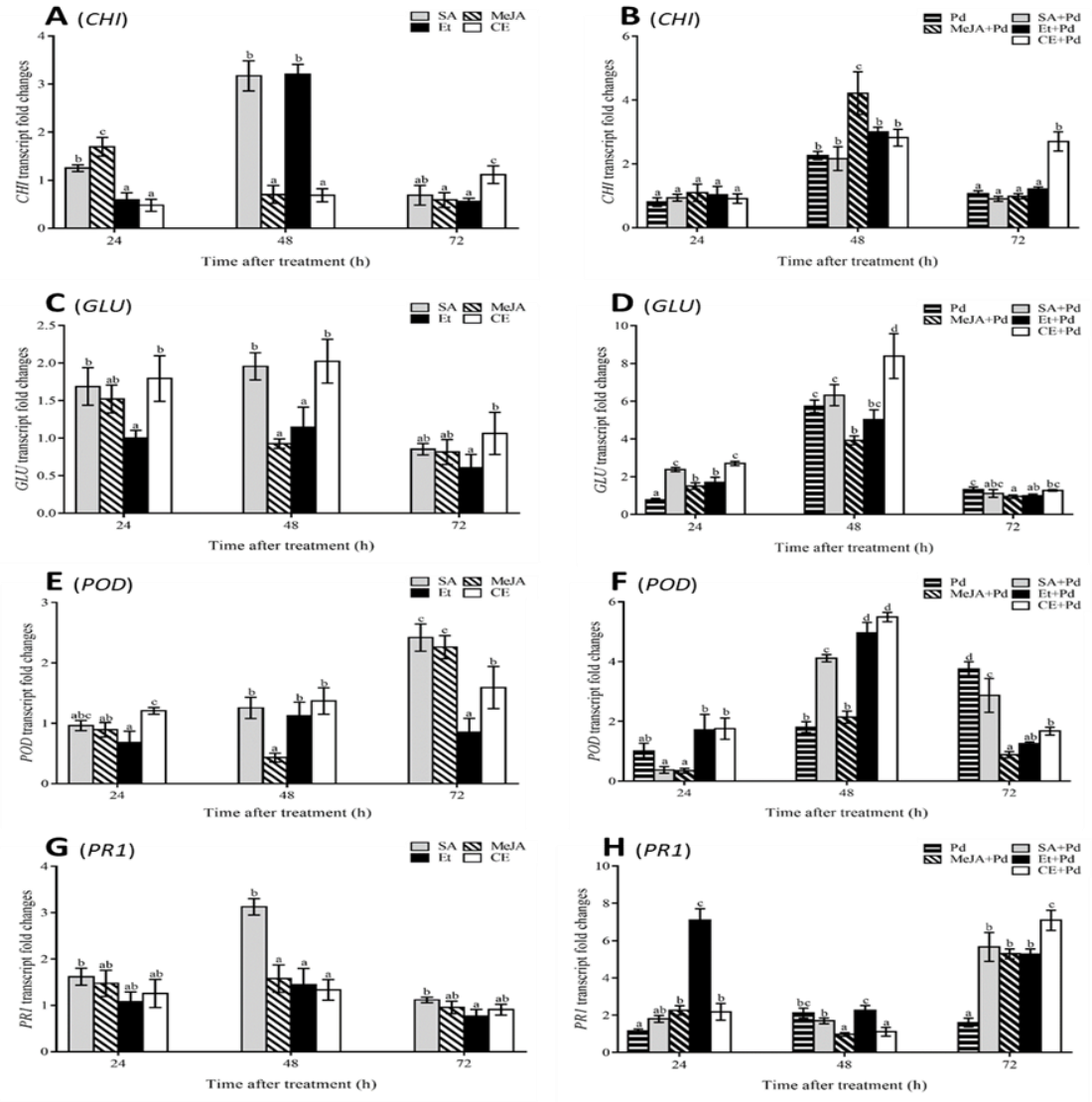

Fig. 3.10 Transcriptional fold changes of plant defensive genes relating to PR proteins by activation of exogenous plant hormones and CLP extract with and without fungal infection. Salicylic acid (SA), methyl jasmonate (MeJA), ethephon (Et), CLP extract (CE), *P. digitatum* (Pd) and *P. digitatum* co-applied with salicylic acid (SA+Pd), methyl jasmonate (MeJA+Pd), ethephon (Et+Pd), and CLP extract (CE+Pd). The treatments with non-fungal infection (A), (C), (E), and (G), and with fungal infection (B), (D), (F), and (H). Transcript abundances of CHI (A), (B), GLU (C), (D), POD (E), (F), and PR1 (G), (H). Vertical bars represent standard errors of the mean value of three trials; columns with the same letter above them show no significant difference to each other at $P \leq 0.05$ according to Tukey's range test.

3.3.3 Distribution of expressed plant proteins attributed by exogenous plant hormones and *B. subtilis* CLP extract

To assess the elicitation ability of CLP extract in comparison to exogenous plant hormones on affecting protein production of the mandarin flavedo tissues, abundance of protein levels in the flavedo tissues treated with CLP extract exogenous plant hormones and sterile distilled water was used as a control. They were determined under wound stress (without fungal invasion), and pathogen infection (Fig. 3.11). Fig. 3.11A shows 3,092 common proteins in all treatments during wound stress while there were 1,628 common proteins which were detected in all elicitor treatments during fungal invasion (Fig. 3.11B). Interestingly, only CLP extract treatment exhibited three and one unique proteins responding to wound stress (Fig. 3.11A) and fungal attack (Fig. 3.11B), respectively. Three unique proteins that were determined to present in the CLP extract treatment (Table 3.1) were calmodulin-binding receptor-like cytoplasmic kinase 2 (CRCK2), molybdenum cofactor (MoCo) sulfurase, and NAD+-dependent glyceraldehyde-3-phosphate dehydrogenase. Noticeably, none of these proteins were detected among the exogenous plant hormone treatments. However, there were 8, 9 and 21 common proteins found in the CLP extract vs SA, CLP extract vs MeJA, and CLP extract vs Et treatments, respectively (Fig. 3.11A). These proteins were identified and characterized as shown in Table 3.1 and the quantified proteins are displayed as a heatmap in Fig. 3.12.

Upon treatment with various exogenous plant hormones or CLP extract coupled with *P. digitatum* inoculation (Table 3.2), significant up-regulated levels of some important relevant plant derived proteins were revealed. Ubiquitin carrier protein (Ubc) was significantly presented only in the co-treatment CLP extract with *P. digitatum.* Ribosome biogenesis protein bop1 was found in both the CLP extract and SA co-treatments with *P. digitatum*. There were four and five proteins (Fig 3.11B) found in common in the CLP extract and MeJA, and CLP extract and Et treatments, respectively. However, none of the relevant proteins were detected in common in the fungal co-

treatment CLP extract and *P. digitatum* treatment. The relative amount of these proteins in all the treatments during fungal invasion is shown as a heatmap in Fig. 3.13.

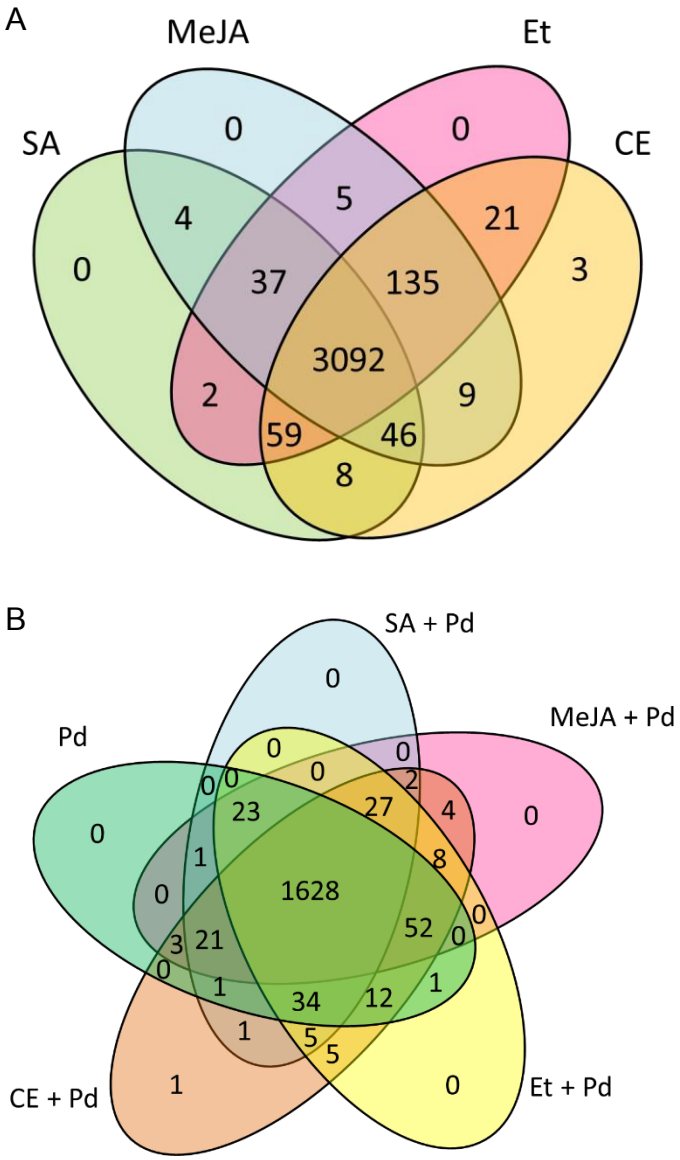

Fig. 3.11 Venn diagram showing the total estimated number of proteins distributed by activation of exogenous plant hormones and CLP extract with and without fungal infection. (A) Effect of salicylic acid (SA), methyl jasmonate (MeJA), ethephon (Et), and CLP extract (CE) in non-fungal infection treatments. (B) Treatments with fungal infection by activation of *P. digitatum* (Pd) including *P. digitatum* co-applied with salicylic acid (SA+Pd), methyl jasmonate (MeJA+Pd), ethephon (Et+Pd), and CLP extract (CE+Pd).

Table 3.1 List of significantly expressed proteins in CLP extract and exogenous plant hormone treatments responding to wound stress.

No.	Protein name	Peptides	Accession No.*	MW (Da)	Elicitors			
					SA	MeJA	Et	CE
1	calmodulin-binding receptor-like cytoplasmic kinase 2	SQMSA	XP_007218022.1	520.32	×	×	×	✓
2	MoCo sulfurase	KNPEXILEISPFSK	ADH82120.1	1617.28	×	×	×	✓
3	NAD+-dependent glyceraldehyde-3-phosphate dehydrogenase	AAVKSA	BAM42682.1	544.22	×	×	×	✓
4	anthocyanin 3'-O-beta-glucosyltransferase-like	AVANGSTK	XP_010687761.1	749.76	✓	×	×	✓
5	gamma tubulin interacting protein	TPGGSR	XP_002953495.1	574.18	✓	×	×	✓
6	inhibitor of trypsin and hageman factor	SSCPGK	P19873.1	639.32	✓	×	×	✓
7	peptide transporter 1	MGIGLFIAILSMAAAALX	ABI97907.1	1824.19	✓	×	×	✓
8	ribosome biogenesis protein slx9-like	GKAESMDF	XP_013701715.1	886.94	✓	×	×	✓
9	trans-2-enoyl-CoA reductase	QLLVGG	EMS47082.1	587.18	✓	×	×	✓
10	tricalbin-3-like	LGDDISIAGSKXSK	XP_008389096.1	1428.41	✓	×	×	✓
11	U-box domain-containing protein 6	ECSSYGSK	XP_010108836.1	920.06	✓	×	×	✓

*Reference: The accession numbers can be obtained from NCBI database. (MW, molecular weight; SA, salicylic acid; MeJA, methyl jasmonate; Et, ethephon; CE, CLP extract).

Table 3.1 List of significantly expressed proteins in CLP extract and exogenous plant hormone treatments responding to wound stress. (Continued)

No.	Protein name	Peptides	Accession No.*	MW (Da)	Elicitors			
					SA	MeJA	Et	CE
12	agmatine coumaroyltransferase	TMTMAR	BAF97628.1	727.02	×	✓	×	✓
13	arabinosyltransferase-like protein	KVPAMK	XP_002978459.1	689.42	×	✓	×	✓
14	arogenate dehydrogenase 1	VRIGEDELR	XP_010435393.1	1085.75	×	✓	×	✓
15	auxin-responsive protein IAA16-like	KMATMHGEER	XP_002281771.1	1225.36	×	✓	×	✓
16	cytochrome P450 709B2	ARAVAR	XP_015633710.1	642.32	×	✓	×	✓
17	mucin-2	SMCIFGLKVILIPYR	XP_003562533.1	1809.95	×	✓	×	✓
18	nudix hydrolase 15	DTTMN	XP_009592215.1	581.31	×	✓	×	✓
19	protein phosphatase 2C 69	GFPSDVAANR	XP_004957026.1	1032.87	×	✓	×	✓
20	ras-related small GTP-binding family protein	RCNSAVTAAVPNR	NP_680628.1	1414.67	×	✓	×	✓
21	60S ribosomal protein L5	GHGMSNXFVR	XP_009625853.1	1151.43	×	×	✓	✓
22	auxin response factor 9	TDNHSN	BAD94156.1	687.74	×	×	✓	✓

*Reference: The accession numbers can be obtained from NCBI database. (MW, molecular weight; SA, salicylic acid; MeJA, methyl jasmonate; Et, ethephon; CE, CLP extract).

Table 3.1 List of significantly expressed proteins in CLP extract and exogenous plant hormone treatments responding to wound stress. (Continued)

No.	Protein name	Peptides	Accession No.*	MW (Da)	Elicitors			
					SA	MeJA	Et	CE
23	cellulose synthase A catalytic subunit 8 [UDP-forming]-like	LGPYRSVIIMR	XP_004485917.1	1321.83	×	×	✓	✓
24	copia protein	NPDAM	KYP51976.1	547.41	×	×	✓	✓
25	DEAD-box ATP-dependent RNA helicase 2-like	IAGGESLFVTAR	XP_018475968.1	1221.85	×	×	✓	✓
26	dicer-like protein 4	LIGILSTFR	XP_002264486.2	1019.00	×	×	✓	✓
27	DNA ligase 1-like	SRVIPTPK	XP_009118391.1	897.02	×	×	✓	✓
28	G patch domain protein	NADVLGHK	NP_001332260.1	851.42	×	×	✓	✓
29	LAGLIDADG homing endonuclease	QSIQKNDL	ALA63887.1	944.11	×	×	✓	✓
30	mitochondrial pyruvate carrier 1-like	SVRAYLNSPMGPK	NP_001316070.1	1436.12	×	×	✓	✓
31	multicopper oxidase LPR1-like	MASELLLLAR	XP_010258781.1	1133.06	×	×	✓	✓
32	myb-related protein 3R-1-like	EDSPSPSSDQK	XP_009367916.1	1180.83	×	×	✓	✓
33	non-LTR retroelement reverse transcriptase	LAETSLAM	ABD91510.1	852.40	×	×	✓	✓

*Reference: The accession numbers can be obtained from NCBI database. (MW, molecular weight; SA, salicylic acid; MeJA, methyl jasmonate; Et, ethephon; CE, CLP extract).

Table 3.1 List of significantly expressed proteins in CLP extract and exogenous plant hormone treatments responding to wound stress. (Continued)

No.	Protein name	Peptides	Accession No.*	MW (Da)	Elicitors			
					SA	MeJA	Et	CE
34	pathogenesis-related genes transcriptional activator	TIMEMYK	XP_002946570.1	930.49	×	×	✓	✓
35	peptidoglycan-binding LysM domain-containing protein	NKTAVD	KZV57878.1	647.42	×	×	✓	✓
36	ribosome-recycling factor-like	SADDMCK	XP_003580029.1	842.58	×	×	✓	✓
37	root cap family protein	DTCKCK	GAQ81227.1	807.87	×	×	✓	✓
38	SPOC domain / Transcription elongation factor S-II protein	QHVPPPQR	NP_196704.2	959.67	×	×	✓	✓
39	tip elongation aberrant protein 1	YDARLDQSVGSMSLK	XP_013638867.1	1685.31	×	×	✓	✓
40	WRKY transcription factor 118	LPSQATT	AGV75978.1	716.41	×	×	✓	✓
41	zinc finger CCCH domain-containing protein 13	LGDQLSSETLK	XP_008801339.1	1189.13	×	×	✓	✓

*Reference: The accession numbers can be obtained from NCBI database. (MW, molecular weight; SA, salicylic acid; MeJA, methyl jasmonate; Et, ethephon; CE, CLP extract).

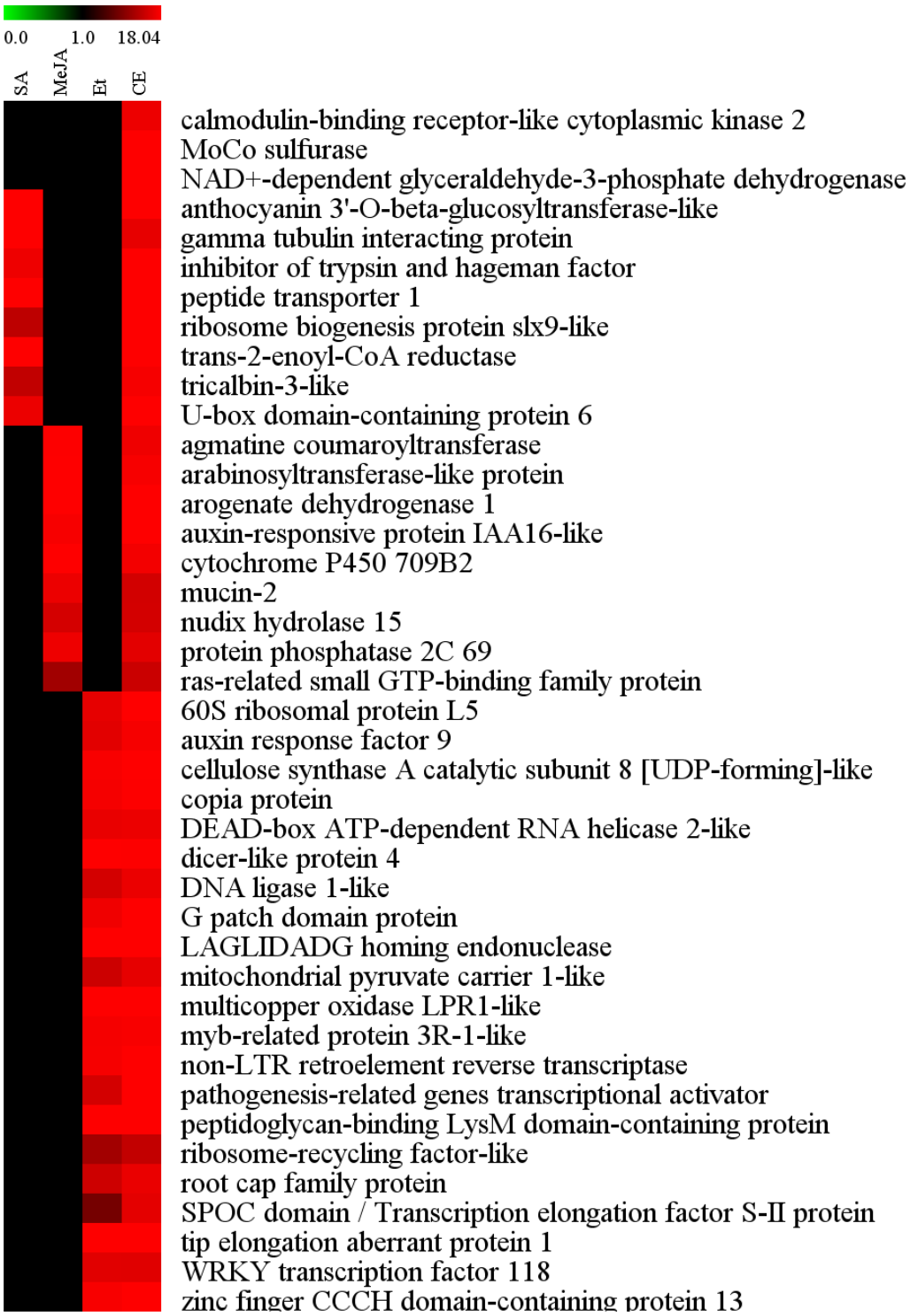

Fig. 3.12 Heatmap showing the relative amount of unique and common proteins in flavedo tissues responding to wound stress (non-infection) by induction of salicylic acid (SA), methyl jasmonate (MeJA), ethephon (Et), and CLP extract (CE). A color bar of green to red color stands for the intensity of the total ion chromatogram from 0.0 to 18.04.

Table 3.2 List of significantly expressed proteins in treatments of CLP extract and exogenous plant hormones co-applied with *Penicillium digitatum* (*Pd*).

No.	Protein name	Peptides	Accession No.*	MW (Da)	Elicitors			
					SA+Pd	MeJA+Pd	Et+Pd	CE+Pd
1	Ubc	GETAM	AAA34128.1	506.98	×	×	×	✓
2	ribosome biogenesis protein bop1	TNGGGVLDCK	KMZ67822.1	1019.39	✓	×	×	✓
3	annexin D8	AMYGEDLLIRLQLASQLK	XP_006826358.1	2077.22	×	✓	×	✓
4	detoxification 49	GIARPK	XP_008369500.1	642.09	×	✓	×	✓
5	factor of DNA methylation 5-like	RSILLGM	XP_015061658.1	809.30	×	✓	×	✓
6	F-box and leucine rich repeat domains containing protein	ESEKNLQAK	EOY08023.1	1042.76	×	✓	×	✓
7	ABC transporter I family member 6	GISMS	XP_009415754.1	510.31	×	×	✓	✓
8	carboxylesterase 6	GATTLTHVTK	XP_010551285.1	1029.91	×	×	✓	✓
9	DNA-directed RNA polymerase I subunit rpa1	EVATAALDMK	XP_004249758.1	1062.22	×	×	✓	✓

*Reference: The accession numbers can be obtained from NCBI database. (MW, molecular weight; Pd, *Penicillium digitatum*; SA, salicylic acid; MeJA, methyl jasmonate; Et, ethephon; CE, CLP extract).

Table 3.2 List of significantly expressed proteins in treatments of CLP extract and exogenous plant hormones co-applied with *Penicillium digitatum* (*Pd*). (Continued)

No.	Protein name	Peptides	Accession No.*	MW (Da)	Elicitors SA+Pd	MeJA+Pd	Et+Pd	CE+Pd
10	mitogen-activated protein kinase kinase kinase 3-like	RQHGYMSSLHRPQQK	XP_006353638.1	1869.42	×	×	✓	✓
11	shaggy-related protein kinase epsilon	MASAGXAPAASAVK	XP_008357735.1	1202.51	×	×	✓	✓

*Reference: The accession numbers can be obtained from NCBI database. (MW, molecular weight; Pd, *Penicillium digitatum*; SA, salicylic acid; MeJA, methyl jasmonate; Et, ethephon; CE, CLP extract).

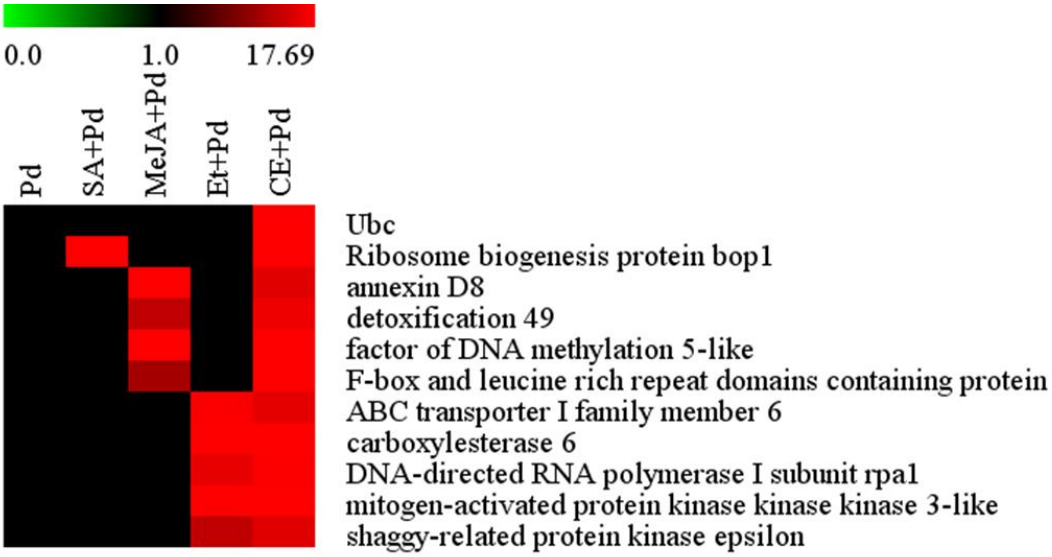

Fig. 3.13 Heatmap showing the relative amount of unique and common proteins in flavedo tissues responding to infection of *P. digitatum* (Pd) including *P. digitatum* co-applied with salicylic acid (SA+Pd), methyl jasmonate (MeJA+Pd), ethephon (Et+Pd), and CLP extract (CE+Pd). A color bar of green to red color stands for the intensity of the total ion chromatogram from 0.0 to 17.69.

3.3.4 Significantly expressed protein patterns in plant defense responses with and without fungal pathogen challenge

The list of significantly expressed proteins presented in the exogenous plant hormone and CLP extract treatments which accumulated during non- and pathogen infection are summarized in Table 3.3. With non- fungal infection, CRCK2, trans-2-enoyl-CoA reductase, LAGLIDADG homing endonuclease, mitochondrial pyruvate carrier 1-like and non-LRT retroelement reverse transcriptase were all present in the CLP extract treatment and also in the Et and SA treatments. However, a distinct pattern of presented protein was revealed in the fungal infection co-treatments. This was most apparent in the fungal-infection-alone treatment, but elevated levels of the same four proteins were also seen in the treatments with exogenous plant hormones and were also detected when CLP extract was co-applied with the pathogen. These proteins were: Annexin D8, ABC transporter I family member 6, carboxylesterase 6, and shaggy-related protein kinase epsilon. Furthermore, these four proteins were significantly detected in all the treatments without fungal infection and were absent in the fungal infection alone treatment, and in the SA and MeJA co-applied with *P. digitatum*. The characteristics of the presented proteins are shown in Table 3.3. The relative amount of the proteins in all the treatments are displayed as a heatmap in Fig. 3.14. In summary, nine proteins were consistently found both in treatments with stand-alone CLP extract and also those coupled with the pathogen.

Table 3.3 Comparison of significantly expressed proteins in each treatment which occurred with and without pathogen infection.

No.	Protein name	Elicitors								
		Non-fungal infection				With fungal infection				
		SA	MeJA	Et	CE*	Pd	SA+Pd	MeJA+Pd	Et+Pd	CE+Pd
Significantly expressed proteins in the treatments without fungal infection										
1	calmodulin-binding receptor-like cytoplasmic kinase 2	×	×	×	✓	✓	×	✓	✓	✓
2	trans-2-enoyl-CoA reductase	✓	×	×	✓	✓	✓	✓	✓	✓
3	LAGLIDADG homing endonuclease	×	×	✓	✓	✓	✓	✓	✓	✓
4	mitochondrial pyruvate carrier 1-like	×	×	✓	✓	✓	×	✓	✓	✓
5	non-LTR retroelement reverse transcriptase	×	×	✓	✓	×	✓	✓	✓	✓
Significantly expressed proteins in the treatments with fungal infection										
6	annexin D8	✓	✓	✓	✓	×	×	✓	×	✓
7	ABC transporter I family member 6	✓	✓	✓	✓	×	×	×	✓	✓
8	carboxylesterase 6	✓	✓	✓	✓	×	×	×	✓	✓
9	shaggy-related protein kinase epsilon	✓	✓	✓	✓	×	×	×	✓	✓

(Pd, *Penicillium digitatum*; SA, salicylic acid; MeJA, methyl jasmonate; Et, ethephon; CE, CLP extract).

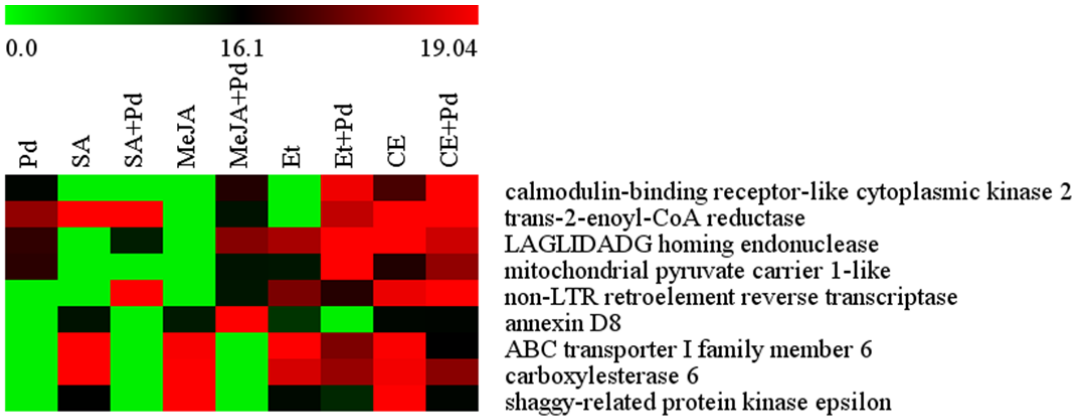

Fig. 3.14 Heatmap showing the relative amount of unique and common proteins in flavedo tissues found to be significantly present in treatments of salicylic acid (SA), methyl jasmonate (MeJA), ethephon (Et), and CLP extract (CE) including infection of *P. digitatum* (Pd) and *P. digitatum* co-applied with salicylic acid (SA+Pd), methyl jasmonate (MeJA+Pd), ethephon (Et+Pd), and CLP extract (CE+Pd). A color bar of green to red color stands for the intensity of the total ion chromatogram from 0.0 to 19.04.

3.3.5 Effect of CLP extract and exogenous plant hormones on plant defensive proteins associated with gene transcripts involved in signal transduction pathway

The elicitation level of *PAL*, *LOX*, *ACS1*, *CHI*, *GLU*, *POD*, and *PR1* transcripts were determined and their encoded protein products were investigated in the various treatments of mandarins without pathogen infection, by proteome profiling. Without fungal attack, certain amounts of PAL3, LOX, ACS, CHI (PR4), GLU, POD, and PR1 proteins were discovered in the flavedo treatments with both CLP extract and exogenous plant hormones. Interestingly, the PAL and PR1 proteins were disappeared during green mold attack while the other proteins remained. The relative amount of the proteins in the individual treatment was illustrated as a heatmap in Fig. 3.15.

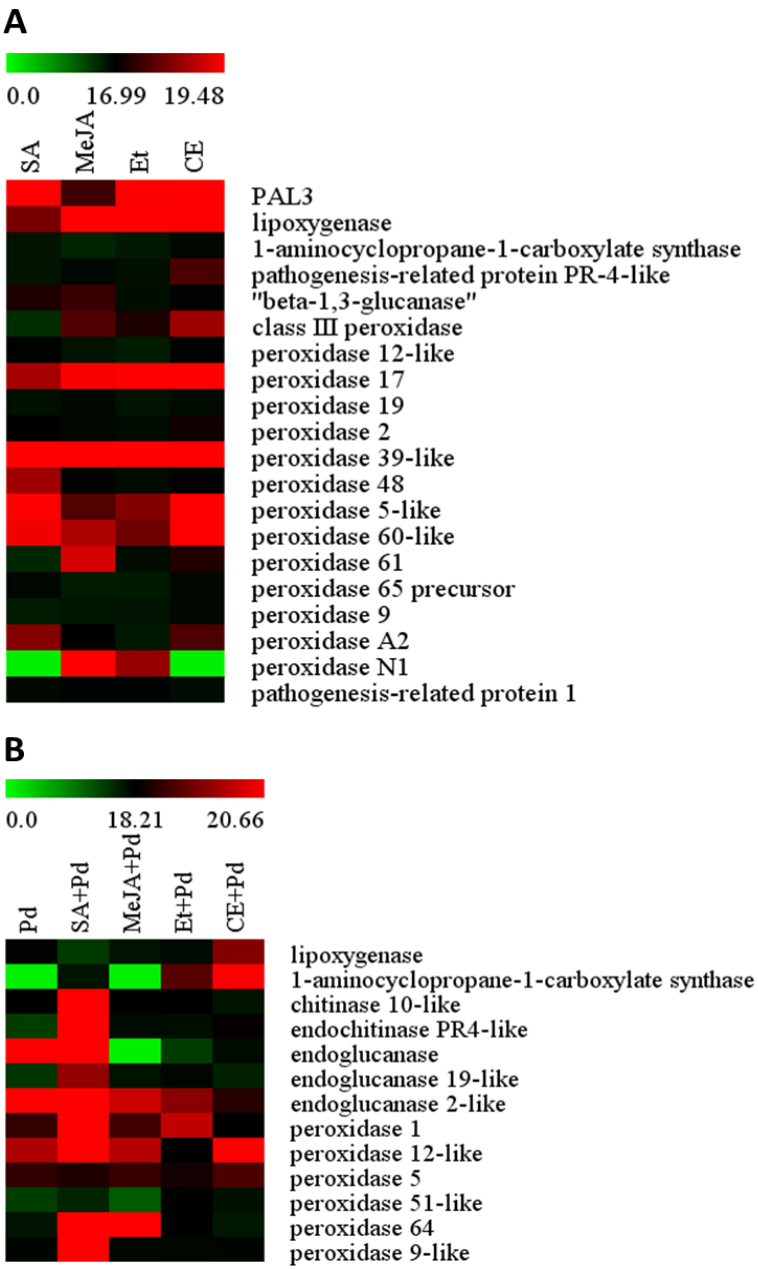

Fig. 3.15 Heatmap showing the relative amount of the proteins in flavedo tissues with associated gene transcripts. (A) non-fungal infection treatments of salicylic acid (SA), methyl jasmonate (MeJA), ethephon (Et) and CLP extract (CE). (B) treatments following with infection of *P. digitatum* (Pd) and *P. digitatum* co-applied with salicylic acid (SA+Pd), methyl jasmonate (MeJA+Pd), ethephon (Et+Pd), and CLP extract (CE+Pd). A color bar of green to red color stands for the intensity of the total ion chromatogram from 0.0 to 19.48 in (A) and 0.0 to 20.66 in (B).

3.4 Transcriptional analysis and targeted proteomics derived from individual CLP-protein binding assay

3.4.1 Activation of gene expression relating to plant hormone modulating signaling pathways by *B. subtilis* individual CLP

Induction of the expression of *PAL, LOX*, *ACS1* and *ACO*, key genes involved in the SA (*PAL*), JA (*LOX)* and ET (*ACS1* and *ACO*) signaling pathways, by *B. subtilis* CLPs alone was conducted. In the fengycin treated flavedo tissues, the maximum expression of the *PAL* gene (3.5-fold) was induced at 24 h post-treatment in response to wound stress (Fig. 3.16A). The abundance of *PAL* transcripts decreased continually from 24 to 72 h in all the CLP treatments (Fig. 3.16A and B). During fungal infection, the pathogen itself had only a small effect on all the gene expressions tested except in *LOX* gene expression (Fig. 3.16B, D, F and H). Iturin A triggered the highest amount of *PAL* transcripts (6.9-fold) at 24 h (Fig. 3.16B) in flavedo tissues. Iturin A showed the greatest induction of *LOX* transcripts (6-fold) at 72 h without fungal attack (Fig. 3.16C). During green mold attack, *P. digitatum* elicited the highest level of *LOX* gene expression (2.6-fold) as early as 24 h post-inoculation (Fig. 3.16D), while the same activity was detected later in surfactin-treated tissues at 72 h post-treatment. In Fig. 3.16E, fengycin presented the highest effect on the *ACS1* transcript level at 24 h (2.1-fold), but this was gradually declined towards 72 h post-treatment. However, iturin A elicited the highest *ACS1* transcription (3.5-fold) at 24 h which was then decreased at 48 and 72 h during green mold attack (Fig. 3.16F). In fengycin the treated tissues revealed a constant level of *ACO* transcripts without fungal infection, but there was a non-significant difference of *ACO* expression by other CLPs at later treatment times (Fig. 3.16G). It was noticeable that iturin A showed the strongest elicitation of *ACO* at 24 h (8.9-fold) with only a small decline at 48 h (8.3-fold) during fungal infection but a lesser effect on the elicitation of *ACO* expression was detected in the fengycin-treated tissues (Fig. 3.16H).

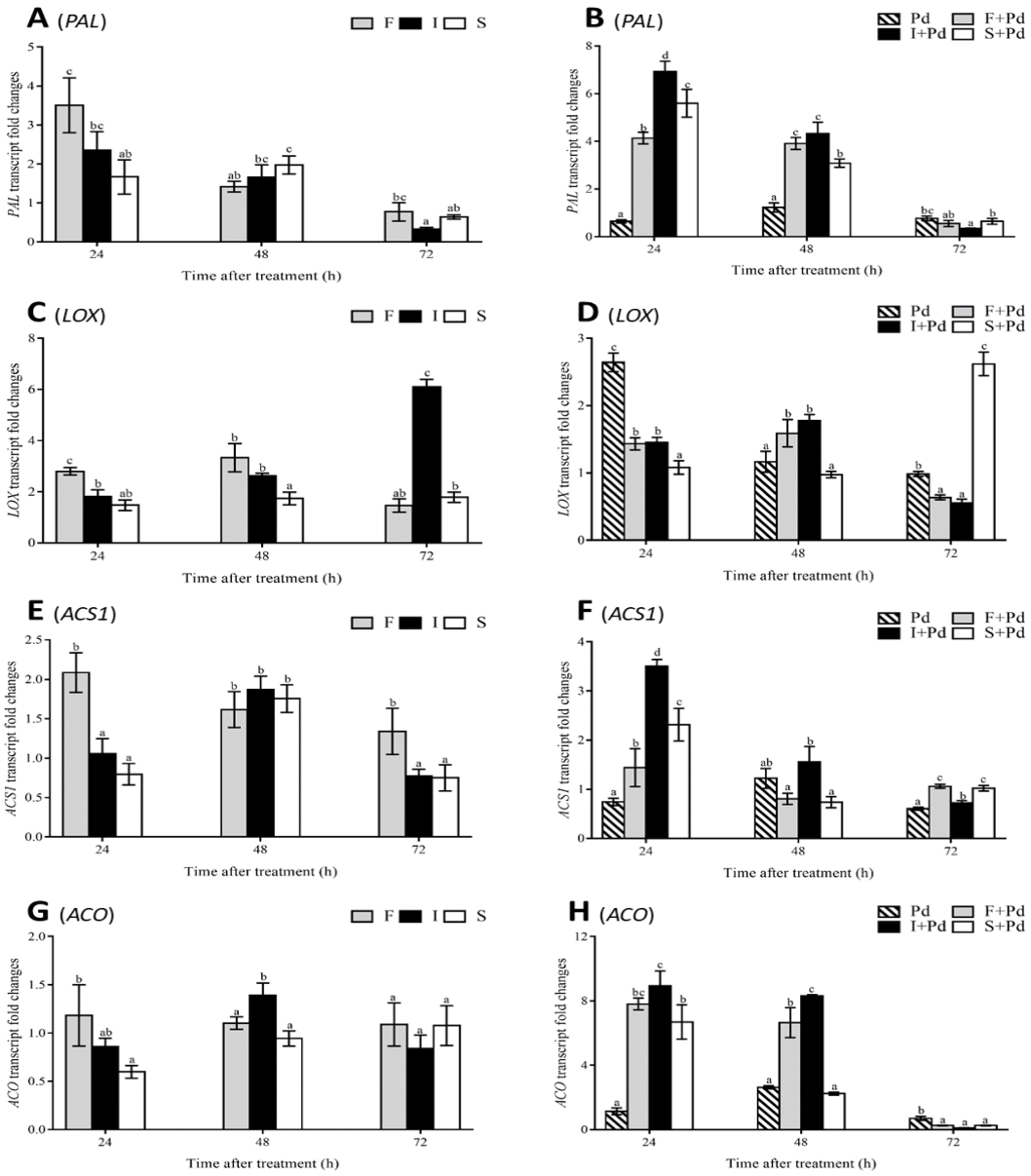

Fig. 3.16 Transcriptional fold changes in mandarin fruit of genes involving in plant hormone signaling pathway activated by individual CLP with and without fungal infection. Fengycin (F), iturin A (I), and surfactin (S), *Penicillium digitatum* (Pd), and *P. digitatum* co-applied with fengycin (F+Pd), iturin A (I+Pd), and surfactin (S+Pd). Transcript abundances with and without fungal infection (A), (B) *PAL*, (C), (D) *LOX,* (E), (F) *ACS1* and (G), (H) *ACO*. Vertical bars represent standard errors of the mean value of three trials; columns with the same letter above them show no significant difference to each other at $P \leq 0.05$ according to the Tukey's range test.

3.4.2 Activation of PR protein gene expression by *B. subtilis* individual CLP

To confirm the effects of CLPs alone on eliciting plant PR protein production, a comparative study among the individual CLP was conducted. Changes in the transcription of *CHI*, *GLU*, *POD*, and *PR1* in flavedo tissues treated with individual CLP, with and without pathogen attack were demonstrated. The level of induction of *CHI* transcripts reached a maximum in the fengycin treatment within 24 h post-treatment and thereafter continually decreased, whereas an increase in the *CHI* transcript level was detected in surfactin-treated fruit between 24 and 72 h in response to wound stress (Fig. 3.17A). Following infection with *P. digitatum,* the fengycin treatment showed a marked increase in the induction of the *CHI* gene at 48 h (2.3-fold) and 72 h (2.5-fold) (Fig.3.17B). Moreover, fengycin produced an increasing trend of *CHI* transcripts from 24 to 72 h, which was opposite to the decreasing trend detected in the iturin A treatment. The expression of the *GLU* gene displayed a decreasing trend in the fengycin treatment which was the opposite of the trend in the iturin A-treated flavedo in response to wound stress (Fig. 3.17C).

As can be observed in Fig. 3.17D, fengycin co-applied with *P. digitatum* synergistically activated the highest level of *GLU* accumulation (7.2-fold) at 48 h post-treatment. The treated flavedo showed the highest level of *POD* expression at 72 h. induced by surfactin (3.4-fold), and by surfactin co-applied with *P. digitatum* (5.6-fold) (Fig. 3.17E and F, respectively). The abundance of *PR1* transcripts reached its maximum when induced by iturin A (2.2-fold) at 48 h without fungal attack (Fig. 3.17G). In contrast, surfactin showed a significant effect when co-applied with *P. digitatum* on the accumulation of *PR1* transcripts at 24 h (9.7-fold) which declined at 72 h (7.3-fold) during fungal infection (Fig. 3.17H).

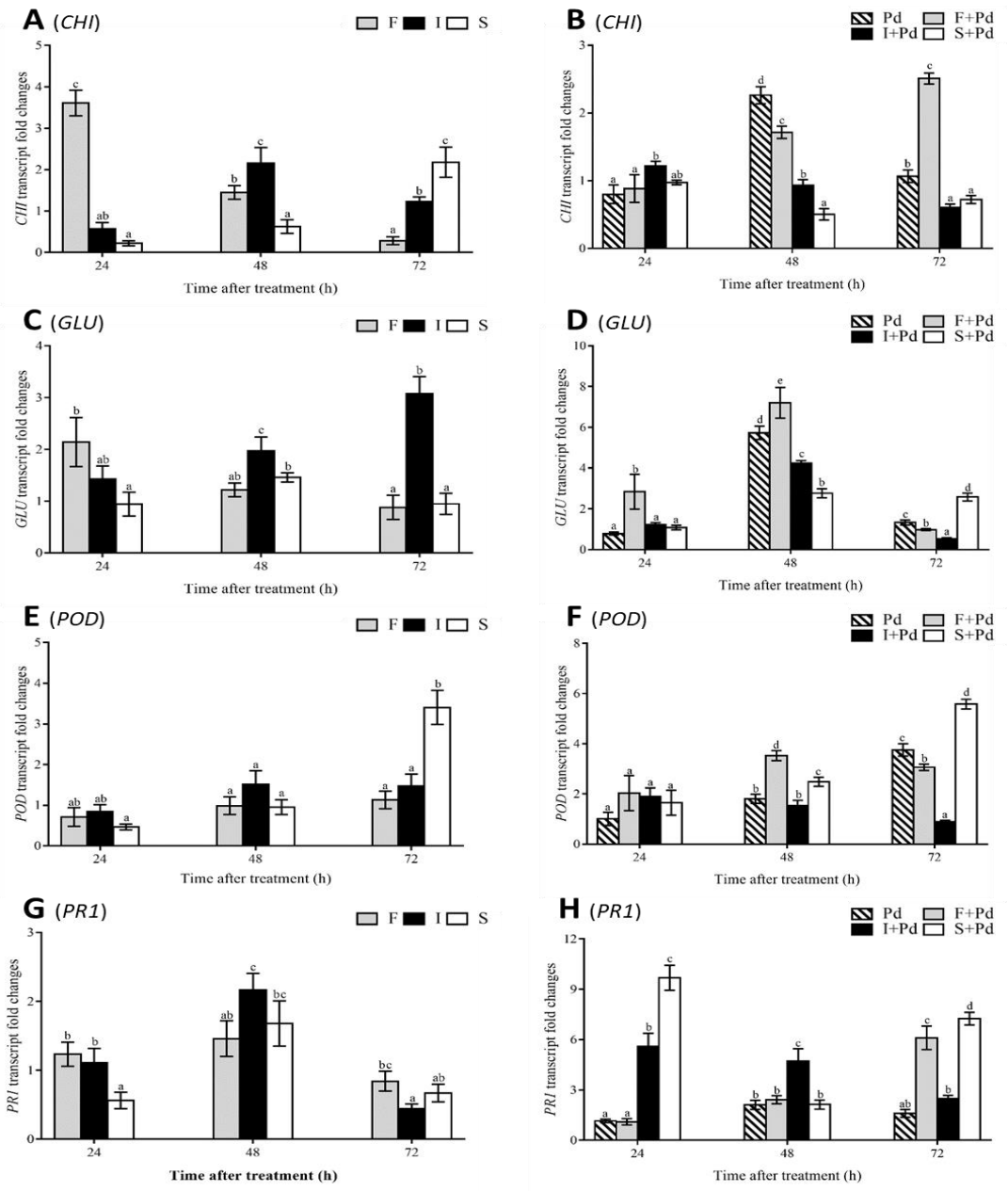

Fig. 3.17 Transcriptional fold changes in mandarin fruit of *PR* genes activated by individual CLP with and without fungal infection. Fengycin (F), iturin A (I), and surfactin (S), *Penicillium digitatum* (Pd), and *P. digitatum* co-applied with fengycin (F+Pd), iturin A (I+Pd), and surfactin (S+Pd). Transcript abundances with and without fungal infection (A), (B) *CHI*, (C), (D) *GLU,* (E), (F) *POD* and (G), (H) *PR1*. Vertical bars represent standard errors of the mean value of three trials; columns with the same letter above them show no significant difference to each other at $P \leq 0.05$ according to the Tukey's range test.

3.4.3 Plant protein production up-regulated by individual CLP

The members *of B. subtilis* CLPs induced distinct patterns of plant defensive proteins under wound stress and fungal infection. Fig. 3.18A shows the 3,081 common proteins which were found in the flavedo tissues treated with fengycin, iturin A, and surfactin in response to wound stress. Fengycin and iturin A produced a common effect in inducing 136 proteins in the flavedo tissues while 73 and 55 proteins were observed in common between the groups of fengycin and surfactin treatments, and the groups of iturin A and surfactin treatments, respectively. There were 16, 29, and 20 proteins uniquely produced by the fengycin-, iturin A-, and surfactin-treated groups, respectively. During green mold attack, a large number (1,656) of proteins in host plants were determined in common (Fig. 3.18B) while only eight proteins were detected in common in the fengycin and iturin A treatment groups, and there were only two common proteins found in the treatments of fengycin and surfactin co-applied with *P. digitatum*. The tissues treated with iturin A and surfactin shared 11 identical proteins responding to fungal attack. One and two unique proteins, respectively, were found in the surfactin and iturin A treatments co-applied with *P. digitatum* while in the fengycin counterpart, no unique proteins were found. A list of the proteins with their unique characteristics, and significant roles in biological processes obtained from each treatment, with and without fungal infection are shown in Table 3.4. The relative amount of each protein is presented as a heatmap in Fig. 3.19

.

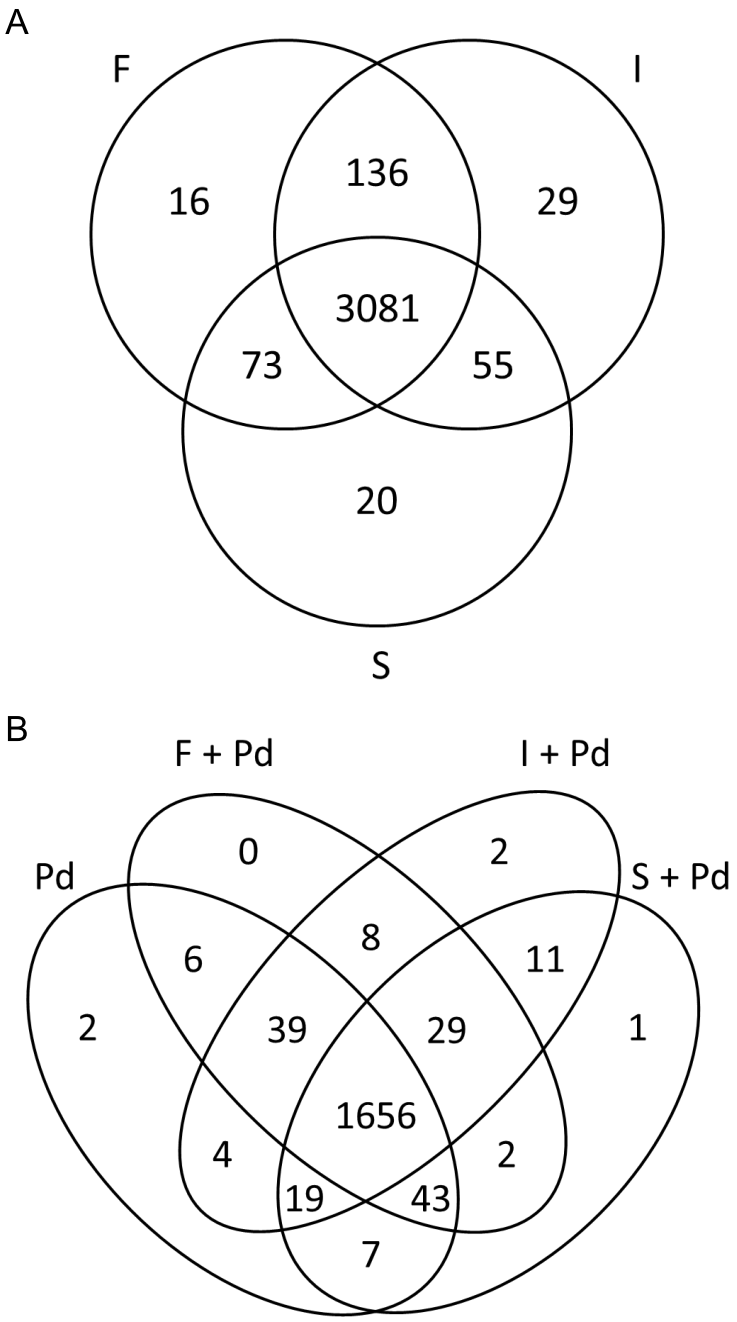

Fig. 3.18 Venn diagram showing the total estimated number of protein distribution activated by individual CLP with and without fungal infection. (A) the four groups of elicitors responding to wound stress induced by fengycin (F), iturin A (I), and surfactin (S). (B) the five groups of elicitors stimulated by *Penicillium digitatum* (Pd) and *P. digitatum* co-applied with fengycin (F+Pd), iturin A (I+Pd), and surfactin (S+Pd).

Table 3.4 List of interestingly unique proteins presented in the individual CLP treatment with and without fungal infection.

No.	Protein name	Accession No.*	Elicitor	Biological process
1	ABC1 family protein	XP_002311218.1	fengycin	ubiquinone biosynthetic process
2	glutamate synthase	XP_002501855.1	fengycin	glutamate biosynthetic process
3	pathogenesis-related genes transcriptional activator	XP_002946570.1	fengycin	defense response
4	peptidoglycan-binding LysM domain-containing protein	KZV57878.1	fengycin	immune response
5	agmatine coumaroyltransferase	BAF97628.1	iturin A	defense response
6	auxin-responsive protein IAA16-like	XP_002281771.1	iturin A	auxin-activated signaling pathway
7	copalyl diphosphate synthase	ADO61011.1	iturin A	gibberellin biosynthetic process
8	cytochrome P450 709B2	XP_015633710.1	iturin A	stress response
9	NAC domain-containing protein 21/22-like	XP_010904650.1	iturin A	auxin-activated signaling pathway
10	peroxidase N1	EOX98840.1	iturin A	response to oxidative stress
11	raffinose synthase	KVI06732.1	iturin A	response to abscisic acid

*Reference: The accession numbers can be obtained from NCBI database.

Table 3.4 List of interestingly unique proteins presented in the individual CLP treatment with and without fungal infection. (Continued)

No.	Protein name	Accession No.*	Elicitor	Biological process
12	auxin transport protein BIG-like	XP_008379461.1	surfactin	auxin-activated signaling pathway
13	calcium-dependent protein kinase 33	KZV34889.1	surfactin	abscisic acid-activated signaling pathway
14	F-box and leucine rich repeat domains containing protein	EOY08023.1	iturin A co-applied with *P. digitatum*	ubiquitin-dependent protein catabolic process
15	two-component response regulator-like APRR2	KHN21028.1	iturin A co-applied with *P. digitatum*	phosphorelay signal transduction system
16	DNA-directed RNA polymerase I subunit rpa1	XP_004249758.1	surfactin co-applied with *P. digitatum*	negative regulation of protein localization to nucleolus

*Reference: The accession numbers can be obtained from NCBI database.

Fig. 3.19 Heatmap showing the relative amount of each protein activated by individual CLP with and without fungal infection. (A) the three groups of elicitors responding to wound stress induced by fengycin (F), iturin A (I), and surfactin (S). (B) the four groups of elicitors stimulated by *Penicillium digitatum* (Pd) and *P. digitatum* co-applied with fengycin (F+Pd), iturin A (I+Pd), and surfactin (S+Pd). A color bar of green to red color stands for the intensity of the total ion chromatogram from 0.0 to 17.2 in (A) and 0.0 to 16.3 in (B).

3.4.4 Specific individual CLP-binding proteins

To emphasize the role of the important function of CLP members in signal transduction pathways involved in ISR elicitation in host plants against pathogen infection, mass spectrometry and a proteomic approach were applied to monitor the mediator protein molecules that are responsible for their interaction. Scans of iindividual saturated CLP in C18 Ziptip® with maximum concentration CLP solutions (5 µg) were manually performed following the data obtained from a NanoDrop® spectrophotometer. The maximum binding of the CLPs to the C18 was respectively 5, 6, and 7 µg of iturin A, fengycin, and surfactin, which bound to the C18 at 96 %, 95 %, and 94 % (iturin A), 98 %, 97 % and 96% (fengycin), and 98 %, 97 % and 94 % (surfactin).

The majority of the commonly expressed plant proteins present in the *P. digitatum* treated and control groups, which were bound to the saturated individual CLP in the C18 columns, are illustrated in Venn diagrams in Fig. 3.20A-C. To confirm the binding ability of extracted proteins to CLP molecules, the bound proteins which were found in both CLP-C18-pipette tips and C18-pipette tips were subtracted from the expressed proteins in Fig. 3.20. Fengycin captured 81 and 82 proteins in the treated and control groups, respectively as shown in the Venn diagram in Fig. 3.20A. Of those, 78 common proteins were entrapped in the saturated C18 column for both groups while three proteins were present only in the fungal-treated group and four proteins were present only in the control group. For the iturin A-saturated C18–protein interactions, there were 82 differentially expressed proteins out of a total identified of 85 which were common to the treated and control groups as shown in Fig. 3.20B. It was nnoticeable that only iturin A was able to capture the three unique proteins expressed in the fungal-treated group whereas the surfactin-protein binding trapped only one protein found in the control group out of the 83 common proteins detected in both groups as shown in Fig. 3.20C.

The proteins attached to each CLP which were detected both in with and without fungal invasion treatments were determined, and only a small number of unique proteins were found to be present in specific protein-CLP binding groups. Fig. 3.21A illustrates the three unique proteins characterized in fungal-treated hosts which interacted

with fengycin and were identified as follows; 1) ATP-dependent DNA helicase Q-like SIM, 2) glycogen debranching enzyme, and 3) myb-related protein 330 occurring in the green mold attack condition. In contrast, there were four unique proteins bound to fengycin in response to wound stress, which were characterized as 1) A/G-specific adenine DNA glycosylase, 2) flavin monooxygenase-like protein, 3) inner membrane protein yieG, and 4) ribosome-binding ATPase YchF (Fig. 3.21A). Interestingly, in the fungal-treated protein extract, the three unique proteins bound to iturin A were determined to be 1) 12-oxophytodienoate reductase 2, 2) beta' subunit of RNA polymerase, and 3) UDP-N-acetylmuramoyl-L-alanyl-D-glutamate--2,6-diaminopimelate ligase (Fig. 3.21B). In addition, A/G-specific adenine DNA glycosylase was the only unique protein attached to surfactin in response to wound stress (Fig. 3.21C). The biological processes of the unique proteins binding to CLPs are displayed in Table 3.5. The relative amount of each protein is also shown as a heatmap (Fig. 3.21A-C).

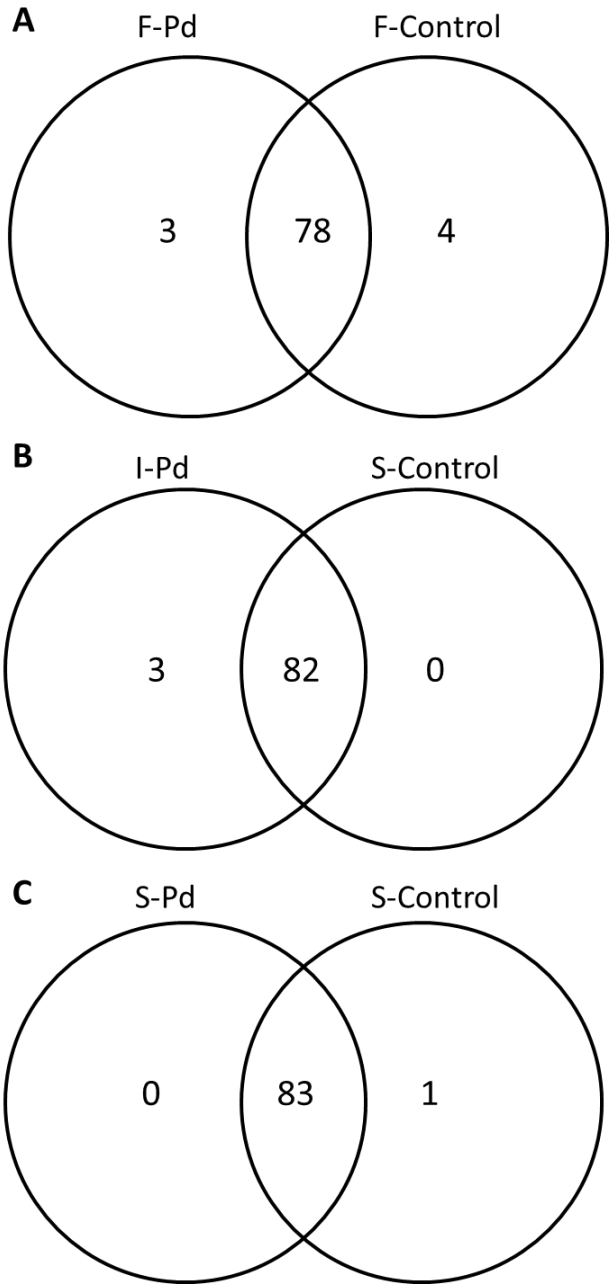

Fig. 3.20 Venn diagram showing the total estimated number of proteins distributed in individual CLP-protein association. (A) treatments of fengycin-attaching proteins induced by *Penicillium digitatum* (F-Pd) and sterile distilled water (F-Control). (B) treatments of iturin A-attaching proteins induced by *Penicillium digitatum* (I-Pd) and sterile distilled water (I-Control). (C) treatments of surfactin-attaching proteins induced by *Penicillium digitatum* (S-Pd) and sterile distilled water (S-Control).

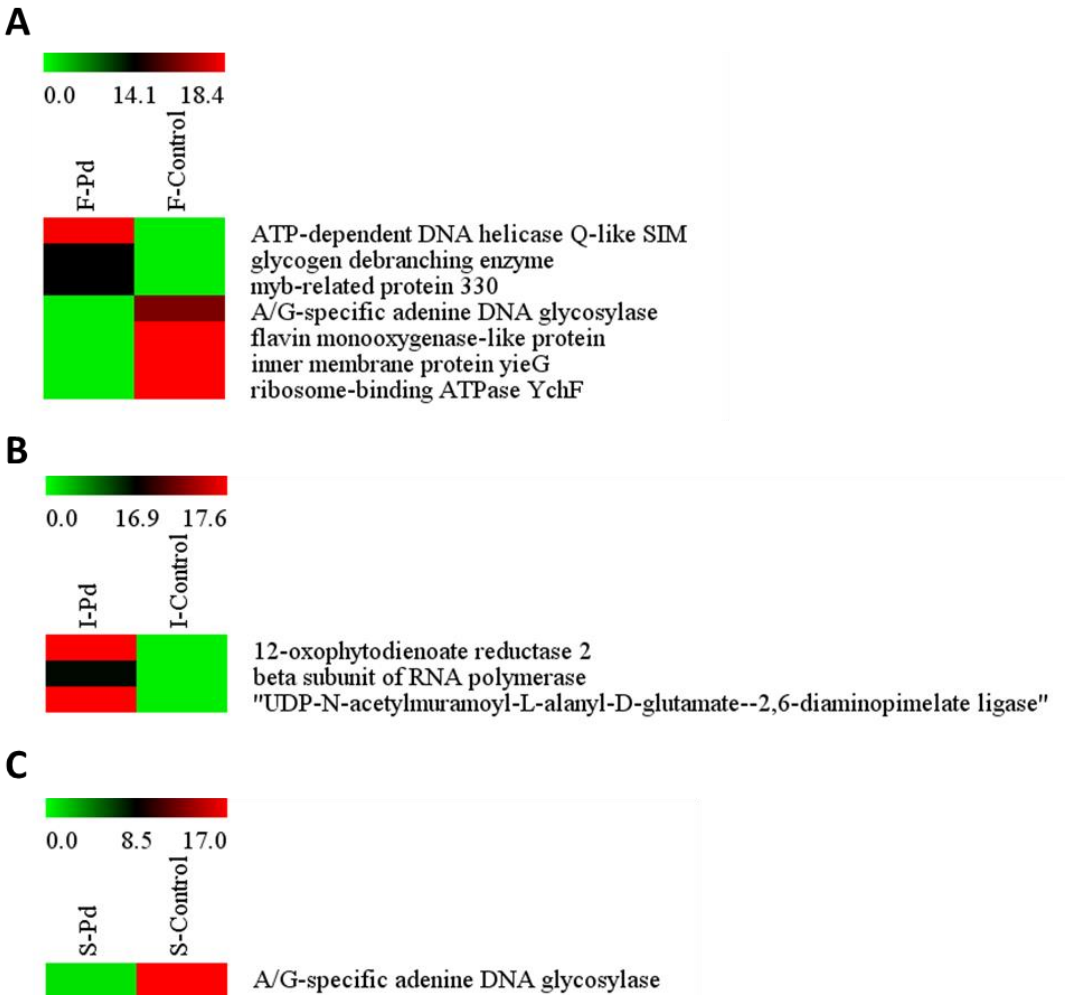

Fig. 3.21 Heatmap showing the relative amount of each protein in individual CLP-protein association. (A) groups of fengycin-attaching proteins induced by *Penicillium digitatum* (F-Pd) and sterile distilled water (F-Control). (B) groups of iturin A-attaching proteins induced by *Penicillium digitatum* (I-Pd) and sterile distilled water (I-Control). (C) groups of surfactin-attaching proteins induced by *Penicillium digitatum* (S-Pd) and sterile distilled water (S-Control). A color bar of green to red color stands for the intensity of the total ion chromatogram from 0.0 to 18.4 in (A), 0.0 to 17.6 in (B), and 0.0 to 17.0 in (C).

Table 3.5 List of unique proteins attached to individual CLP-C18 with and without fungal infection.

No.	Protein name	Accession No.*	CLPs	Condition	Biological process
1	ATP-dependent DNA helicase Q-like SIM	XP_004960267.1	fengycin	fungal infection	DNA repair
2	glycogen debranching enzyme	XP_013432022.1	fengycin	fungal infection	glycogen catabolic process
3	MYB-related protein 330	XP_013659104.1	fengycin	fungal infection	transcription
4	A/G-specific adenine DNA glycosylase	XP_013632165.1	fengycin/surfactin	wound stress	base-excision repair
5	flavin monooxygenase-like protein	OAA54389.1	fengycin	wound stress	oxidation-reduction process
6	inner membrane protein yieG	XP_003176899.1	fengycin	wound stress	transport
7	ribosome-binding ATPase YchF	XP_017602863.1	fengycin	wound stress	response to oxidative stress
8	12-oxophytodienoate reductase 2	XP_015643914.1	iturin A	fungal infection	oxylipin biosynthetic process
9	beta subunit of RNA polymerase	YP_002000409.1	iturin A	fungal infection	transcription
10	UDP-N-acetylmuramoyl-L-alanyl-D-glutamate--2,6-diaminopimelate ligase	JAT63352.1	iturin A	fungal infection	cell wall organization

*Reference: The accession numbers can be obtained from NCBI database.

3.5 Metabolomic study of mandarin defense responses upon applications of *B. subtilis* CLPs in comparison to plant hormones and *P. digitatum* infection

3.5.1 Submetabolome profiling and metabolite identification

Metabolites in the treated flavedo tissues of the mandarin fruit were profiled using ^{12}C-/^{13}C-dansylation LC-MS analysis. A total of 4,914±111 peak pairs or metabolites were detected in the duplicate analysis of 90 flavedo samples. Note that IsoMS filtered out all redundant peak pairs of the same metabolite, such as adducts or dimers, and retained only one peak pair for one labeled metabolite. Thus, the number of peak pairs reflects the number of metabolites detected. Among these, 77 metabolites were positively identified using a dansyl standard library search based on accurate mass and retention time matches. In addition, 666 and 2,769 peak pairs were mass-matched to metabolites in the HMDB library and the EML library, respectively. These results indicated that dansylation LC-MS could be used to detect a large number of amine- and phenol-containing metabolites. More importantly, judging from the number of detected metabolites, the metabolome composition of the flavedo samples appeared to be very complex. Due to a limited number of available metabolite standards, only a very small fraction of the submetabolome (77 metabolites) were positively identified. Nevertheless, the 77 positively identified metabolites and some putatively matched metabolites were found to involve in metabolic pathways, as it will be discussed in the section of pathway analysis.

3.5.2 Plant metabolome profiles and comparison

From the data set of 180 samples, the statistical tools were used to analyze the metabolome differences among different groups of samples. PCA showed distinct separations from tested samples using different treatments of various substances and from samples of different time points as well as the 19 QC runs (Fig. 3.22A). It was shown that the metabolomic data set could be clearly separated into four major groups plus the QC group. Very tight clustering of the QC samples indicated the high performance of the analysis and the reliability of data quality. It was not surprising as in our work, the ^{13}C-labeled pool was used as the internal control for analyzing all the ^{12}C-labeled individual sample. Using a differential isotope labeled internal control greatly reduced the ion suppression and matrix effects as well as compensated for instrument sensitivity drift, if any, during the sample runs for accurate and precise relative quantification of individual metabolite. In Fig. 3.22A, each major group could be identified from the different color-labeled samples detected in the treatments with similar elicitors being categorized into the same group. Fig. 3.22B shows the four-color PCA plot of the samples detected in various treatments. The green-color samples which labeled with sterile distilled water and ethanol were clustered together and defined as the control group for wound stress. The sample groups in light blue, blue and red represented treatments with *P. digitatum*, exogenous plant hormones, and *B. subtilis* ABS-S14 CLPs group (CLP extract, fengycin, iturin A, and surfactin), respectively. Based on time point analysis of each treatment (Fig. 3.22C), it was apparent that in the *P. digitatum* treatment, the samples at each time point stood alone, unlike the other groups. It was notable that the samples at 24 and 48 h were grouped together closer than those at 72 h, as shown in Fig. 3.22C. Likewise, the PCA plot of the metabolome data from the treatment group of exogenous plant hormones showed that they were similar at 24 and 48 h and differed from the 72 h samples.

The activation of a number of metabolites was demonstrated by the Venn diagram which shows the metabolite number distribution of the four treatment groups. Most of the metabolites (Fig 3.23) were commonly detected among the four groups. Only a very small fraction of the metabolites was uniquely detected in each group. To determine

the metabolic changes, we further analyzed the data set using binary comparison of different groups. The resulting volcano plots were shown in Fig. 3.24 for the metabolite changes after exposure to fungal pathogen, exogenous plant hormones, or *B. subtilis* ABS-S14 CLPs, as compared to their corresponding control group. In the preparation of the *P. digitatum* spore suspension, sterile distilled water was used, whereas ethanol was used for the CLPs and exogenous plant hormone solutions. Therefore, the effect of water or ethanol was discounted using binary comparison analysis of the submetabolome in the treated group vs. the proper control (i.e., *P. digitatum* treatment vs. water, CLPs vs. ethanol and exogenous plant hormones vs. ethanol).

In the volcano plots shown in Fig. 3.24, any change in metabolite concentration of more than 1.5-fold and a q-value of below 0.05 was considered as being significant. The volcano plot analysis of the *P. digitatum* group vs. control (Fig. 3.24A) indicates that out of 4,577 metabolites, 1,061 metabolites were down-regulated (i.e., lower metabolite concentration in the treated samples than that of the control) and 407 metabolites were up-regulated (i.e., higher metabolite concentration in the treated samples). In the group of exogenous plant hormones vs. control (Fig. 3.24B), out of 4,545 metabolites, only three metabolites were found to be down-regulated and 17 metabolites were up-regulated. Interestingly, in the group of CLPs vs. control (Fig. 3.24C), out of 4,594 metabolites, 748 metabolites were down-regulated and 600 metabolites were up-regulated. Regarding the significantly changed metabolites in the three binary comparisons, the group of CLPs showed the greatest number of up-regulated metabolites. This group also showed the greatest numbers of identified metabolites among the tested groups, based on a search in the dansyl standard library.

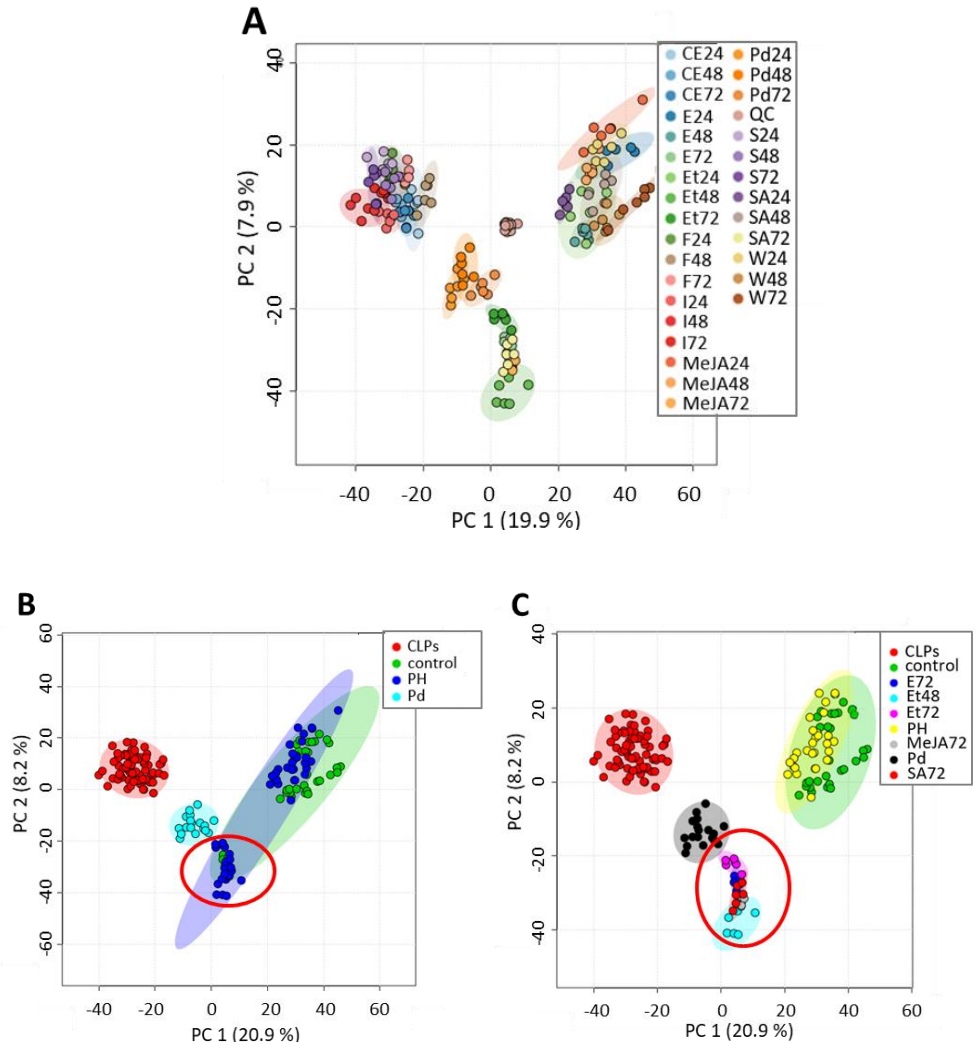

Fig. 3.22 PCA plots of the metabolomic data obtained from different groups of samples including QC samples. (A) Color-coded groups according to the treatment elicitors at all-time points and the QC group. (B) Color-coded groups according to the treatment times of 24, 48 and 72 h from four major groups of elicitors. (C) Color-coded sub-groups within the control and exogenous plant hormone groups. W, sterile distilled water; E, ethanol; Pd, *Penicillium digitatum*; SA, salicylic acid; MeJA, methyl jasmonate; Et, ethephon; CE, CLP extract; F, fengycin; I, iturin A; S, surfactin; CLPs, cyclic lipopeptide group; PH, exogenous plant hormones; 24, 24 h; 48, 48 h; 72, 72 h.

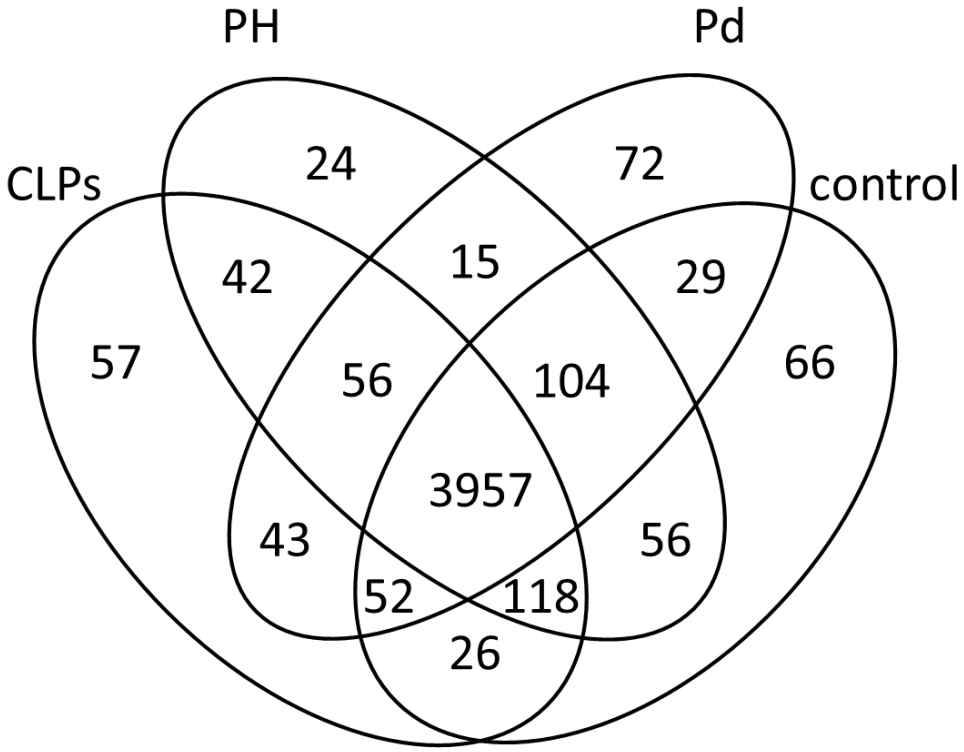

Fig. 3.23 Venn diagram showing the total estimated number of metabolites distributed in the four major groups of treatments. C, control stress; CLPs, cyclic lipopeptide group; PH, exogenous plant hormones; Pd, *Penicillium digitatum*.

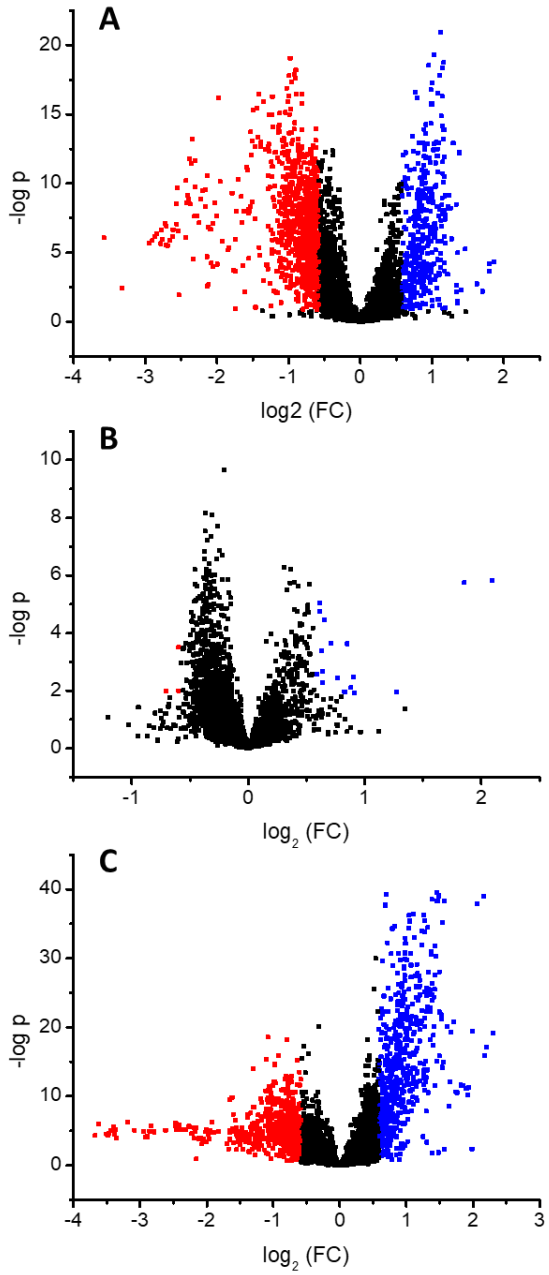

Fig. 3.24 Volcano plots of binary comparisons of metabolites in treatment vs. control. (A) *Penicillium digitatum* treatment group vs. water group. (B) Exogenous plant hormone treatment group vs. ethanol group. (C) CLP treatment group vs. ethanol group. The significant metabolites are shown in red or blue with fold change > 1.5 and q=value < 0.05 with corresponding *P*-value < 0.134 in (A), *P*-value < 0.014 in (B) and *P*-value < 0.216 in (C).

3.5.3 Metabolite regulation in plant defense to stress responses

The first conclusion was drawn from this metabolomic study in accordance with the greater numbers of metabolite changes in the plant stress responses elicited by the group of *B. subtilis* CLPs than other elicitor groups. The group of CLPs was better elicitors for triggering the synthesis of plant defense metabolites when compared with the exogenous plant hormones, SA, MeJA and Et. Seventy-seven metabolites were positively identified from the treatments of CLPs. These metabolites were exported for pathway analysis using the Metaboanalyst 4.0 software based on the *Arabidopsis thaliana* database since no citrus plant database was available. The positively identified metabolites means the metabolites that matched to the metabolite database in a dansyl standard library upon accurate mass and retention time searching. The metabolites which were putatively identified metabolites are mass-matched to metabolites in the HMDB library and the EML library. There were 39 pathways which matched to the 77 positively identified metabolites. Each pathway contained an impact and a *P*-value according to numbers of 'hits' recorded and the significance factors of the detected metabolites. The highest pathway impact and statistical significance was located on the top right corner as shown in Fig. 3.25. The metabolism of glycine, serine and threonine showed the highest pathway impact and statistical significance. Moreover, the activation of some other metabolites was detected in pathways that played a role in postharvest stress responses such as alanine, aspartate and glutamate metabolism, beta alanine metabolism, isoquinoline alkaloid biosynthesis, tyrosine (Tyr) metabolism, pantothenate and CoA biosynthesis, carbon fixation in photosynthetic organisms, aminoacyl-tRNA biosynthesis, phenylpropanoid biosynthesis, pyrimidine metabolism, glutathione metabolism and lysine biosynthesis.

The relationship of the metabolites displayed in Fig. 3.25 was expanded upon in Figs. 3.26-3.31. Fig. 3.26 shows that 6 out of the 77 positively identified metabolites contributed in the metabolism of glycine, serine and threonine. The metabolites shown in the light blue boxes in Figs. 3.26-3.31 were not yet identified. The positively identified metabolites were highlighted in green, whiles the putatively identified

metabolites were highlighted in orange. The box plot of each positively or putatively identified metabolite in the pathway was included to show the significant level changes compared to the control group. There were two metabolites in the Tyr metabolism positively identified in this work, i.e., Tyr and tyramine (in green in Fig. 3.27) and three metabolites putatively identified (in orange). In Fig. 3.27, 2 out of 77 identified metabolites were involved in Tyr metabolism. The 6 out of 77 identified metabolites were related in alanine, aspartate, and glutamate metabolism (Fig. 3.28). There were 3 out of 77 identified metabolites; aspartic acid, beta-alanine, and pantothenic acid playing in beta alanine metabolism (Fig. 3.29). Moreover, Fig. 3.30 represents Tyr and tyramine were 2 out of 77 identified metabolites that were involved in isoquinoline alkaloid biosynthesis, and (pantothenic acid, beta-alanine), and valine were 3 out of 77 identified metabolites that were contributed in panthotenate and CoA biosynthesis, respectively (Fig. 3.31).

In summary, the CLP extract and individual CLP obtained from *B. subtilis* ABS-S14 were able to trigger the synthesis of serotonin (Fig. 3.32A) and 5-hydroxy-*N*-methyltryptamine (Fig. 3.32B) in flavedo tissues. Tyr has been demonstrated to be a precursor of tyramine. Accordingly, the box plot of Tyr concentration in the CLPs treated group was seen to be at a lower level than those found in the other elicitor tests (Fig. 3.32C). This confirmed that Tyr had been immediately changed to tyramine as validated by the box plot of Tyramine/Tyr (Fig. 3.32D). Thus, the elicitors in the CLPs group were able to highly activate tyramine production, compared to the other groups (Fig. 3.32E). Thus, the comparative metabolic studies of the mandarin fruit in response to fungal infection, exogenous plant hormones and CLPs, their impacts on the Trp and Tyr pathways as well as the metabolism of serotonin (Fig. 3.32A), 5-hydroxy-*N*-metyltryptamine (Fig. 3.32B), Tyr (Fig. 3.32C) and tyramine (Fig. 3.32E) provide evidence that *P. digitatum* had only a minor effect on those metabolites. In the same manner, the effects of exogenous plant hormones were similar to fungal infection on those metabolites with the exception that SA, MeJA and Et were able to elicit greater accumulations of Tyr than in CLPs and the fungal pathogen treated tissues.

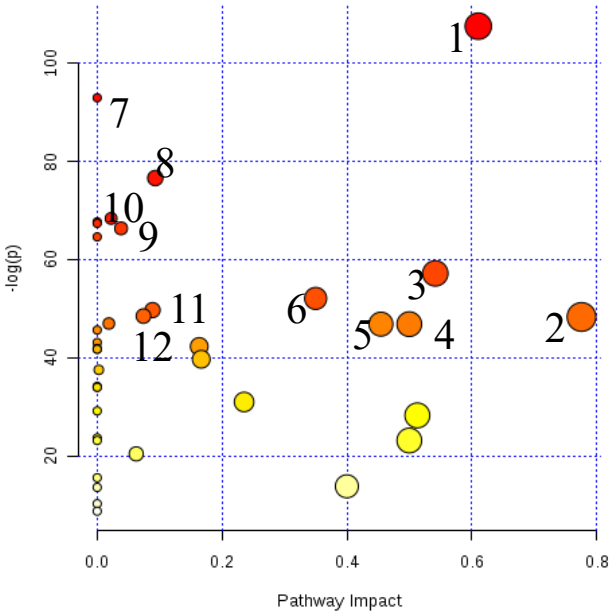

1	Glycine, serine and threonine metabolism
2	Alanine, aspartate and glutamate metabolism
3	Beta alanine metabolism
4	Isoquinoline alkaloid biosynthesis
5	Tyrosine metabolism
6	Pantothenate and CoA biosynthesis
7	Carbon fixation in photosynthetic organisms
8	Aminoacyl-tRNA biosynthesis
9	Phenylpropanoid biosynthesis
10	Pyrimidine metabolism
11	Glutathione metabolism
12	Lysine biosynthesis

Fig. 3.25 Overview of metabolomic pathway analysis relating to stress responses.

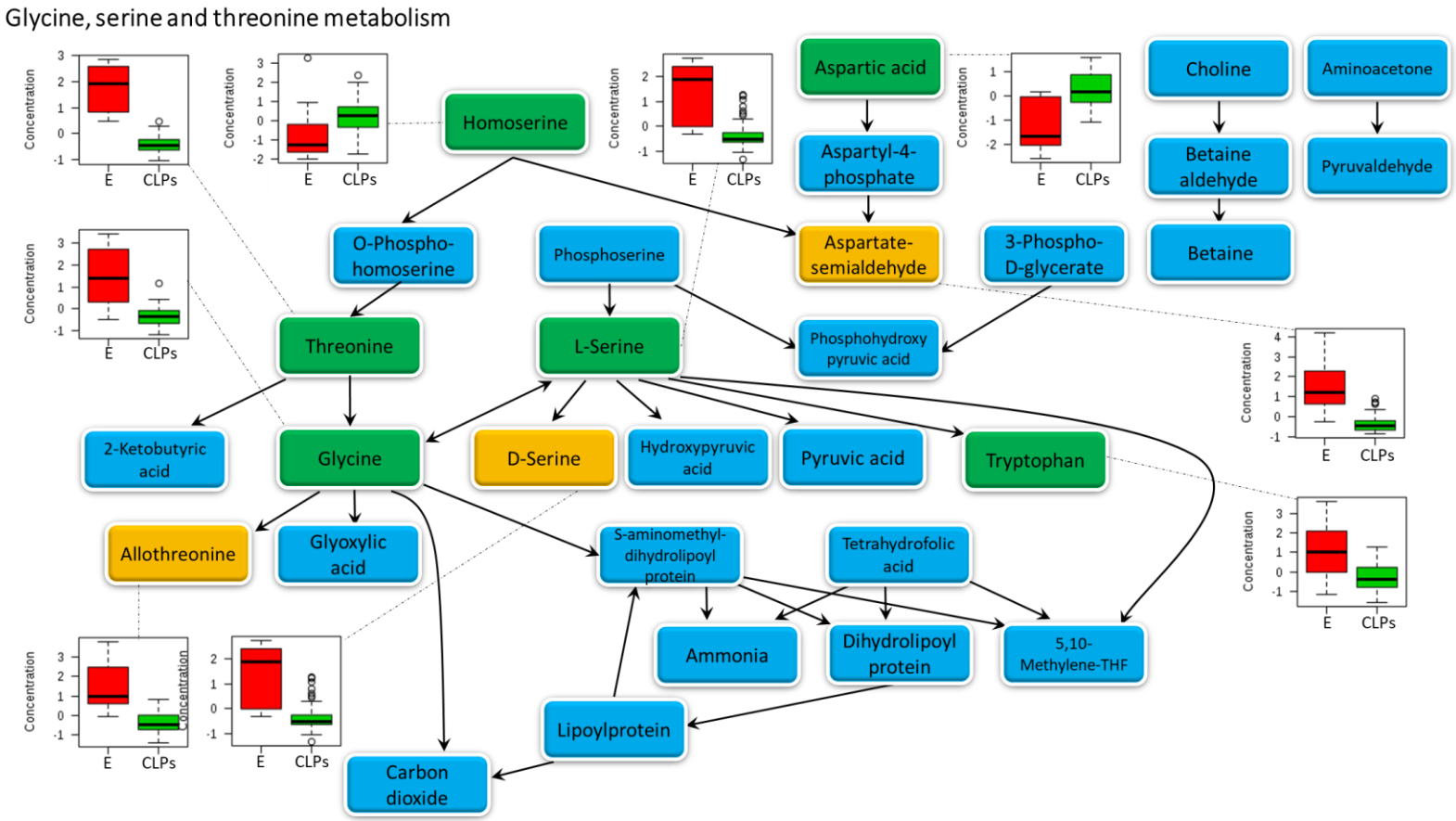

Fig. 3.26 Pathway of glycine, serine and threonine metabolism. The metabolite in green box represents the positive ID, orange box represents the putative ID, and blue box represents no ID, and the box plots of identified metabolites are displayed beside the corresponding metabolites. E, ethanol; CLPs, cyclic lipopeptide group.

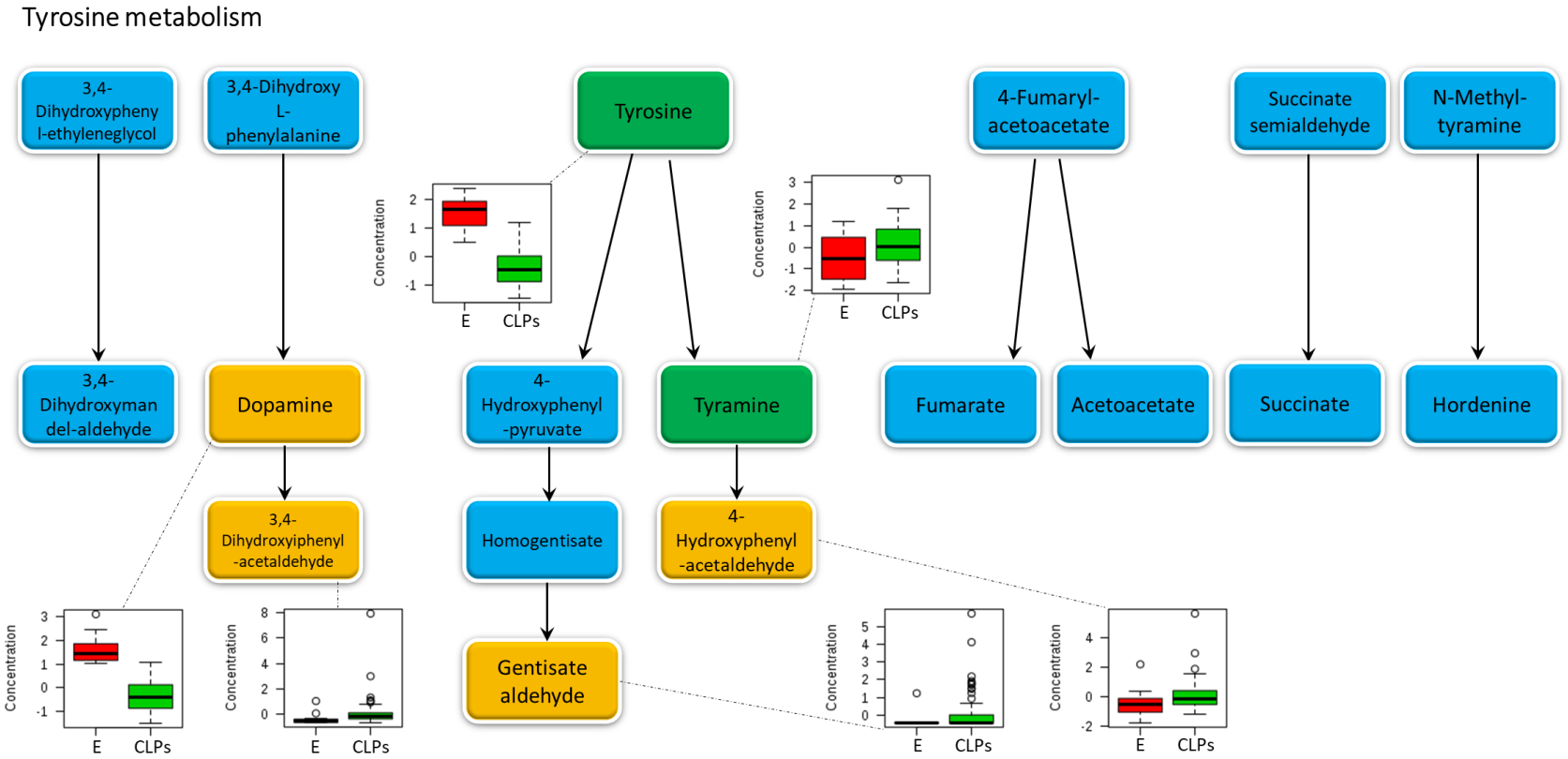

Fig. 3.27 Pathway of tyrosine metabolism. The metabolite in green box represents the positive ID, orange box represents the putative ID, and blue box represents no ID, and the box plots of identified metabolites are displayed beside the corresponding metabolites. E, ethanol; CLPs, cyclic lipopeptide group.

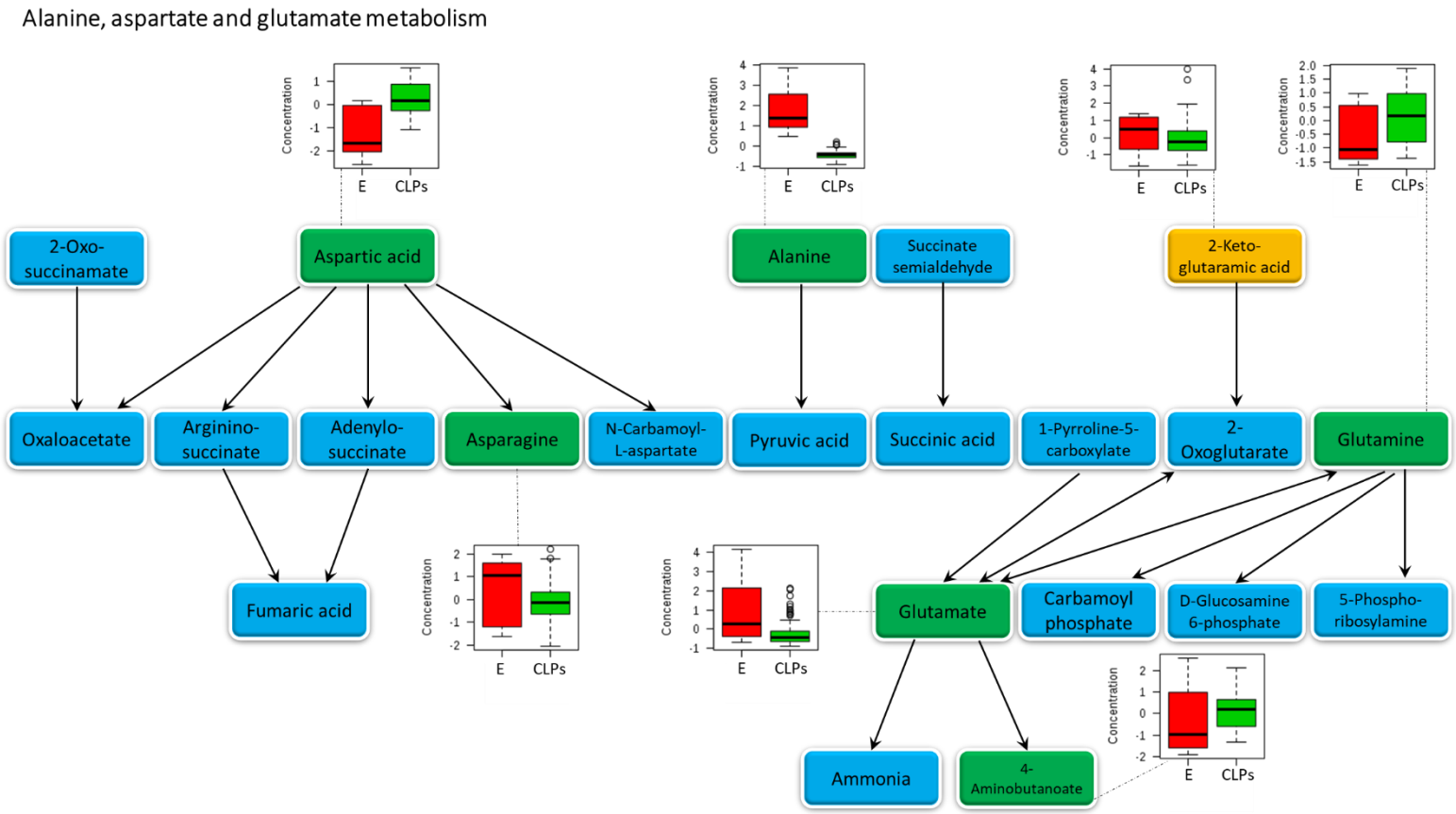

Fig. 3.28 Pathway of alanine, aspartate and glutamate metabolism. The metabolite in green box represents the positive ID, orange box represents the putative ID, and blue box represents no ID, and the box plots of identified metabolites are displayed beside the corresponding metabolites. E, ethanol; CLPs, cyclic lipopeptide group.

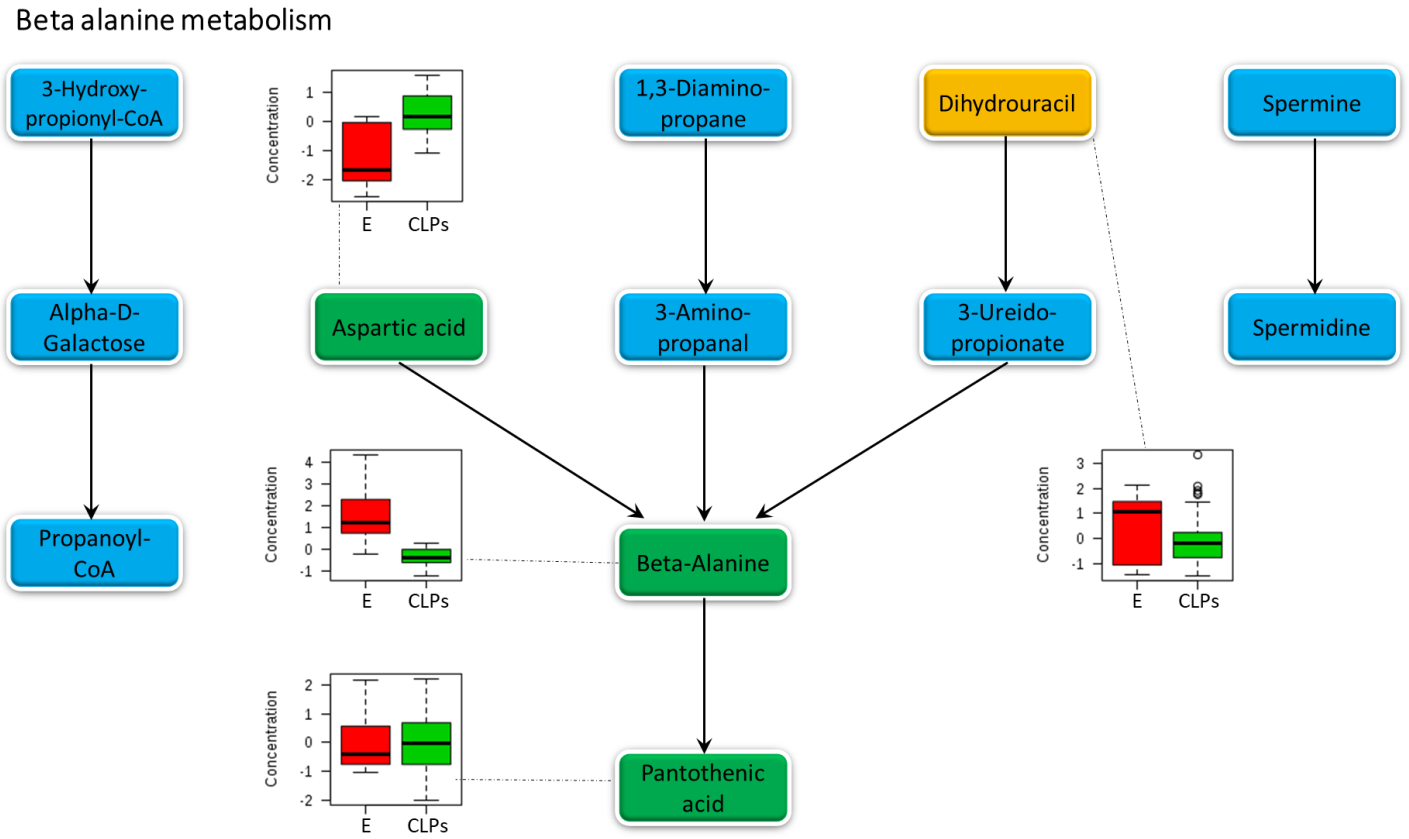

Fig. 3.29 Pathway of beta alanine metabolism. The metabolite in green box represents the positive ID, orange box represents the putative ID, and blue box represents no ID, and the box plots of identified metabolites are displayed beside the corresponding metabolites. E, ethanol; CLPs, cyclic lipopeptide group.

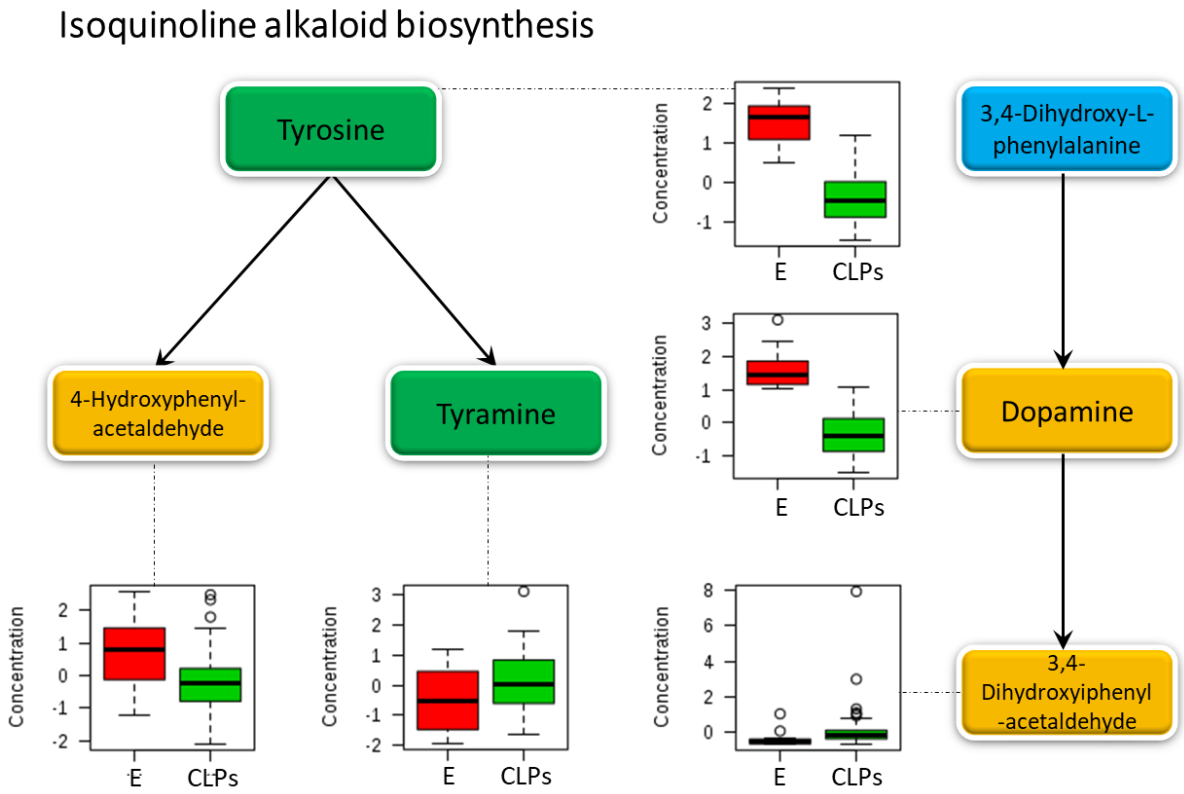

Fig. 3.30 Pathway of isoquinoline alkaloid biosynthesis. The metabolite in green box represents the positive ID, orange box represents the putative ID, and blue box represents no ID, and the box plots of identified metabolites are displayed beside the corresponding metabolites. E, ethanol; CLPs, cyclic lipopeptide group.

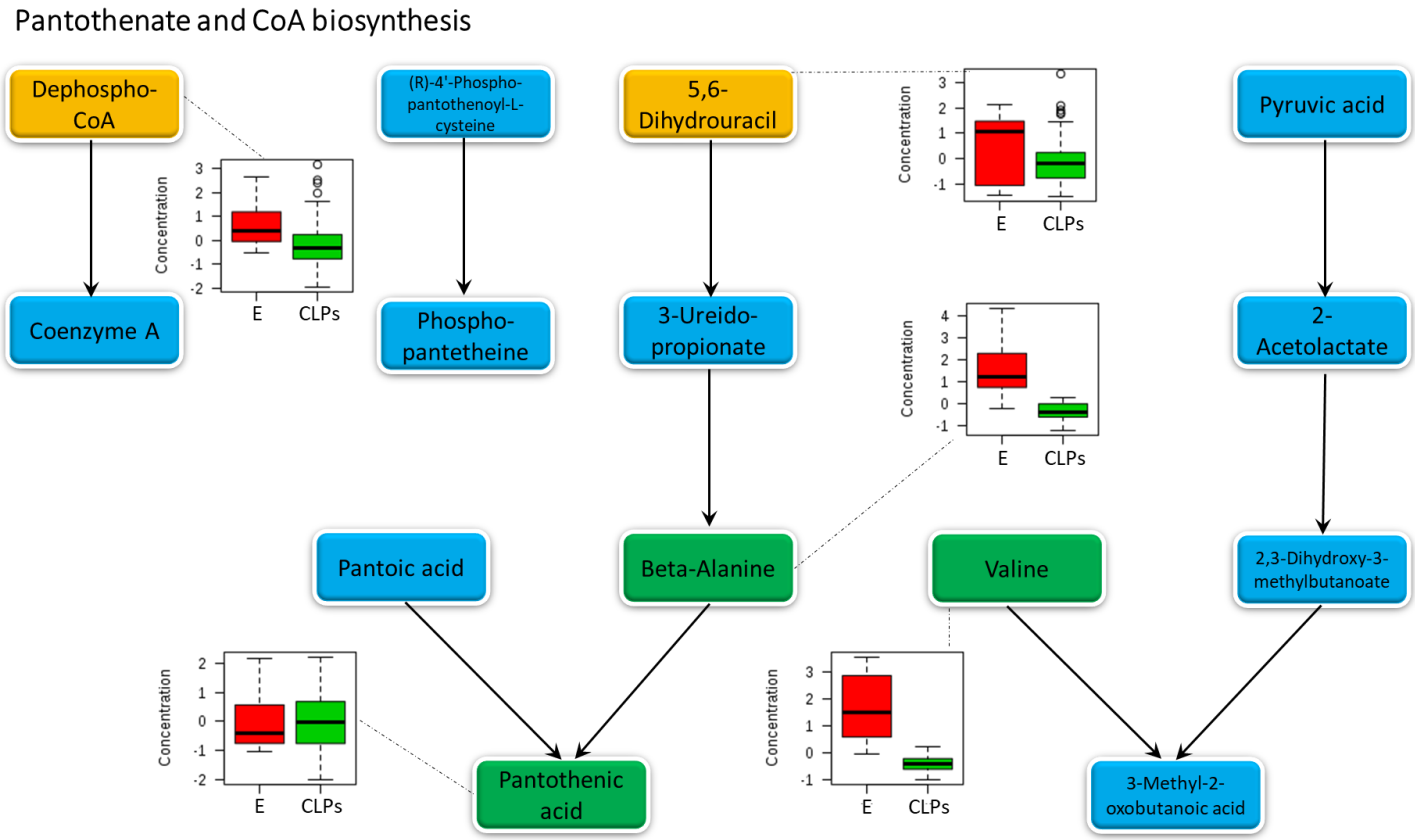

Fig. 3.31 Pathway of pantothenate and CoA biosynthesis. The metabolite in green box represents the positive ID, orange box represents the putative ID, and blue box represents no ID, and the box plots of identified metabolites are displayed beside the corresponding metabolites. E, ethanol; CLPs, cyclic lipopeptide group.

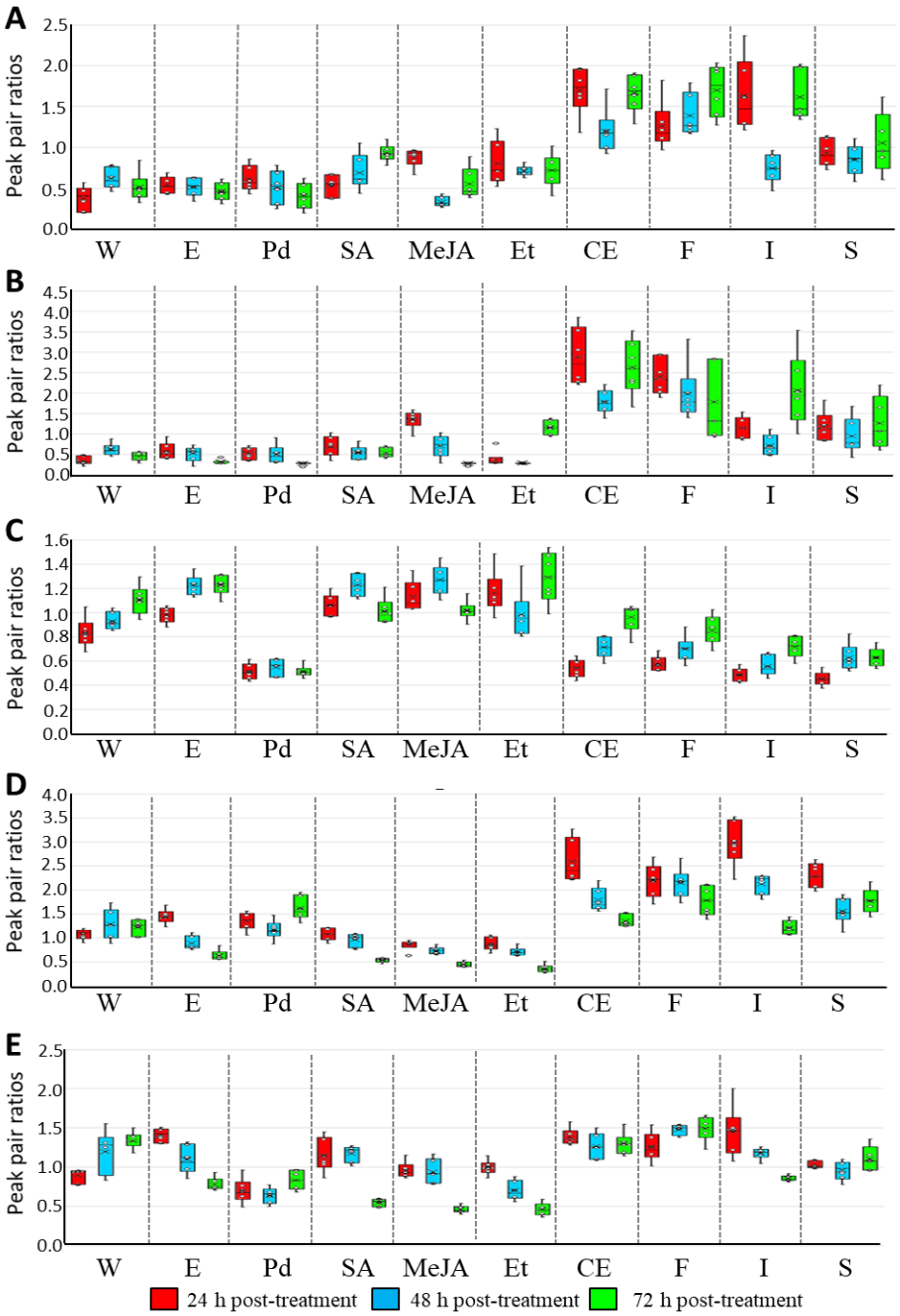

Fig. 3.32 Box plots of positively identified metabolites related to plant defense pathway. (A) serotonin, (B) 5-hydroxy-N-methyltryptamine, (C) tyrosine, (D) tyramine/tyrosine, and (E) tyramine. Tyr, tyrosine; W, sterile distilled water; E, ethanol; Pd, *Penicillium digitatum*; SA, salicylic acid; MeJA, methyl jasmonate; Et, ethephon; CE, CLP extract; F, fengycin; I, iturin A; S, surfactin. Vertical bars represent standard errors of the mean value of six trials.

CHAPTER 4

DISCUSSION

The work described herein focused on the changes of transcript pattern of genes involved in the signal transduction pathway, including PR proteins and the analysis of changes in protein abundance based on the proteomic study of mandarin fruit responding to CLP extract and exogenous plant hormones with and without fungal infection. Evidences that have been reviewed in many reports revealed the secondary metabolites of *B. subtillis* strains, produced and excreted into the medium culture. A strong antifungal activity against the growth and spore germination of several pathogenic fungi were exhibited, such as *Rhizoctonia solani*, *Penicillium digitatum* (Leelasuphakul et al., 2006, 2008), *Aspergillus flavus* (Gong et al., 2014), *Sclerotinia sclerotiorum* (Kumar et al., 2012), *P. roqueforti* (Chitarra et al., 2003), *Gaeumannomyces graminis* (Yang et al., 2015). The secondary metabolites produced by *B. subtillis* ABS-S14 so called CLPs were used in this experiment. The cell-free supernatant and CLP extract gave the consistent results with previous findings that showed the remarkable inhibition on the mycelial growth of *P. digitatum*. Moreover, CLP production of *B. subtilis* ABS-S14 comprised three main families; fengycins, iturins, and surfactin after RP-HPLC and MALDI-TOF MS analysis, they were corresponded to those detected in a previous report (Waewthongrak et al., 2014).

4.1 Transcription and proteome analysis of defense-related genes in mandarins triggered by *B. subtilis* CLP extract and exogenous plant hormones upon *P. digitatum* infection

In the event of a plant being attacked, the host plant's immunity is primarily activated to provide signal molecules to other parts of the plant in order to respond to the attacking pathogen. Sequential pathways in plant are elicited, such as those in both SAR and ISR which contribute to the plant's defense mechanism. Moreover, during ISR, CLP members produced by *Bacillus* spp. are well-known as one of the most powerful chemicals in mediating the defense response mechanism to protect the host plant. JA

and ET are also important hormones in the regulation of rhizobacteria-mediated ISR, as reviewed by Pieterse et al. (2014). Rhizobacteria-mediated ISR was initially thought to be mechanistically similar to pathogen-induced SAR and has been shown to have a broad spectrum effectiveness. To provide clear evidence that the *Bacillus* strain has the ability to trigger the key genes in the plant hormone regulating signaling pathways, the effect of CLPs produced by *B. subtilis*-S14 on the immune response to green mold infection in postharvest mandarins was investigated and compared to those of the applied exogenous plant hormones.

4.1.1 Effect of *B. subtilis* CLP extract and exogenous plant hormones on gene expression and protein production involving in plant defense mechanism

The mechanisms that citrus fruit use to protect themselves from stresses and infections have been intensively studied. These mechanisms include transcriptomic responses to *P. digitatum* infection on ISR genes, including genes involved in the phenylpropanoid biosynthetic pathway, and pathogenesis-related proteins, and it has been demonstrated that the enzymes remain active and are retained over time after induction (Ballester et al., 2010; González-Candelas et al., 2010). The patterns of *PAL*, *LOX*, and *ACS1* gene expression in the treated mandarin tissues based on both transcription and proteome patterns present in current work confirmed that *B. subtilis* CLP extract activated the key genes which are well-known as being involved in the SA and ET signaling pathways which promote the plant's immunity response to stresses (Lu et al., 2014; Shine et al., 2018). These findings are in agreement with the effect of CLP extract from *B. subtilis* on the induction of PAL enzyme activity in infected mandarin tissues (Waewthongrak et al., 2015) including the effects of the fengycin and surfactin in *B. subtilis* CLP extract on *ACS1* gene expression (Chandler et al., 2015). The present work also elucidated the occurrence of early gene activation by CLP extract involving in the SA and ET signaling pathways leading to up regulation in production of the precursors of the plant's defensive proteins.

The group of *PR* genes is affected by SAR via the SA signaling pathway and ISR via the JA, and ET signaling pathways which trigger the plant's immunity. In the present work exogenous plant hormones and CLP extract had distinct effects in eliciting *PR* gene expression in treated mandarins. CLP extract showed the minor effect among the various treatments to induce *CHI* gene expression both with and without fungal attack. When mandarins were exposed to fungal infection, CLP extract elicited more abundances of *GLU* and *POD* transcripts than those found in the non-infection treatments. *CHI*, *GLU*, and *POD* are classified as *PR* genes. *CHI* was reported in *PR3*, *PR4*, and *PR11* forms while *GLU* was reported as *PR2* and *POD* as *PR9* (Ali et al., 2018). *PR1*, *GLU* (*PR2*), and *POD* (*PR9*) play an important role in inducing plant defensive mechanisms via SAR signaling pathway (Ali et al., 2018; Coqueiro et al., 2015), while *CHI* (*PR3* and *PR4*) were reported to be involved in plant immunity involving the ISR mechanism (Ali et al., 2018), which functions through the JA and ET signaling pathways (reviewed in Pieterse et al., 2014). The high expression of *PR1* in fruit tissues by SA elicitation in the current study agreed with the previous study (Zhang et al., 2010) which reported enhanced *PR1* transcript abundance due to SA induction. *B. subtilis*-S14 CLP extract showed a greater effect than did exogenous plant hormones in inducing *PR1* accumulation at later time point (72 h post-treatment) during *P. digitatum* infection. *PR1* transcription was reported to be increased by the induction of iturin A (Kawagoe et al., 2015).

The results of proteomic profiling demonstrated the existence of PAL3, LOX, ACS, CHI (PR4), GLU, POD, and PR1 proteins in the fruit tissues activated by both CLPs and exogenous plant hormones during wound stress, and these proteins were found in all the treatments. CLP extract showed the same ability as exogenous plant hormones to regulate the production of these proteins in the signal transduction pathways in host plants. The absence of the PAL and PR1 proteins, which are important in SAR in triggering the plant's resistance system was notable in this study when CLP extract was applied to the flavedo during fungal infection. This finding is in agreement with a previous report of fengycin and iturin A lacking the power to induce *PR1* when exposed to pathogens in maize seeds (Gond et al., 2015). CLP extract and exogenous plant hormones mostly

participated in the enhancement of LOX, ACS, CHI, GLU, and POD protein accumulations during green mold attack. It was of interest that ISR associated with *B. subtilis* appears to be an important system in mandarin fruit in triggering host immunity and producing stress responses during fungal infections as previously reported (Waewthongrak et al., 2014; Waewthongrak et al., 2015). This finding confirms that CLP extract has potential as an elicitor to increase the production of proteins which involved in ISR signaling pathway responding to stress.

4.1.2 Effect of *B. subtilis* CLP extract on inducing defensive protein production in mandarins during non-*P. digitatum* infection

The induction of plant defensive proteins by CLP extract obtained from *B. subtilis* ABS-S14 and exogenous plant hormones with and without fungal infection revealed the unique proteins which play major roles in distinct pathways. It is interesting to note that CLP extract showed an ability to induce important proteins which were not found in the exogenous plant hormone treatments. However, CLP extract has the same effect as exogenous plant hormones in the SA, JA and ET signaling pathways through activating the biosynthesis of common proteins which were present in the exogenous plant hormone treatments. This is the first report to demonstrate that CLP extract possesses the unique ability to activate CRCK2, MoCo sulfurase, and NAD+-dependent glyceraldehyde-3-phosphate dehydrogenase. These proteins were not activated by exogenous plant hormones, but are known to be involved in plant defensive mechanisms responding to stresses. CRCK2 was reported to be involved in signaling transduction for plant development (Boavida et al., 2009) and interacts with calmodulin (CaM), a Ca^{2+} sensor protein, which plays a vital role in the Ca^{2+} signaling pathway in response to stress (Zeng et al., 2015). Moreover, some common proteins which related to Ca^{2+} signaling pathway were found in the CLP extract treatment of this study such as calcium/calmodulin dependent protein kinase kinase 1, calcium-binding protein, and calcium-dependent protein kinase. MoCo sulfurase was reported to contribute to significantly increased expression of genes related to abscisic (ABA) signaling transduction during drought

stress (Lu et al., 2013) and it is a co-factor required by aldehyde oxidase, which functions in the last step of ABA biosynthesis in response to stress (Xiong et al., 2001). To support the effect of CLP extract on activation of ABA signaling pathway, some common proteins such as abscisic acid receptor PYL9, ABA-insensitive 5-like protein, and transcription factor ABA-inducible bHLH-type-like were discovered in CLP extract treatment. In addition, NAD+-dependent glyceraldehyde-3-phosphate dehydrogenase is an enzyme which catalyzes D-glyceraldehyde 3-phosphate to 3-phosphoglycerate (Brunner et al., 1998) in glycolysis relating to energy metabolism. This enzyme was reported to interact with the plasma membrane-associated phospholipase D which was also revealed in the proteome analysed data in this study to transduce H_2O_2 signals via reactive oxygen species (ROS) in response to stress (Guo et al., 2012). It could, therefore, be suggested that CLP extract might play a major role in stress responses by enhancing the protein production involved in Ca^{2+} signaling pathway, ABA signal transduction, energy metabolism and ROS signal transduction. It was the same manner as shown in the previous study (Ma et al., 2017), which reported that CLPs triggered plant resistance via the ABA signaling pathway.

4.1.3 Elicitation of defensive protein production in mandarin fruit by *B. subtilis* CLP extract during *P. digitatum* infection

CLP extract empowers the plant's immunity by enhancing its defensive gene expression and the production of proteins in mandarins during postharvest period with or without fungal infection. The proteomic pattern of CLP extract induction during *P. digitatum* infection was different from that without fungal infection. The total number of proteins identified decreased when the mandarin fruit were treated with exogenous plant hormones and CLP extract and also exposed to the fungal pathogen.

CLP extract obtained from *B. subtilis* ABS-S14 after being applied to the peel of mandarin fruit during *P. digitatum* attack and of it being the only elicitor to cause production of the Ubc protein, corresponded to that as was reported in the recent study (Zhou et al., 2017). Ubc was demonstrated to play a role in ubiquitination, which aids the

plant's immunity against pathogens. In this study, ubiquitin-activating enzyme (E1), ubiquitin-conjugating enzyme (E2), and ubiquitin-protein ligase (E3), all of which facilitate the ubiquitin pathway, were discovered and identified following CLP extract induction. Similarly, Ubc was reported to be involved in the ubiquitin pathway which plays a role responding to stress (Belknap and Garbarino, 1996). This finding suggests that CLP extract increase Ubc production serving for ubiquitination, which degraded the abnormal proteins, which occur during infection, in order to maintain the environmental conditions in the cell, through the mechanism reported in the previous study of Sharma et al.(2016). Furthermore, CLP extract also triggered the proteins which were commonly found in the exogenous plant hormone treatments during fungal infection. This might explain the fact that CLP extract elicits plant immunity via the ubiquitination process and at the same time triggers the defensive proteins which play a role in plant hormone signal transduction.

4.1.4 Difference in regulation of specific protein production in mandarins treated with *B. subtilis* CLP extract followed by fungal and non-fungal infection

The effect of CLP extract in the induction of plant defensive proteins which elicit immunity in mandarin fruit in response to stresses with and without *P. digitatum* attack, revealed a distinct pattern in the proteome. CLP extract elicited different kinds of proteins in response to stress, such as the Ca^{2+} signaling pathway, glycolysis, ROS, and ABA signal transduction. These were significantly up-regulated productions in fruit tissues by CLP extract only in non-fungal infection treatment, but the ubiquitin pathway was vitally activated during fungal infection. However, there were five common proteins with specific functions, which presented in all the non-fungal infected treatments, were also detected in the fungal-infection treatments with exogenous plant hormones and CLP extract. Biological function characterization of these proteins was shown that CRCK2 is a mediator in signaling transduction for plant development (Boavida et al., 2009) including in the Ca^{2+} signaling pathway (Zeng et al., 2015). The mechanism of Ca^{2+} signal transduction may be controlled by the ubiquitin-proteasome process in the plant's defense response (Zhang et al., 2014). Trans-2-enoyl-CoA reductase is an enzyme which was reported to catalyze

the reduction of enoyl-CoA to acyl-CoA which is related to fatty acid and polyketide biosynthesis, including NAD(P)H-dependent acyl-CoA synthesis (Hoffmeister et al., 2005). LAGLIDADG homing endonucleases (LHEs) are DNA cleaving enzymes also called meganucleases (Taylor et al., 2012) and are responsible for unique catalytic activity, being comprised largely of amino acid residues (Epinat et al., 2003). Mitochondrial pyruvate carrier 1-like is a mitochondrial pyruvate carrier functioning as a transporter to send pyruvate to cytosol for cellular substance and energy metabolism and it has also been reported to associate with ABA for stomatal movements in *Arabidopsis* (Wang et al., 2014). Non-LRT retroelement reverse transcriptase was reported to be present in *Arabidopsis* pollen (Loraine et al., 2013) and it was observed that these proteins might be necessary during fungal infection to enhance the attack of green mold rot.

In addition, four proteins which played an important role during fungal attack were found in the treatments without fungal infection, but with induction by exogenous plant hormones and CLP. Annexin D8 is a form of annexin present in stress responses (Cantero et al., 2006) and it functions in the host plant as a Ca^{2+}-permeable signal of an oxidized membrane which activates ROS signaling transduction (Laohavisit et al., 2010). ABC transporter I family member 6 is a member of the ABC transporter family which function as transporters related to detoxification mechanisms including those active in plant development and stress responses (Kang et al., 2011). Carboxylesterase 6 is a multiple carboxyesterase, which were reported to work like phytotoxic acids on hydrolysis via herbicide esters (Gershater et al., 2007). Shaggy-related protein kinase epsilon is a shaggy-like kinase which is presented by a plant during stress as a process in the plant's development system (Charrier et al., 2002). It is intriguing that these proteins were all suppressed during fungal infection, but some elicitors had the power to trigger them as part of stress responses.

A hypothetical model of action of *B. subtilis* CLP extract in activating plant defense in mandarin fruit with and without *P. digitatum* invasion were shown as in Fig. 4.1.

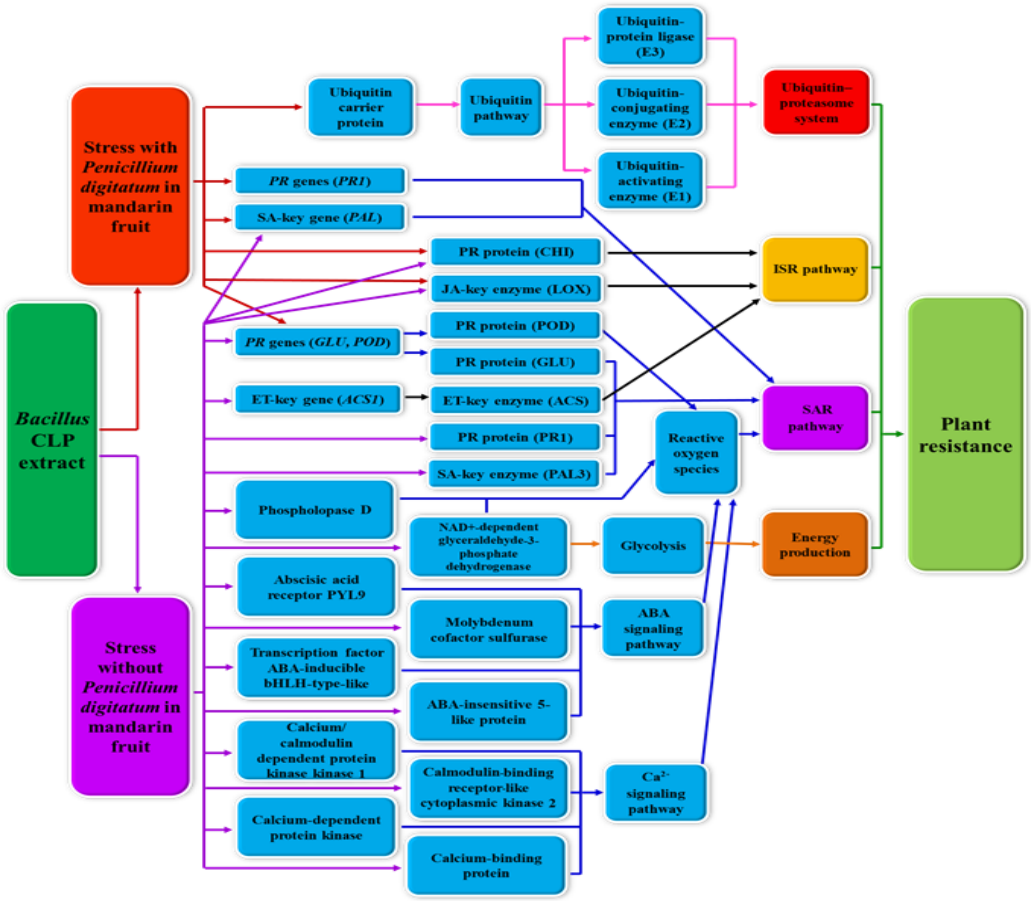

Fig. 4.1 Proposed model of *Bacillus* CLP extract to induce plant resistance in postharvest mandarin fruit with and without *P. digitatum* infection. CLP extract in non-*P. digitatum* infection treatment increased the protein production in Ca^{2+} signaling pathway, ABA signaling pathway, and glycolysis for energy production including ROS signaling pathway. Ca^{2+} and ABA signaling pathways also affected ROS signaling pathway which elicits SAR pathway for plant resistance and ubiquitin-proteasome system was elicited during fungal invasion. Furthermore, CLP extract triggered the expression of *PAL*, *GLU*, *POD*, *PR1* genes or proteins resulting in activation of SAR pathway for plant resistance. CLP extract also activated ISR pathway by enhancing expression of *ACS1* gene and production of LOX and CHI protein in mandarin fruit. (Arrows in purple, responding to stress; red arrow, responding to fungal infection; blue, activating SAR pathway; black, ISR pathway; pink, ubiquitin/proteasome system; orange, responding to energy production; green, activating plant defense).

4.2 Transcriptional analysis and targeted proteomics derived from individual CLP-protein binding assay to elucidating ISR elicitation of mandarin resistance during *P. digitatum* infection

Innate immune responses in plants were induced by creating biotic stresses based on a pathogen infection. The activation of defense pathways employed systemic signaling molecules, termed 'phytohormones', which regulated various stages of the development and coordination of defense responses. The induction of the defense response in higher plants was shown to be widely triggered by non-pathogenic rhizobacteria which increase the plant's systemic resistance to subsequent pathogen challenge (Ongena and Jacques, 2008). Elicitors like lipopeptides with varying sizes and lengths of lipid tails such as the CLPs produced by the rhizobacteria *Bacillus* species, are powerful in stimulating ISRs in many plants as has been shown in previous work, particularly in citrus biocontrol (Lopes et al., 2018; Waewthongrak et al., 2014). *In vivo* experiments with the control of green mold fungus in postharvest citrus fruit by *B.* citrus *subtilis* and its CLPs has demonstrated their effectiveness in eliciting ISRs in flavedo tissues. This data leads to the question of how different CLPs act on the priming process and signal transduction pathways to increase the defense response. In this study, the mechanisms by which fengycin, iturin A, and surfactin initiate host plant stimulation in response to stress and the expression of the genes which play key roles in plant defense were investigated proteomic profiling was conducted and the specific defensive proteins were established by a CLP-protein association assay.

4.2.1 Effect of *B. subtilis* individual CLP on gene expression that are involved in plant defense mechanism

ISR is an important system for protecting a host plant from pathogens by the induction of phenylpropanoid pathways including the JA and ET signaling pathways (Romanazzi et al., 2016). All the CLPs obtained from *B. subtlis*-S14 were able to boost the abundance of *PAL* transcripts. However, fengycin and iturin A showed powerful

enhancement of *PAL* gene expression at the earliest time post-treatment during wound stress and fungal infection. The *PAL* gene plays a crucial role not only in SA biosynthesis, but also in the phenylpropanoid pathway which produces lignins, flavanoids, and coumarins as weapons against pathogens (Zhang and Liu, 2015). The results obtained in this study were similar to those achieved in a previous study of PAL enzyme activity elicited by *B. subtlis*-S14 CLPs in infected mandarin fruit (Waewthongrak et al., 2015). Further, iturin A showed better ability to amplify the level of *LOX* transcripts than other CLPs as a reaction to wound stress. An invasion of green mold in citrus flavedo increased the expression of the *LOX* gene at an early stage which was equal to that found in the surfactin treatment at a later time point. This result was similar to that established in a previous study which investigated the action of surfactin in citrus flavedo tissues during fungal attack (Waewthongrak et al., 2014).

The current study reveals that fengycin and iturin A possess a high potential to trigger the *ACS1* and *ACO* productions, even without green mold attack at 24 h and 48 h post-treatment, respectively. During fungal infection, iturin A was the best elicitor triggering *ACS1* and *ACO* transcriptions. These results agreed with a previous work that reported the induction of the *ACS1* transcription level elicited by fengycin and the iturin family in the ET signaling pathway in rice (Chandler et al., 2015). However, the accumulation of JA is dependent on the expression of the *LOX* gene (Kazan and Manners, 2008), and for ET production, *ACS* and *ACO* gene expression are required (Wang et al., 2002). Therefore, the present work firstly demonstrates that fengycin, iturin A and surfactin stimulate the immune system via the JA/ ET signal transduction pathways to promote the activation of *PR* gene expression in mandarins which leads to PR protein synthesis with antimicrobial and antifungal compounds active against pathogens, as shown in previous reports (Ali et al., 2018; Kawagoe et al., 2015; Ongena et al., 2007).

Increase in PR protein production is known to be one of a host plant's strategies to protect itself from pathogen attack (Ali et al., 2018). The present investigation demonstrates the potent action of *B. subtlis* CLPs on inducing *PR* gene expression of PR proteins like *CHI*, *GLU*, *POD*, and *PR1* in mandarins. The potential of fengycin, iturin A,

and surfactin to stimulating the accumulation of transcripts of *CHI* was showed at 24, 48, and 72 h post-treatment during wound stress. Interestingly however, only in the fengycin treatment the expression of *CHI* did increase in mandarin flavedo during fungal invasion, Moreover, this trend was similarly observed in the iturin A treatment on the induction of *GLU* gene expression in response to wound stress although the greatest accumulation of *GLU* transcript abundance during fungal infection was detected in the fengycin treatment. Surfactin has the ability to enhance *POD* expression both with and without fungal attack. *PR1* abundance reached its highest level at 48 h in the flavedo tissues treated with iturin A, both with and without green mold infection, while surfactin co-applied with *P. digitatum* triggered the greatest level of *PR1* transcription at 24 and 72 h post-treatment. These results correspond to previous works that have reported the effect of fengycin, iturin A, and surfactin on the activation of *CHI*, *GLU*, and *POD* in mandarin fruit with fungal infection (Waewthongrak et al., 2014), as well as the enhancement of the *PR1* gene by iturin A elicitation in *Arabidopsis* plants (Kawagoe et al., 2015). It can, therefore, be concluded that *B. subtlis*-S14 CLPs are potent elicitors activating the key genes in the phenylpropanoid pathway and JA, and ET biosynthesis, which results in the elicitation of *PR* gene expression in mandarins.

4.2.2 Activation of plant defensive protein production by *B. subtilis* individual CLP

In the present study CLPs were found to induce the flavedo tissues of mandarin fruit to synthesize various plant defensive proteins which are associated with many significant pathways vital to plant immunity against *P. digitatum* invasion or responding to other stresses. This work focused on the functionally active proteins discovered in the fengycin, iturin A and surfactin treatments which are associated with significant biological processes in plant defense during wound stress and green mold infection. Four proteins present in the fengycin treated flavedo's response to wound stress are major proteins those are involved in most important biological processes. For examples, the ABC1 family protein which is involved in plant development and supports secondary metabolite accumulation for plant defense (Hwang et al., 2016), and also

functions in the ubiquinone biosynthetic process (Chen et al., 2017). Ubiquinone plays a crucial role relating to reactive oxygen species (ROS) in stress responses (Liu and Lu, 2016). Glutamate synthase functions in the glutamate biosynthetic process (Chen et al., 2017) and glutamate metabolism is involved in plant defense by playing a role in amino acid metabolism and other crucial metabolic functions (Seifi et al., 2013). PR genes transcriptional activators play an interesting role in defense responses (Chen et al., 2017) and support the expression of *PR* genes, which are pivotal weapons in responding to stress (Ali et al., 2018). Lastly, peptidoglycan-binding LysM domain-containing protein is linked to microbe-associated molecular patterns (MAMP) (Gust, 2015) in immunity responses (Chen et al., 2017). However, in this study no unique protein appeared in the fengycin treatment during fungal infection.

In the iturin A treatment, distinct patterns of proteins of the flavedo tissues were revealed in both with and without fungal attack. Seven characterized proteins discovered in the iturin A treated mandarins are known to play a role in a plant's response to stress. They are (1) Agmatine coumaroyltransferase, which has the ability to enhance the *Arabidopsis* plant's immunity response for defense against stress (Muroi et al., 2012) (Chen et al., 2017). (2) Auxin-responsive protein IAA16-like, and (3) NAC domain-containing protein 21/22-like, which functions in the auxin-activated signaling pathway (Chen et al., 2017). Auxin is a phytohormone in plants acting in plant growth and plant defense. Auxin signaling shares a lot of common components with JA signaling, resulting in plant resistance outcomes (Kazan and Manners, 2009). (4) Copalyl diphosphate synthase (CPS) plays a pivotal role in the gibberellin biosynthetic process (Chen et al., 2017). CPS was reported to function in plant growth and plant defense via the biosynthesis of phytoalexins (Toyomasu et al., 2015). (5) Cytochrome P450 (CYP) 709B2 which is produced in response to stress (Chen et al., 2017). CYP acts as a defensive protein by its involvement in secondary metabolite and phytoalexin biosynthesis, including hormone metabolism (Xu et al., 2015). (6) POD N1, which is connected to the response to oxidative stress (Chen et al., 2017). POD has many roles in physiological processes for plant resistance such as lignin and suberin formation, phytoalexin biosynthesis, and ROS

metabolism (Almagro et al., 2009). Finally, (7) raffinose synthase, which is related to the abscisic acid (ABA) response (Chen et al., 2017; Sui et al., 2012). ABA is involved in plant defense due to its healing properties and plays a role in defending against environmental stress (Wasilewska et al., 2008). Noticeably, higher numbers of unique proteins were observed to be activated by iturin A in stress response than iturin A co-applied with the fungal pathogen. In the treatment of iturin A co-applied with *P. digitatum*, two unique proteins were stimulated, F-box and leucine rich repeat domains containing protein, which is related to the ubiquitin-dependent protein catabolic process (Chen et al., 2017). Ubiquitin is a vital component in the ubiquitin pathway which is instrumental in responding to stress (Belknap and Garbarino, 1996). Furthermore, ubiquitination plays a role in the defense mechanism by degrading the abnormal proteins which appear during infection (Sharma et al., 2016). A second protein was discovered in this work, namely two-component response regulator-like APRR2 which functions in the phosphorelay signal transduction system (Chen et al., 2017). Phosphorelays have been reported to be implicated in cytokinin regulation and signal responses for higher plants in response to bacteria (Hoch, 2000).

In wound stress, the results from the surfactin-treated flavedo tissues revealed that two unique proteins are involved in the biological processes of interest relating to the plant hormone pathway. (1) Auxin transport protein BIG-like and (2) calcium-dependent protein kinase 33, which are associated with the auxin-activated (Chen et al., 2017; Kazan and Manners, 2009) and abscisic acid-activated signaling pathway (Chen et al., 2017; Wasilewska et al., 2008), respectively. Furthermore, DNA-directed RNA polymerase I subunit rpa1 was the only unique protein detected in the surfactin treatment co-applied with *P. digitatum,* which functions in the negative regulation of protein localization to the nucleolus (Chen et al., 2017). Therefore, CLPs alone were able to trigger unique proteins, which functioned directly via ABA-, gibberellin-, auxin-signal transductions, ubiquitination, and ROS metabolism to promote the plant defense response during wound stress and fungal infection as reported in previous work (Chandler et al., 2015). A hypothetical model of action of *B. subtilis* fengycin, iturin A, and surfactin

in activating plant defense in mandarin fruit with and without *P. digitatum* invasion were shown as in Fig. 4.2-4.4, respectively.

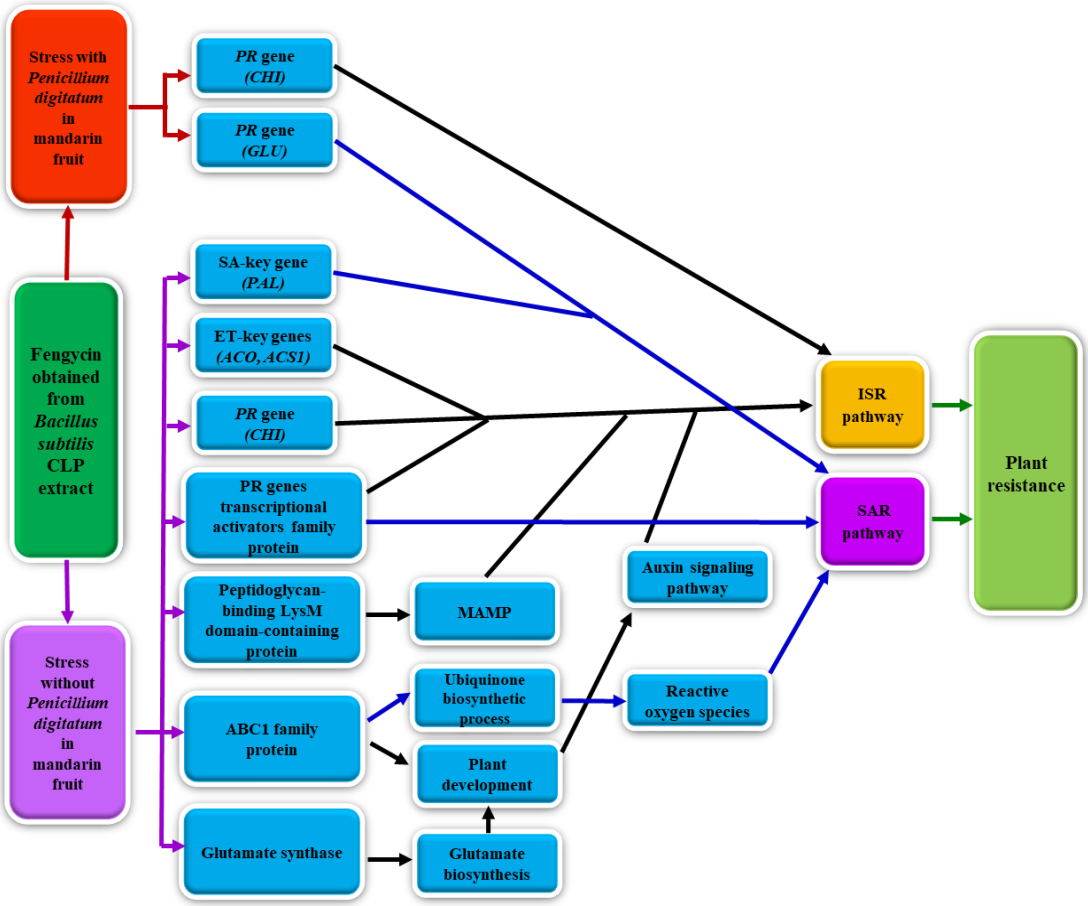

Fig. 4.2 Proposed model of fengycin to induce plant resistance in postharvest mandarin fruit with and without *P. digitatum* infection. Fengycin in non-*P. digitatum* infection treatment increased the protein production in MAMP, ubiquinone biosynthetic process, glutamate biosynthesis, and plant development which affected by auxin signaling pathway resulting in ISR activation. Ubiquinone biosynthetic process affected ROS pathway resulting in SAR induction for plant resistance. Furthermore, fengycin triggered the expression of *PAL* and *GLU* genes resulting in activation of SAR pathway. Fengycin also activated ISR pathway by enhancing expression of *ACS1, ACO*, and *CHI* genes in mandarin fruit. (Arrows in purple, responding to stress; red arrow, responding to fungal infection; blue, activating SAR pathway; black, ISR pathway; green, activating plant defense).

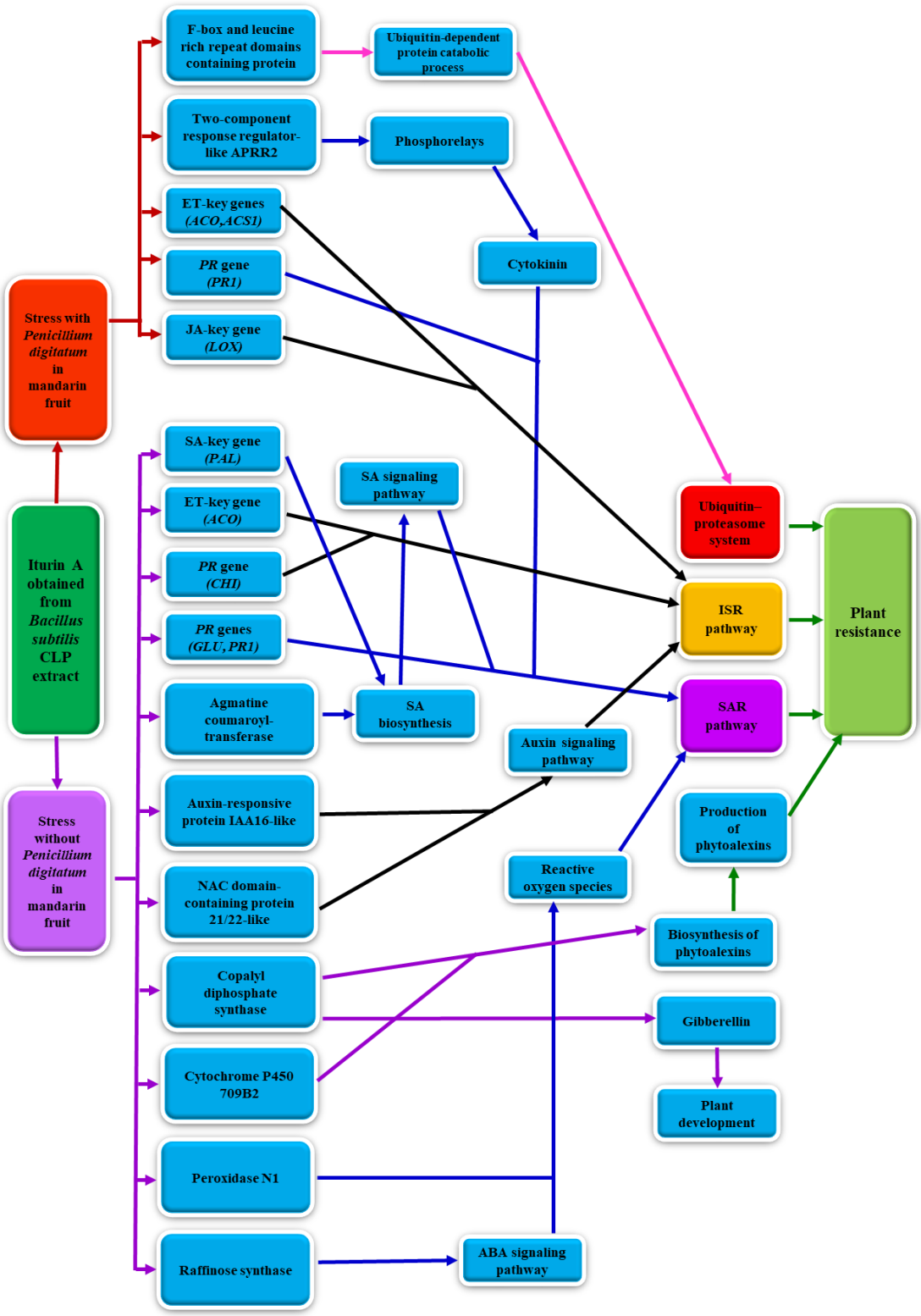

Fig. 4.3 Proposed model of iturin A to induce plant resistance in postharvest mandarin fruit with and without *P. digitatum* infection. Iturin A treatments increased the

protein production in SA biosynthesis, which is affected SA signaling pathway, ABA signal transduction (affecting ROS pathway), and phosphorelays (affecting cytokinin signaling pathway) resulting in SAR activation for plant resistance. Including an increase protein production in auxin signaling pathway for ISR elicitation. Iturin A also enhances plant resistance by increasing the production of proteins which involve in phytoalexin biosynthesis and gibberellin for plant development. Ubiquitin/proteasome system is also affected by the induction of iturin A during fungal infection. Furthermore, iturin A triggered the expression of *PAL, GLU,* and *PR1* genes resulting in activation of SAR pathway. ISR pathway was also acitivaed in iturin A treatments by enhancing expression of *LOX, ACS1, ACO*, and *CHI* genes in mandarin fruit. (Arrows in purple, responding to stress; red arrow, responding to fungal infection; blue, activating SAR pathway; black, ISR pathway; pink, ubiquitin/proteasome system; green, activating plant defense).

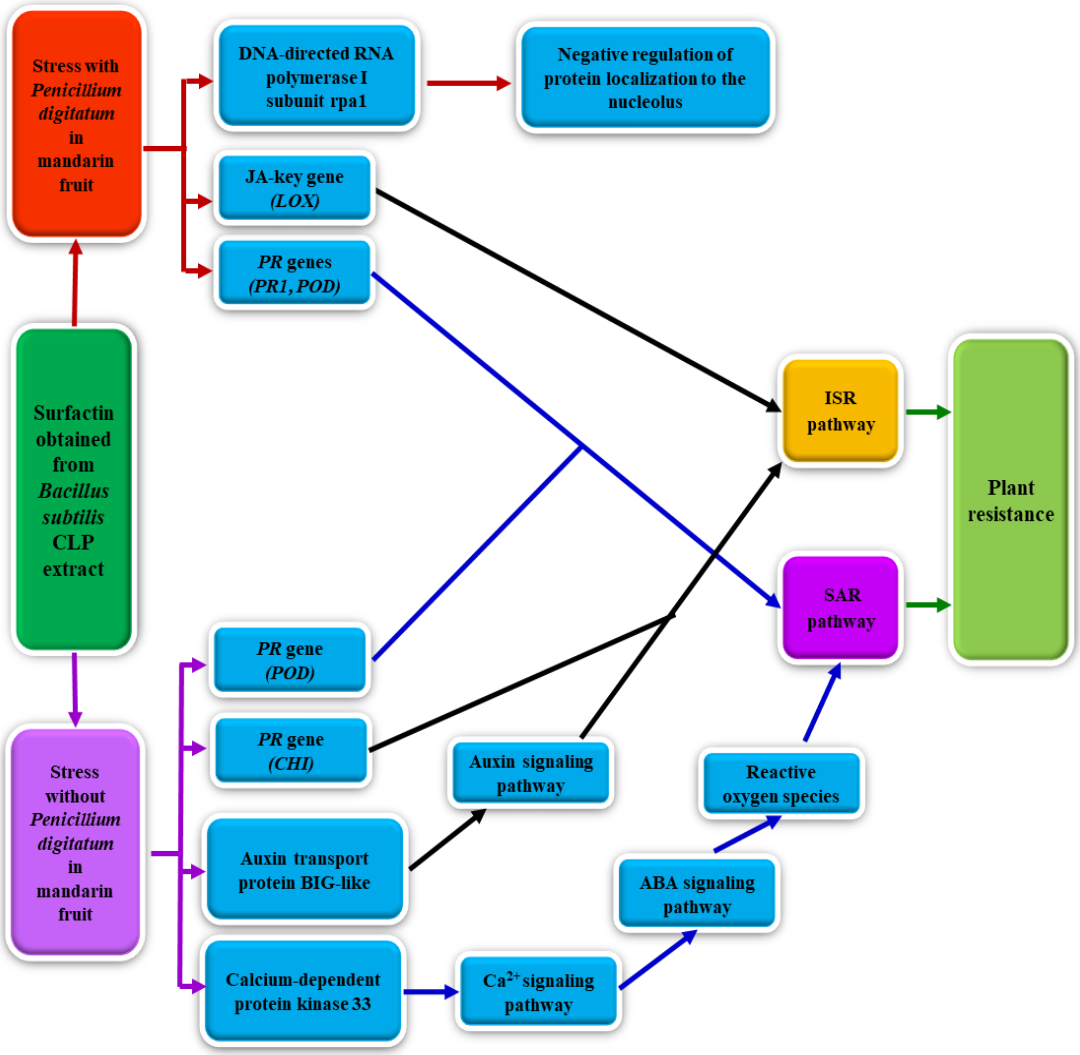

Fig. 4.4 Proposed model of surfactin to induce plant resistance in postharvest mandarin fruit with and without *P. digitatum* infection. Surfactin treatments increased the protein production in auxin signaling pathway, Ca^{2+} pathway which affected ABA signaling pathway. Resulting in ROS activation for SAR induction. During fungal infection, surfactin plays a role in negative regulator of protein localization in to the nucleus by enhancing the protein production involved in this system. Furthermore, surfactin triggered the expression of *POD* and *PR1* genes resulting in activation of SAR pathway. surfactin also activated ISR pathway by enhancing expression of *LOX* and *CHI* genes in mandarin fruit. (Arrows in purple, responding to stress; red arrow, responding to fungal infection; blue, activating SAR pathway; black, ISR pathway; green, activating plant defense).

4.2.3 Specific models of *B. subtilis* individual CLP on binding property to plant proteins implied for disease resistance

In this study, the binding of individual CLP to different targeted proteins occurring during wound stress or fungal infection was noted and the binding potentiality of fengycin, iturin A, and surfactin to the flavedo-extracted proteins obtained under the conditions of wound stress and green mold invasion was demonstrated. During fungal attack, fengycin had the ability to attach three unique proteins derived from host plant tissues, which were; 1) ATP-dependent DNA helicase Q-like SIM; 2) glycogen debranching enzyme; and 3) MYB-related protein 330, relating to DNA repair, glycogen catabolic process, and transcription, respectively, through biological processes, (Chen et al., 2017). One of the effects of fungal attack is DNA damage. Fengycin is able to trigger the proteins implicated in the DNA repair process, which is involved in the repair of lesions in DNA for specialized proteins and regulatory pathways (Gimenez and Manzano-Agugliaro, 2017). The glycogen catabolic process relates to the serving energy system (Cano et al., 2018). Moreover, MYB-related proteins have been reported to monitor the cell cycle in plants and to be involved in ABA-mediated responses (Ambawat et al., 2013).

The four unique proteins which showed up in the wound stress condition attaching to fengycin were (1) A/G-specific adenine DNA glycosylase; (2) flavin monooxygenase-like protein; (3) inner membrane protein yieG; and (4) ribosome-binding ATPase YchF, which have functions in base-excision repair, the oxidation-reduction process, transport, and the response to oxidative stress, respectively, through biological processes, (Chen et al., 2017). Base excision repair plays a role in correcting DNA damage or base lesions (Krokan and Bjoras, 2013). Flavin-containing monooxygenases affect the catalyzation of glucosinolates which are implicated in secondary metabolites and stress responses (Kong et al., 2016).

Interestingly, no unique binding protein was found in the non-fungal infected iturin A treatment. However, the three unique proteins attaching to iturin A following *P. digitatum* invasion were characterized as (1) 12-oxophytodienoate reductase 2; (2) beta subunit of RNA polymerase; and (3) UDP-N-acetylmuramoyl-L-alanyl-D-

glutamate-2,6-diaminopimelate ligase, which are associated with the oxylipin biosynthetic process, transcription, and cell wall organization, respectively, through biological processes (Chen et al., 2017). The oxylipin biosynthetic process produces an accumulation of JA, which plays a vital role in the JA signaling pathway for the elicitation of plant immunity (Kazan and Manners, 2008) and is effective in the production of PR proteins (Ali et al., 2018).

In addition, A/G-specific adenine DNA glycosylase was the only unique protein attaching to surfactin in the wound stress condition. This protein has been demonstrated to function in the base-excision repair process (Chen et al., 2017; Krokan and Bjoras, 2013). The mechanism of individual CLP attaching to unique proteins for plant resistance depends on the type of stress condition. Iturin A was able to attach to unique proteins from the fungal-infected flavedo tissues, whereas surfactin linked to a unique protein responding to wound stress and fengycin interacted with unique proteins in both conditions which gave rise to a plant defense response. Overall, fengycin may play a role in the enhancement of the plant's defensive-protein production system during wound stress and fungal infection by connecting to the proteins involved in the transcription process. Similarly, surfactin operated through an equivalent mechanism in the reaction to wound stress, while iturin A prefers to stimulate plant immunity via the JA signaling pathway for ISR activation against green mold infection, a different mechanism to that operating for fengycin and surfactin in the wound-stress response.

4.3 Metabolomic study of defense responses in mandarins upon applications of *B. subtilis* CLPs in comparison to plant hormones, and *P. digitatum* infection

Metabolomics of plant-microbe/biotic elicitor interactions using mandarin fruit and *B. subtilis* CLPs /exogenous plant hormones as well as *P. digitatum* as a model of study was firstly revealed in this report. Dansylation labeling method was employed and discovered and quantified many interesting metabolites that were involved in various pathways in the host plant, especially defense responses. The effects of each elicitor in major groups; CLPs, exogenous plant hormones, fungal pathogen and wound stress on

submetabolome profiles and identified metabolites had different levels of capability to trigger metabolite accumulations in the treated flavedo tissues. However, a close relationship between the exogenous plant hormones and wounding effects in metabolite induction was observed in their treatments at the early time point (24 h) and the late time points (48 and 72 h). They shared a common pathway in their metabolite regulation function in mandarin peel as it was previously demonstrated in citrus leaves that both Trp and serine were highly sensitive to stress treatments (Asai et al., 2017). The wounding and MeJA treatment showed that amino acid abundances like Trp which was up-regulated with serine being down-regulated, indicating that the *de novo* synthesis of Trp occurred due to the conversion of serine and indole (Asai et al., 2017).

In current study, the metabolomic data were clearly elucidated that the *B. subtilis* CLP mixtures, fengycin, iturin A and surfactin, which were the members of the CLPs group, possessed the powerful elicitor function in triggering metabolic changes in the flavedo tissues due to stress responses during the postharvest period. This metabolomic finding was consistent with the results shown in a previous study where the authors demonstrated the elicitation of defense–related gene expression and ISR involving enzyme accumulation by *B. subtilis* ABS-S14 CLPs (Waewthongrak et al., 2014). This work firstly demonstrated the metabolites which were induced by an individual elicitor in *B. subtilis* CLPs group were involved in the 6 major pathways; 1) The metabolism of glycine, serine and threonine, 2) alanine, aspartate and glutamate metabolism, 3) beta alanine metabolism, 4) isoquinoline alkaloid biosynthesis, 5) Tyr metabolism, and 6) pantothenate and CoA biosynthesis. These results strongly suggested that glycine, serine and threonine metabolism played significant physiological roles in some aspects of stress response in mandarin flavedo tissues induced by bacterial CLPs. On the other hand, in stresses such as wounding, MeJA and SA treatments, increasing phenylalanine, Trp and Tyr level were found to be located in the same cluster and might exhibit the same behavior with some suggestion of tissue dependent regulation (Asai et al., 2017).

The overall functional categories of each amino acid and their derivatives described in this report were: 1) aspartic acid not only acts as the precursor for the

synthesis of asparagine which mediates nitrogen transport and storage in plants, but is also the precursor for generating aspartate-derived amino acids which are located in leaves, seeds and roots (Azevedo et al., 2006); 2) homoserine has been reported as activating plant growth (Palmer et al., 2014); 3) threonine, a substrate of threonine deaminase in α-ketobutyrate and ammonia biosynthesis, involved in plant defense (Gonzales-Vigil et al., 2011); 4) serine was one of the most important amino acids discovered in the photorespiratory glycolate pathway for plant metabolism and development (Ros et al., 2014); 5) glycine has been reported to be involved in plant development via the root system (Domínguez-May et al., 2013); and 6) Trp was a precursor for generating secondary metabolites in plant immunity (Dixon and Paiva, 1995; Servillo et al., 2013).

Trp has been reported to function in plant defense (Ishihara et al., 2008; Servillo et al., 2013) and also acts as the precursor of serotonin (Ishihara et al., 2008). In the present study, serotonin was found to be one of the significantly up-regulated metabolites in the treatment group of *B. subtilis* CLPs, as was 5-hydroxy-*N*-methyltryptamine which is a serotonin derivative (Servillo et al., 2013; Servillo et al., 2015). The bacterial substances could be emphasized on the activation of the serotonin and 5-hydroxy-*N*-methyltryptamine synthesis at a higher level than the other elicitors used in this experiment at all time-points as shown in the box plots. Serotonin involved in the plant defense mechanism (Servillo et al., 2015), serving as a substrate of peroxidase to create polymers like lignin that functioned as a physical barrier inhibiting the spread of the pathogen infection (Ishihara et al., 2008). Even though the direct function of 5-hydroxy-*N*-methyltryptamine in plant defense is still unclear, it can act as a precursor for glucosylated serotonin derivatives which have been reported to produce toxic aglycones to attack the pathogen via glycosidase activity (Servillo et al., 2015).

In addition, this finding confirmed the role of tyramine as the precursor of tyramine derivatives that involved in the pathways of the plant defense mechanism (Servillo et al., 2017). More importantly, tyramine derivatives were coproduced with specialized defensive secondary metabolites, such as toxic substances produced by the

plant in response to an infection in order to attack the pathogen (Servillo et al., 2014). The large abundance of Tyr induced by exogenous plant hormones might be a precursor in the pathway to produce downstream substances from the metabolism of Tyr, but it did not influence tyramine accumulation. It could be remarked that *P. digitatum* and exogenous plant hormones did not play any important role on serotonin, 5-hydroxy-*N*-metyltryptamine, Tyr or tyramine in the metabolism of Trp and Tyr and in the mandarin's response to stress. There were 4 putatively identified metabolites in this pathway from this study: dopamine, 3,4-dihydroxyiphenyl-acetaldehyde, gentisate aldehyde and 4-hydroxyphenyl-acetaldehyde. In addition, Tyr and tyramine involved in isoquinoline alkaloid biosynthesis pathway.

In alanine, aspartate and glutamate metabolism, there were 1) aspartic acid (Azevedo et al., 2006); 2) asparagine (Azevedo et al., 2006); 3) alanine which is directly converted to pyruvate, an essential chemical for plant energy (Bolton, 2009; Hildebrandt et al., 2015); 4) glutamine which functioned in plant growth and stress responses via plant nutrition and signal transduction mechanism (Kan et al., 2015); 5) glutamate which was reported to involve in plant defense in host plant during pathogen challeng (Seifi et al., 2013); and 6) gamma-aminobutyric acid or GABA which was a mobile signal responding to biotic and abiotic stress (Roberts, 2007). Likewise, in beta alanine metabolism, high level of beta-alanine found in *Bacillus* CLPs treated flavedo tissues was consistent with the previous report where it was found to be increased in response to heat and drought stress (Rizhsky et al., 2004) and also pantothenic acid which functioned as a cofactor of cell metabolism in plant growth-promoting bacteria (Palacios et al., 2014). In pantothenate and CoA biosynthesis, pantothenic acid, beta-alanine, and valine were elucidated in this work, which are in agreement with those found accumulated after exposure to pathogens (Rojas et al., 2014). The mechanism of action of *B. subtilis* ABS-S14 CLPs on postharvest mandarins exhibited in present work was also discussed by Spadaro and Droby (2016) that once host resistant systems were stimulated, plants would be able to develop an increased resistance to pathogen infection and as a result fruit decay was reduced.

It could be suggested that CLPs isolated from *B. subtilis* ABS-S14 induced the primary metabolism including the secondary metabolism through six major pathways in stimulating plant immunity. Obviously, in CLP treated flavedo tissues glycine, serine and threonine metabolism which contains a number of vital amino acids and their derivatives in plant defense in responding to stress was increased. Thus, the effectiveness of *B. subtilis* ABS-S14 CLPs in elicitation of mandarin defense response through metabolic pathways discovered in this report was endorsed to protect fruit against pathogen invasion during postharvest storage.

4.4 Integration of the results from different omics technologies on defense responses in mandarin fruit upon applications of *B. subtilis* CLPs

This study used the omics technologies such as proteomics and metabolomics including transcription data to explain the actions of *B. subtilis* CLPs on induction of defensive system responding to stresses in mandarin fruit. CLPs showed abilities to induce various gene expression and increase the protein accumulation including metabolite production which involved in plant immunity.

The results of gene expression, proteomics, and metabolomics in CLP treatment were indicated that Trp metabolism was the one of important mechanisms playing a key role during stress response. In metabolomic study, Trp was found in CLP treatments as primary metabolites which played a role responding to stress in mandarin fruit. Trp is the precursor to produce serotonin and tryptamine which was reported to be involved in defensive mechanism (Ishihara et al., 2008; Servillo et al., 2013). It was the same manner as proteomic study, Trp aminotransferase-related protein 3 and Trp synthase beta chain 1-like were up-regulated proteins in the treatments of CLPs. Those proteins are the enzymes which function in Trp biosynthesis. In transcriptomic study, expression of *POD* gene was induced by the activation of CLP treatment. Serotonin was reported to be a substrate to produce peroxidase resulting in inhibitory effect against pathogen attack (Ishihara et al., 2008). It could be suggested that Trp metabolism played a key role in CLP treated-mandarin fruit during postharvest period based on the results

from gene and -omics technologies that are leading to plant resistance responding to stresses.

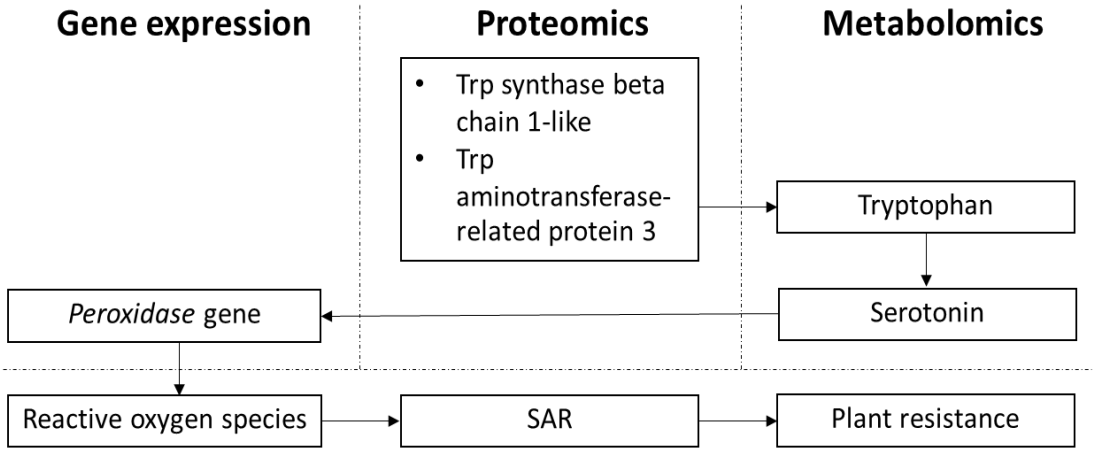

Fig. 4.5 Integration of the results from gene and omics technologies on defense responses in mandarin fruit upon applications of *B. subtilis* CLPs.

In summary, this study focused on the action of CLPs obtained from *B. subtilis* ABS-S14 on the induction of plant defensive systems responding to wound stress and *P. digitatum* infection in postharvest mandarin fruit comparing with the application of exogenous plant hormones. The evidences from the results of expression of genes and production of proteins and metabolites involving in plant defensive systems confirmed the ability of CLPs obtained from *B. subtilis* ABS-S14 to be the potential agents for enhancing plant immunity in mandarin fruit better than the application of exogenous plant hormones. Proteomics and metabolomics were the powerful approaches to fulfill the understanding of CLP action on activation of plant defense via SAR and ISR including the primary and secondary metabolism relating to plant immunity. It could be indicated that the extracted products from *B. subtilis* ABS-S14; CLP extract, fengycin, iturin A, and surfactin were the effective biological control agents against *P. digitatum* infection in postharvest mandarin fruit.

CHAPTER 5

CONCLUSION

This study investigated the induction effect of CLPs produced by *B. subtilis* ABS-S14 on plant defensive genes, proteins, and metabolites and how that differed from the application of exogenous plant hormones to mandarin fruit with and without *P. digitatum* infection for suggestion of the agents in biological control approaches instead of the use of synthetic fungicides. Insight findings were obtained as follows.

1. *B. subtilis* CLP was considered to be an alternative agent for utilization in biological control approaches because it is not only easy to handling and maintenance and antimicrobial ability, but also its strong ability in plant defensive induction comparing with exogenous plant hormones. Thus, *B. subtilis* CLP is suggested to be the one of potential biological control agents when compared with exogenous plant hormones to inhibit *P. digitatum* infection during postharvest period in mandarin fruit.

2. Transcription data of the key enzymes which are involved in plant hormone-mediated signal transduction pathways and PR protein accumulation provides important evidences relating to the action of *B. subtilis* CLPs in mandarin fruit with and without *P. digitatum* infection.

3. Proteomics data in this study provided significant data relating to the proteome and signaling pathways in *B. subtilis* CLP treatments leading to plant resistance including the distinctive up-regulated patterns of individual CLP-protein association relating to stress response and *P. digitatum* infection.

4. The approach of dansylation LC-MS in metabolomic analysis indicated that *B. subtilis* CLPs highlighted the greater effect than exogenous plant hormones on the elicitation of the synthesis of primary and secondary metabolites involving in plant defense mechanism in postharvest mandarin fruit. The glycine, serine and threonine metabolism pathways including the metabolism of Trp and Tyr were suggested as being the major responses.

REFERENCES

Adie, B., Chico, J.M., Rubio-Somoza, I., Solano, R., 2007. Modulation of plant defenses by ethylene. J. Plant Growth Regul. 26, 160-177.

Ali, S., Ganai, B.A., Kamili, A.N., Bhat, A.A., Mir, Z.A., Bhat, J.A., Tyagi, A., Islam, S.T., Mushtaq, M., Yadav, P., Rawat, S., Grover, A., 2018. Pathogenesis-related proteins and peptides as promising tools for engineering plants with multiple stress tolerance. Microbiol. Res. 212-213, 29-37.

Almagro, L., Gomez Ros, L.V., Belchi-Navarro, S., Bru, R., Ros Barcelo, A., Pedreno, M.A., 2009. Class III peroxidases in plant defence reactions. J. Exp. Bot. 60, 377-390.

Ambawat, S., Sharma, P., Yadav, N.R., Yadav, R.C., 2013. MYB transcription factor genes as regulators for plant responses: an overview. Physiol Mol Biol Plants. 19, 307-321.

Asai, T., Matsukawa, T., Kajiyama, S., 2017. Metabolomic analysis of primary metabolites in citrus leaf during defense responses. J. Biosci. Bioeng. 123, 376-381.

Azevedo, R.A., Lancien, M., Lea, P.J., 2006. The aspartic acid metabolic pathway, an exciting and essential pathway in plants. Amino Acids. 30, 143-162.

Ballester, A. R., Izquierdo, A., Lafuente, M.T., and González-Candelas, L., 2010. Biochemical and molecular characterization of induced resistance against *Penicillium digitatum* in citrus fruit. Postharvest Biol. Technol. 56, 31-38.

Barkai-Golan, R., 2001. Postharvest diseases of fruit and vegetables: Development and Control. Elsevier Sciences, Amasterdam, The Netherlands.

Belknap, W.R., Garbarino, J.E., 1996. The role of ubiquitin in plant senescence and stress responses. Trends Plant Sci. 1, 331-335.

Blum, H., Beier, H., Gross Hans, J., 1987. Improved silver staining of plant proteins, RNA and DNA in polyacrylamide gels. Electrophoresis. 8, 93-99.

Boavida, L.C., Shuai, B., Yu, H.J., Pagnussat, G.C., Sundaresan, V., McCormick, S., 2009. A collection of Ds insertional mutants associated with defects in male gametophyte development and function in *Arabidopsis thaliana*. Genetics 181, 1369-1385.

Bolton, M.D., 2009. Primary metabolism and plant defense--fuel for the fire. Mol. Plant Microbe Interact. 22, 487-497.

Brunner, N.A., Brinkmann, H., Siebers, B., Hensel, R., 1998. NAD+-dependent glyceraldehyde-3-phosphate dehydrogenase from *Thermoproteus tenax*. The first identified archaeal member of the aldehyde dehydrogenase superfamily is a glycolytic enzyme with unusual regulatory properties. J. Biol. Chem. 273, 6149-6156.

Burketova, L., Trda, L., Ott, P.G., Valentova, O., 2015. Bio-based resistance inducers for sustainable plant protection against pathogens. Biotechnol. Adv. 33, 994-1004.

Cano, M., Holland, S.C., Artier, J., Burnap, R.L., Ghirardi, M., Morgan, J.A., Yu, J., 2018. Glycogen synthesis and metabolite overflow contribute to energy balancing in Cyanobacteria. Cell Rep. 23, 667-672.

Cantero, A., Barthakur, S., Bushart, T.J., Chou, S., Morgan, R.O., Fernandez, M.P., Clark, G.B., Roux, S.J., 2006. Expression profiling of the *Arabidopsis* annexin gene family during germination, de-etiolation and abiotic stress. Plant Physiol. Biochem. 44, 13-24.

Cawoy, H., Mariutto, M., Henry, G., Fisher, C., Vasilyeva, N., Thonart, P., Dommes, J., Ongena, M., 2014. Plant defense stimulation by natural isolates of *Bacillus* depends on efficient surfactin production. Mol. Plant Microbe Interact. 27, 87-100.

Chandler, S., Van Hese, N., Coutte, F., Jacques, P., Höfte, M., De Vleesschauwer, D., 2015. Role of cyclic lipopeptides produced by *Bacillus subtilis* in mounting induced immunity in rice (*Oryza sativa* L.). Physiol. Mol. Plant Pathol. 91, 20-30.

Charrier, B., Champion, A., Henry, Y., Kreis, M., 2002. Expression profiling of the whole *Arabidopsis* shaggy-like kinase multigene family by real-time reverse transcriptase-polymerase chain reaction. Plant Physiol. 130, 577-590.

Chen, C., Huang, H., Wu, C.H., 2017. Protein bioinformatics databases and resources. Methods Mol. Biol. 1558, 3-39.

Chitarra, G., Breeuwer, P., Nout, M., Van Aelst, A., Rombouts, F., and Abee, T., 2003. An antifungal compound produced by *Bacillus subtilis* YM 10–20 inhibits germination of *Penicillium roqueforti* conidiospores. J. Appl. Microbiol. 94, 159-166.

Chong, J., Soufan, O., Li, C., Caraus, I., Li, S., Bourque, G., Wishart, D.S., Xia, J., 2018. MetaboAnalyst 4.0: towards more transparent and integrative metabolomics analysis. Nucleic Acids Res. 46, W486-W494.

Choudhary, D.K., Prakash, A., Johri, B.N., 2007. Induced systemic resistance (ISR) in plants: mechanism of action. Indian J. Microbiol. 47, 289-297.

Cook. R.J., 1993. Making greater use of introduced microorganisms for biological control of plant pathogens. Annu Rev Phytopathol. 31, 53-80.

Coqueiro, D.S., de Souza, A.A., Takita, M.A., Rodrigues, C.M., Kishi, L.T., Machado, M.A., 2015. Transcriptional profile of sweet orange in response to chitosan and salicylic acid. BMC Genomics. 16, 288.

Deleu, M., Paquot, M., Nylander, T., 2005. Fengycin interaction with lipid monolayers at the air-aqueous interface-implications for the effect of fengycin on biological membranes. J Colloid Interface Sci. 283, 358-365.

Dixon, R.A., Paiva, N.L., 1995. Stress-induced phenylpropanoid metabolism. Plant Cell. 7, 1085-1097.

Domínguez-May, Á.V., Carrillo-Pech, M., Barredo-Pool, F.A., Martínez-Estévez, M., Us-Camas, R.Y., Moreno-Valenzuela, O.A., Echevarría-Machado, I., 2013. A novel effect for glycine on root system growth of habanero pepper. J. Am. Soc. Hortic. Sci. 138, 433-442.

Droby, S., Wisniewski, M., Macarisin, D., Wilson, C., 2009. Twenty years of postharvest biocontrol research: Is it time for a new paradigm? Postharvest Biol. Technol. 52, 137-145.

Dutt, M., Barthe, G., Irey, M., Grosser, J., 2015. Transgenic citrus expressing an *Arabidopsis* NPR1 gene exhibit enhanced resistance against Huanglongbing (HLB; Citrus Greening). PLoS ONE. 10, e0137134.

Eckert, J.W., 1978. Post-harvest diseases of citrus fruits. Outlook Agric. 9, 225-232.

Eckert, J.W., Eaks, I.L., 1989. Postharvest disorders and diseases of citrus fruits. In: Reuther,W., Calavan, E.C., Carman, G.E. (Eds.), In: The Citrus Industry, vol. 4. University of California Press, Berkeley, USA. 179-260.

Epinat, J.-C., Arnould, S., Chames, P., Rochaix, P., Desfontaines, D., Puzin, C., Patin, A., Zanghellini, A., Pâques, F., Lacroix, E., 2003. A novel engineered meganuclease induces homologous recombination in yeast and mammalian cells. Nucleic Acids Res. 31, 2952-2962.

Etebu, E., and Nwauzoma, A. B. 2014. A review on sweet orange (*Citrus sinensis* Osbeck): Health, diseases, and management. Am J Res Commun. 2, 33-70.

Falardeau, J., Wise, C., Novitsky, L., Avis, T.J., 2013. Ecological and mechanistic insights into the direct and indirect antimicrobial properties of *Bacillus subtilis* lipopeptides on plant pathogens. J. Chem. Ecol. 39, 869-878.

Fan, H., Ru, J., Zhang, Y., Wang, Q., Li, Y., 2017. Fengycin produced by *Bacillus subtilis* 9407 plays a major role in the biocontrol of apple ring rot disease. Microbiol. Res. 199, 89-97.

Farace, G., Fernandez, O., Jacquens, L., Coutte, F., Krier, F., Jacques, P., Clement, C., Barka, E.A., Jacquard, C., Dorey, S., 2015. Cyclic lipopeptides from *Bacillus subtilis* activate distinct patterns of defence responses in grapevine. Mol. Plant Pathol. 16, 177-187.

Fu, Z.Q., Dong, X., 2013. Systemic acquired resistance: turning local infection into global defense. Annu Rev Plant Biol. 64, 839-863.

Gamliel, A., Katan, J., Cohen, E., 1989. Toxicity of chloronitrobenzenes to *Fusarium oxysporum* and *Rhizoctonia solani* as related to their structure. Phytoparasitica. 17, 101-106.

Gershater, M.C., Cummins, I., Edwards, R., 2007. Role of a carboxylesterase in herbicide bioactivation in *Arabidopsis thaliana*. J. Biol. Chem. 282, 21460-21466.

Gimenez, E., Manzano-Agugliaro, F., 2017. DNA damage repair system in plants: A Worldwide Research Update. Genes (Basel). 8, 299.

Gond, S.K., Bergen, M.S., Torres, M.S., White, J.F., Jr., 2015. Endophytic *Bacillus* spp. produce antifungal lipopeptides and induce host defence gene expression in maize. Microbiol. Res. 172, 79-87.

Gong, Q., Zhang, C., Lu, F., Zhao, H., Bie, X., Lu, Z., 2014. Identification of bacillomycin D from *Bacillus subtilis* fmbJ and its inhibition effects against *Aspergillus flavus*. Food Control. 36, 8-14.

González-Candelas, L., Alamar, S., Sánchez-Torres, P., Zacarías, L., Marcos, J.F., 2010 A transcriptomic approach highlights induction of secondary metabolism in citrus fruit in response to *Penicillium digitatum* infection. BMC Plant Biol. 10, 194-211.

Gonzalez-Vigil, E., Bianchetti, C.M., Phillips, G.N., Jr., Howe, G.A., 2011. Adaptive evolution of threonine deaminase in plant defense against insect herbivores. Proc. Natl. Acad. Sci. U.S.A. 108, 5897-5902.

Guo, J., Fang, W., Lu, H., Zhu, R., Lu, L., Zheng, X., Yu, T., 2014. Inhibition of green mold disease in mandarins by preventive applications of methyl jasmonate and antagonistic yeast *Cryptococcus laurentii*. Postharvest Biol. Technol. 88, 72-78.

Guo, K., Li, L., 2009. Differential 12C-/13C-isotope dansylation labeling and fast liquid chromatography/mass spectrometry for absolute and relative quantification of the metabolome. Anal. Chem. 81, 3919-3932.

Guo, L., Devaiah, S.P., Narasimhan, R., Pan, X., Zhang, Y., Zhang, W., Wang, X., 2012. Cytosolic glyceraldehyde-3-phosphate dehydrogenases interact with phospholipase Ddelta to transduce hydrogen peroxide signals in the *Arabidopsis* response to stress. Plant Cell. 24, 2200-2212.

Gust, A.A., 2015. Peptidoglycan perception in plants. PLoS Pathog. 11, e1005275.

Hall, R., Beale, M., Fiehn, O., Hardy, N., Sumner, L., Bino, R., 2002. Plant metabolomics: the missing link in functional genomics strategies. Plant Cell. 14, 1437-1440.

Han, W., Sapkota, S., Camicioli, R., Dixon, R.A., Li, L., 2017. Profiling novel metabolic biomarkers for Parkinson's disease using in-depth metabolomic analysis. Mov. Disord. 32, 1720-1728.

Hildebrandt, T.M., Nunes Nesi, A., Araujo, W.L., Braun, H.P., 2015. Amino acid catabolism in plants. Mol Plant. 8, 1563-1579.

Hoch, J.A., 2000. Two-component and phosphorelay signal transduction. Curr. Opin. Microbiol. 3, 165-170.

Hoffmeister, M., Piotrowski, M., Nowitzki, U., Martin, W., 2005. Mitochondrial trans-2-enoyl-CoA reductase of wax ester fermentation from *Euglena gracilis* defines a new family of enzymes involved in lipid synthesis. J. Biol. Chem. 280, 4329-4338.

Hooton, K., Han, W., Li, L., 2016. Comprehensive and quantitative profiling of the human sweat submetabolome using high-performance chemical isotope labeling LC-MS. Anal. Chem. 88, 7378-7386.

Horn, J.N., Romo, T.D., Grossfield, A., 2013. Simulating the mechanism of antimicrobial lipopeptides with all-atom molecular dynamics. Biochemistry. 52, 5604-5610.

Howe, E., Holton, K., Nair, S., Schlauch, D., Sinha, R., Quackenbush, J., 2010. MeV: MultiExperiment viewer. Biomedical Informatics for Cancer Research. Springer, Boston, MA. 267-277.

Huan, T., Wu, Y., Tang, C., Lin, G., Li, L., 2015. DnsID in MyCompoundID for rapid identification of dansylated amine- and phenol-containing metabolites in LC-MS-based metabolomics. Anal. Chem. 87, 9838-9845.

Hwang, J.U., Song, W.Y., Hong, D., Ko, D., Yamaoka, Y., Jang, S., Yim, S., Lee, E., Khare, D., Kim, K., Palmgren, M., Yoon, H.S.,Martinoia, E., Lee, Y., 2016. Plant ABC transporters enable many unique aspects of a terrestrial plant's lifestyle. Mol Plant. 9, 338-355.

Ishihara, A., Hashimoto, Y., Tanaka, C., Dubouzet, J.G., Nakao, T., Matsuda, F., Nishioka, T., Miyagawa, H., Wakasa, K., 2008. The tryptophan pathway is involved in the defense responses of rice against pathogenic infection via serotonin production. Plant J. 54, 481-495.

Janisiewicz, W.J., Tworkoski, T.J., Sharer, C., 2000. Characterizing the mechanism of biological control of postharvest diseases on fruit with a simple method to study competition for nutrients. Phytopathology. 90, 1196-1200.

Jiang, C., Shi, J., Liu, Y., Zhu, C., 2014. Inhibition of *Aspergillus carbonarius* and fungal contamination in table grapes using *Bacillus subtilis*. Food Control. 35, 41-48.

Jiwanit, P., Pitakpornpreecha, T., Pisuchpen, S., Leelasuphakul, W., 2018. The use of Aloe vera gel coating supplemented with *Pichia guilliermondii* BCC5389 for enhancement of defense-related gene expression and secondary metabolism in mandarins to prevent postharvest losses from green mold rot. Biol. Control. 117, 43-51.

Johansson, C., Samskog, J., Sundstrom, L., Wadensten, H., Bjorkesten, L., Flensburg, J., 2006. Differential expression analysis of *Escherichia coli* proteins using a novel software for relative quantitation of LC-MS/MS data. Proteomics. 6, 4475-4485.

John-Karuppiah, K.-J., Burns, J.K., 2010. Expression of ethylene biosynthesis and signaling genes during differential abscission responses of sweet orange leaves and mature fruit. J. Am. Soc. Hortic. Sci. 135, 456-464.

Kan, C.C., Chung, T.Y., Juo, Y.A., Hsieh, M.H., 2015. Glutamine rapidly induces the expression of key transcription factor genes involved in nitrogen and stress responses in rice roots. BMC Genomics. 16, 731.

Kang, J., Park, J., Choi, H., Burla, B., Kretzschmar, T., Lee, Y., Martinoia, E., 2011. Plant ABC transporters. Arabidopsis Book. 9, e0153.

Kawagoe, Y., Shiraishi, S., Kondo, H., Yamamoto, S., Aoki, Y., Suzuki, S., 2015. Cyclic lipopeptide iturin A structure-dependently induces defense response in *Arabidopsis* plants by activating SA and JA signaling pathways. Biochem. Biophys. Res. Commun. 460, 1015-1020.

Kazan, K., Manners, J.M., 2008. Jasmonate signaling: toward an integrated view. Plant Physiol. 146, 1459-1468.

Kazan, K., Manners, J.M., 2009. Linking development to defense: auxin in plant-pathogen interactions. Trends Plant Sci. 14, 373-382.

Kinay, P., Mansour, M.F., Mlikota Gabler, F., Margosan, D.A., Smilanick, J.L., 2007. Characterization of fungicide-resistant isolates of *Penicillium digitatum* collected in California. Crop Prot. 26, 647-656.

Kong, W., Li, J., Yu, Q., Cang, W., Xu, R., Wang, Y., Ji, W., 2016. Two novel flavin-containing monooxygenases involved in biosynthesis of aliphatic glucosinolates. Front Plant Sci. 7, 1292.

Krokan, H.E., Bjoras, M., 2013. Base excision repair. Cold Spring Harb Perspect Biol. 5, a012583.

Kumar, D., 2014. Salicylic acid signaling in disease resistance. Plant Sci. 228, 127-134.

Kumar, P., Dubey, R.C., Maheshwari, D.K., 2012. *Bacillus* strains isolated from rhizosphere showed plant growth promoting and antagonistic activity against phytopathogens. Microbiol. Res. 167, 493-499.

Laohavisit, A., Brown, A.T., Cicuta, P., Davies, J.M., 2010. Annexins: components of the calcium and reactive oxygen signaling network. Plant Physiol. 152, 1824-1829.

Leelasuphakul, W., Hemmanee, P., Chuenchitt, S., 2008. Growth inhibitory properties of *Bacillus subtilis* strains and their metabolites against the green mold pathogen (*Penicillium digitatum* Sacc.) of citrus fruit. Postharvest Biol. Technol. 48, 113-121.

Leelasuphakul, W., Sivanunsakul, P., Phongpaichit, S., 2006. Purification, characterization and synergistic activity of β-1,3-glucanase and antibiotic extract from an antagonistic *Bacillus subtilis* NSRS 89-24 against rice blast and sheath blight. Enzyme Microb. Technol. 38, 990-997.

Lerma-Garcia, M.J., D'Amato, A., Simo-Alfonso, E.F., Righetti, P.G., Fasoli, E., 2016. Orange proteomic fingerprinting: From fruit to commercial juices. Food Chem. 196, 739-749.

Liu, M., Lu, S., 2016. Plastoquinone and ubiquinone in plants: Biosynthesis, physiological function and metabolic engineering. Front Plant Sci. 7, 1898.

Lopes, R., Tsui, S., Goncalves, P., de Queiroz, M.V., 2018. A look into a multifunctional toolbox: endophytic Bacillus species provide broad and underexploited benefits for plants. World J. Microbiol. Biotechnol. 34, 94.

Loraine, A.E., McCormick, S., Estrada, A., Patel, K., Qin, P., 2013. RNA-seq of *Arabidopsis* pollen uncovers novel transcription and alternative splicing. Plant Physiol. 162, 1092-1109.

Lu, L., Xu, S., Zeng, L., Zheng, X., Yu, T., 2014. *Rhodosporidium paludigenum* induced resistance in Ponkan mandarin against *Penicillium digitatum* requires ethylene-dependent signaling pathway. Postharvest Biol. Technol. 97, 93-101.

Lu, Y., Li, Y., Zhang, J., Xiao, Y., Yue, Y., Duan, L., Zhang, M., Li, Z., 2013. Overexpression of *Arabidopsis* molybdenum cofactor sulfurase gene confers drought tolerance in maize (*Zea mays* L.). PLoS ONE. 8, e52126.

Luo, X., Zhao, S., Huan, T., Sun, D., Friis, R.M., Schultz, M.C., Li, L., 2016. High-performance chemical isotope labeling liquid chromatography-mass spectrometry for profiling the metabolomic reprogramming elicited by ammonium limitation in yeast. J. Proteome Res. 15, 1602-1612.

Ma, Z., Ongena, M., Hofte, M., 2017. The cyclic lipopeptide orfamide induces systemic resistance in rice to *Cochliobolus miyabeanus* but not to *Magnaporthe oryzae*. Plant Cell Rep. 36, 1731-1746.

Mandal, S., Mandal, M., 2016. Tangerine (*Citrus reticulata* L. var.) Oils, Essential Oils in Food Preservation, Flavor and Safety. 803-811.

McKeen, C.D., Reilly, C.C., Pusey, P.L., 1986. Production and partial characterization of antifungal substances antagonistic to *Monilinia fructicola* from *Bacillus subtilis*. Phytopathology. 76, 136-139.

Moita, C., Feio, S.S., Nunes, L., João Marcelo Curto, M., Carlos Roseiro, J., 2005. Optimisation of physical factors on the production of active metabolites by *Bacillus subtilis* 355 against wood surface contaminant fungi. Int. Biodeterior. Biodegradation. 55, 261-269.

Moscoso-Ramírez, P.A., Palou, L., 2013. Evaluation of postharvest treatments with chemical resistance inducers to control green and blue molds on orange fruit. Postharvest Biol. Technol. 85, 132-135.

Muccilli, V., Licciardello, C., Fontanini, D., Russo, M.P., Cunsolo, V., Saletti, R., Recupero, G.R., Foti, S., 2009. Proteome analysis of *Citrus sinensis* L. (Osbeck) flesh at ripening time. J Proteomics. 73, 134-152.

Muroi, A., Matsui, K., Shimoda, T., Kihara, H., Ozawa, R., Ishihara, A., Nishihara, M., Arimura, G., 2012. Acquired immunity of transgenic torenia plants overexpressing agmatine coumaroyltransferase to pathogens and herbivore pests. Sci Rep. 2, 689.

Narawitseree, T., 2009. Antibiotic production and growth inhibiting activities on fruit rot fungus of antagonistic *Bacillus subtilis* in citrus. A thesis for the degree of master of science in biochemistry, Prince of Songkla University.

Nogata, Y., Ohta, H., Sumida, T., Sekiya, K., 2003. Effect of extraction method on the concentrations of selected bioactive compounds in mandarin juice. J. Agric. Food Chem. 51, 7346-7351.

Obagwu, J., Korsten, L., 2003. Integrated control of citrus green and blue molds using *Bacillus subtilis* in combination with sodium bicarbonate or hot water. Postharvest Biol. Technol. 28, 187-194.

Ongena, M., Jacques, P., 2008. *Bacillus* lipopeptides: versatile weapons for plant disease biocontrol. Trends Microbiol. 16, 115-125.

Ongena, M., Jacques, P., Touré, Y., Destain., J., Jabrane, A. and Thonart, P., 2005. Involvement of fengycin-type lipopeptides in the multifaceted biocontrol potential of *Bacillus subtilis*. Appl. Microbiol. Biotechnol. 69, 29-38.

Ongena, M., Jourdan, E., Adam, A., Paquot, M., Brans, A., Joris, B., Arpigny, J.L., Thonart, P., 2007. Surfactin and fengycin lipopeptides of *Bacillus subtilis* as elicitors of induced systemic resistance in plants. Environ. Microbiol. 9, 1084-1090.

Pal, K.K., McSpadden Gardener, B., 2006. Biological control of plant pathogens. The Plant Health Instructor. 1-25. Availablevia APSnet DOI: 10.1094/PHI-A-2006-1117-02.

Palacios, O.A., Bashan, Y., de-Bashan, L.E., 2014. Proven and potential involvement of vitamins in interactions of plants with plant growth-promoting bacteria—an overview. Biol. Fertil. Soils. 50, 415-432.

Palmer, A.G., Senechal, A.C., Mukherjee, A., Ane, J.M., Blackwell, H.E., 2014. Plant responses to bacterial N-acyl L-homoserine lactones are dependent on enzymatic degradation to L-homoserine. ACS Chem. Biol. 9, 1834-1845.

Peng, J., Guo, K., Xia, J., Zhou, J., Yang, J., Westaway, D., Wishart, D.S., Li, L., 2014. Development of isotope labeling liquid chromatography mass spectrometry for mouse urine metabolomics: quantitative metabolomic study of transgenic mice related to Alzheimer's disease. J. Proteome Res. 13, 4457-4469.

Perkins, D.N., Pappin, D.J., Creasy, D.M., Cottrell, J.S., 1999. Probability-based protein identification by searching sequence databases using mass spectrometry data. Electrophoresis. 20, 3551-3567.

Perotti, V.E., Moreno, A.S., Trípodi, K., Del Vecchio, H.A., Meier, G., Bello, F., Cocco, M., Vázquez, D., Podestá, F.E., 2015. Biochemical characterization of the flavedo of heat-treated Valencia orange during postharvest cold storage. Postharvest Biol. Technol. 99, 80-87.

Peterson, G.L., 1977. A simplification of the protein assay method of Lowry et al. which is more generally applicable. Anal. Biochem. 83, 346-356.

Pfaffl, M.W., 2001. A new mathematical model for relative quantification in real-time RT–PCR. Nucleic Acids Res. 29, e45-e45.

Pieterse, C.M.J., Zamioudis, C., Berendsen, R.L., Weller, D.M., Van Wees, S.C., Bakker, P.A., 2014. Induced systemic resistance by beneficial microbes. Annu Rev Phytopathol. 52, 347-375.

Pisamai, S., Roytrakul, S., Phaonakrop, N., Jaresitthikunchai, J., Suriyaphol, G., 2018. Proteomic analysis of canine oral tumor tissues using MALDI-TOF mass spectrometry and in-gel digestion coupled with mass spectrometry (GeLC MS/MS) approaches. PLoS ONE. 13, e0200619.

Putnik, P., Barba, F.J., Lorenzo, J.M., Gabric, D., Shpigelman, A., Cravotto, G., Bursac Kovacevic, D., 2017. An Integrated approach to mandarin processing: Food safety and nutritional quality, consumer preference, and nutrient bioaccessibility. Compr Rev Food Sci Food Saf. 16, 1345-1358.

Raaijmakers, J.M., de Bruijn, I., de Kock, M.J.D., 2006. Cyclic lipopeptide production by plant-associated *Pseudomonas* spp.: Diversity, activity, biosynthesis, and regulation. Mol. Plant Microbe Interact. 19, 699-710.

Rizhsky, L., Liang, H., Shuman, J., Shulaev, V., Davletova, S., Mittler, R., 2004. When defense pathways collide. The response of Arabidopsis to a combination of drought and heat stress. Plant Physiol. 134, 1683-1696.

Roberts, M.R., 2007. Does GABA act as a signal in plants?: Hints from molecular studies. Plant Signal Behav. 2, 408-409.

Rojas, C.M., Senthil-Kumar, M., Tzin, V., Mysore, K.S., 2014. Regulation of primary plant metabolism during plant-pathogen interactions and its contribution to plant defense. Front Plant Sci. 5, 17.

Rojo, E., Solano, R., Sánchez-Serrano, J.J., 2003. Interactions between signaling compounds involved in plant defense. J. Plant Growth Regul. 22, 82-98.

Romanazzi, G., Sanzani, S.M., Bi, Y., Tian, S., Gutiérrez Martínez, P., Alkan, N., 2016. Induced resistance to control postharvest decay of fruit and vegetables. Postharvest Biol. Technol. 122, 82-94.

Ros, R., Munoz-Bertomeu, J., Krueger, S., 2014. Serine in plants: Biosynthesis, metabolism, and functions. Trends Plant Sci. 19, 564-569.

Ryals, J.A., Neuenschwander, U.H., Willits, M.G., Molina, A., Steiner, H.Y., Hunt, M.D., 1996. Systemic acquired resistance. Plant Cell. 8, 1809-1819.

Sampaio, B.L., Edrada-Ebel, R., Da Costa, F.B., 2016. Effect of the environment on the secondary metabolic profile of *Tithonia diversifolia*: a model for environmental metabolomics of plants. Sci Rep. 6, 29265.

Seifi, H.S., Van Bockhaven, J., Angenon, G., Hofte, M., 2013. Glutamate metabolism in plant disease and defense: friend or foe? Mol. Plant Microbe Interact. 26, 475-485.

Servillo, L., Castaldo, D., Giovane, A., Casale, R., D'Onofrio, N., Cautela, D., Balestrieri, M.L., 2017. Tyramine pathways in citrus plant defense: Glycoconjugates of tyramine and its *N*-methylated derivatives. J. Agric. Food Chem. 65, 892-899.

Servillo, L., Giovane, A., Balestrieri, M.L., Casale, R., Cautela, D., Castaldo, D., 2013. Citrus genus plants contain *N*-methylated tryptamine derivatives and their 5-hydroxylated forms. J. Agric. Food Chem. 61, 5156-5162.

Servillo, L., Giovane, A., Casale, R., D'Onofrio, N., Ferrari, G., Cautela, D., Balestrieri, M.L., Castaldo, D., 2015. Serotonin 5-O-beta-glucoside and its *N*-methylated forms in *Citrus* genus plants. J. Agric. Food Chem. 63, 4220-4227.

Servillo, L., Giovane, A., D'Onofrio, N., Casale, R., Cautela, D., Ferrari, G., Balestrieri, M.L., Castaldo, D., 2014. *N*-methylated derivatives of tyramine in *Citrus* genus plants: identification of *N,N,N*-trimethyltyramine (candicine). J. Agric. Food Chem. 62, 2679-2684.

Sharma, B., Joshi, D., Yadav, P.K., Gupta, A.K., Bhatt, T.K., 2016. Role of ubiquitin-mediated degradation system in plant biology. Front Plant Sci. 7, 806.

Shen, W., Han, W., Li, Y., Meng, Z., Cai, L., Li, L., 2016. Development of chemical isotope labeling liquid chromatography mass spectrometry for silkworm hemolymph metabolomics. Anal. Chim. Acta. 942, 1-11.

Shi, J.X., Chen, S., Gollop, N., Goren, R., Goldschmidt, E.E., Porat, R., 2008. Effects of anaerobic stress on the proteome of citrus fruit. Plant Sci. 175, 478-486.

Shine, M.B., Xiao, X., Kachroo, P., Kachroo, A., 2018. Signaling mechanisms underlying systemic acquired resistance to microbial pathogens. Plant Sci.

Smilanick, J.L., Mansour,M.F., Margosan, D.A., Mlikota Gabler, F., Goodwine, W.R., 2005. Influence of pH and NaHCO3 on effectiveness of imazalil to inhibit germination of *Penicillium digitatum* and to control postharvest green mold on citrus fruit. Plant Dis. 89, 640-648.

Smilanick, J.L., Mansour, M.F., Mlikota Gabler, F., Goodwine,W.R., 2006. The effectiveness of pyrimethanil to inhibit germination of *Penicillium digitatum* and to control citrus green mold after harvest. Postharvest Biol. Technol. 42, 75-85.

Spadaro, D., and Droby, S., 2016. Development of biocontrol products for postharvest diseases of fruit: The importance of elucidating the mechanisms of action of yeast antagonists. Trends Food Sci. Tech. 47, 39-49.

Song, L., Liu, D., 2015. Ethylene and plant responses to phosphate deficiency. Front Plant Sci. 6, 796.

Sui, X.L., Meng, F.Z., Wang, H.Y., Wei, Y.X., Li, R.F., Wang, Z.Y., Hu, L.P., Wang, S.H., Zhang, Z.X., 2012. Molecular cloning, characteristics and low temperature response of raffinose synthase gene in *Cucumis sativus* L. J Plant Physiol. 169, 1883-1891.

Sur, S., Romo, T.D., Grossfield, A., 2018. Selectivity and mechanism of fengycin, an antimicrobial lipopeptide, from molecular dynamics. J. Phys. Chem. B. 122, 2219-2226.

Tan, B.C., Lim, Y.S., Lau, S.E., 2017. Proteomics in commercial crops: An overview. J. Proteomics. 169, 176-188.

Tao, Y., Bie, X.M., Lv, F.X., Zhao, H.Z., Lu, Z.X., 2011. Antifungal activity and mechanism of fengycin in the presence and absence of commercial surfactin against *Rhizopus stolonifer*. J. Microbiol. 49, 146-150.

Taylor, G.K., Petrucci, L.H., Lambert, A.R., Baxter, S.K., Jarjour, J., Stoddard, B.L., 2012. LAHEDES: the LAGLIDADG homing endonuclease database and engineering server. Nucleic Acids Res. 40, W110-116.

Thorsell, A., Portelius, E., Blennow, K., Westman-Brinkmalm, A., 2007. Evaluation of sample fractionation using micro-scale liquid-phase isoelectric focusing on mass spectrometric identification and quantitation of proteins in a SILAC experiment. Rapid Commun. Mass Spectrom. 21, 771-778.

Toyomasu, T., Usui, M., Sugawara, C., Kanno, Y., Sakai, A., Takahashi, H., Nakazono, M., Kuroda, M., Miyamoto, K., Morimoto, Y., Mitsuhashi, W., Okada, K., Yamaguchi, S., Yamane, H., 2015. Transcripts of two ent-copalyl diphosphate synthase genes differentially localize in rice plants according to their distinct biological roles. J. Exp. Bot. 66, 369-376.

Tripoli, E., Guardia, M.L., Giammanco, S., Majo, D.D., Giammanco, M., 2007. Citrus flavonoids: Molecular structure, biological activity and nutritional properties: A review. Food Chem. 104, 466-479.

Tugizimana, F., Piater, L., Dubery, I., 2013. Plant metabolomics: A new frontier in phytochemical analysis. Afr. J. Sci. 109, 1-11.

Van Wees, S.C., Van der Ent, S., Pieterse, C.M., 2008. Plant immune responses triggered by beneficial microbes. Curr. Opin. Plant Biol. 11, 443-448.

Waewthongrak, W., Leelasuphakul, W., McCollum, G., 2014. Cyclic lipopeptides from *Bacillus subtilis* ABS-S14 elicit defense-related gene expression in citrus fruit. PLoS ONE. 9, e109386.

Waewthongrak, W., Pisuchpen, S., Leelasuphakul, W., 2015. Effect of *Bacillus subtilis* and chitosan applications on green mold (*Penicilium digitatum* Sacc.) decay in citrus fruit. Postharvest Biol. Technol. 99, 44-49.

Wang, G., Huang, W., Li, M., Xu, Z., Wang, F., Xiong, A., 2016. Expression profiles of genes involved in jasmonic acid biosynthesis and signaling during growth and development of carrot. Acta Biochim. Biophys. Sin. (Shanghai). 48, 795-803.

Wang, K.L.C., Li, H., Ecker, J.R., 2002. Ethylene biosynthesis and signaling networks. Plant Cell. 14, S131-S151.

Wang, M., Ma, X., Shen, J., Li, C., Zhang, W., 2014. The ongoing story: the mitochondria pyruvate carrier 1 in plant stress response in *Arabidopsis*. Plant Signal Behav. 9, e973810.

Wang, X., Kong, H., Ma, H., 2009. F-box proteins regulate ethylene signaling and more. Genes Dev. 23, 391-396.

Wasilewska, A., Vlad, F., Sirichandra, C., Redko, Y., Jammes, F., Valon, C., Frei dit Frey, N., Leung, J., 2008. An update on abscisic acid signaling in plants and more. Mol Plant. 1, 198-217.

Wasternack, C., 2007. Jasmonates: an update on biosynthesis, signal transduction and action in plant stress response, growth and development. Ann. Bot. 100, 681-697.

Wildermuth, M.C., Dewdney, J., Wu, G., Ausubel, F.M., 2001. Isochorismate synthase is required to synthesize salicylic acid for plant defence. Nature. 414, 562.

Xiong, L., Ishitani, M., Lee, H., Zhu, J.-K., 2001. The *Arabidopsis* LOS5/ABA3 locus encodes a molybdenum cofactor sulfurase and modulates cold stress– and osmotic stress–responsive gene expression. Plant Cell. 13, 2063.

Xu, J., Wang, X.-y., Guo, W.-z., 2015. The cytochrome P450 superfamily: Key players in plant development and defense. J Integr Agric. 14, 1673-1686.

Yang, L., Quan, X., Xue, B., Goodwin, P.H., Lu, S., Wang, J., Du, W., Wu, C., 2015. Isolation and identification of *Bacillus subtilis* strain YB-05 and its antifungal substances showing antagonism against *Gaeumannomyces graminis* var. tritici. Biol. Control. 85, 52–58.

Yang, S.F., Hoffman, N.E., 1984. Ethylene biosynthesis and its regulation in higher plants. Annu. Rev. Plant Physiol. Plant Mol. Biol. 35, 155-189.

Yun, Z., Li, W., Pan, Z., Xu, J., Cheng, Y., Deng, X., 2010. Comparative proteomics analysis of differentially accumulated proteins in juice sacs of ponkan (*Citrus reticulata*) fruit during postharvest cold storage. Postharvest Biol. Technol. 56, 189-201.

Zeng, H., Xu, L., Singh, A., Wang, H., Du, L., Poovaiah, B.W., 2015. Involvement of calmodulin and calmodulin-like proteins in plant responses to abiotic stresses. Front Plant Sci. 6, 600.

Zhang, J., Du, X., Wang, Q., Chen, X., Lv, D., Xu, K., Qu, S., Zhang, Z., 2010. Expression of pathogenesis related genes in response to salicylic acid, methyl jasmonate and 1-aminocyclopropane-1-carboxylic acid in Malus hupehensis (Pamp.) Rehd. BMC Res Notes. 3, 208.

Zhang, L., Du, L., Poovaiah, B.W., 2014. Calcium signaling and biotic defense responses in plants. Plant Signal Behav. 9, e973818.

Zhang, X., Liu, C.J., 2015. Multifaceted regulations of gateway enzyme phenylalanine ammonia-lyase in the biosynthesis of phenylpropanoids. Mol Plant. 8, 17-27.

Zhou, B., Mural, R.V., Chen, X., Oates, M.E., Connor, R.A., Martin, G.B., Gough, J., Zeng, L., 2017. A Subset of ubiquitin-conjugating enzymes is essential for plant immunity. Plant Physiol. 173, 1371-1390.

Zhou, Y., Ma, J., Xie, J., Deng, L., Yao, S., Zeng, K., 2018. Transcriptomic and biochemical analysis of highlighted induction of phenylpropanoid pathway metabolism of citrus fruit in response to salicylic acid, *Pichia membranaefaciens* and oligochitosan. Postharvest Biol. Technol. 142, 81-92.

APPENDIX

The digital supplementary data of this study listed below is available by direct contact Assoc. Prof. Wichitra Leelasuphakul via wichitra.l@psu.ac.th.

1. Lists of supplementary tables

2. Lists of supplementary figures

VITAE

Name Paiboon Tunsagool

Student ID 5610230012

Educational Attainment

Degree	Name of Institution	Year of Graduation
Bachelor of Science (Traditional Thai Medicine)	Prince of Songkla University	2013

Scholarship Awards during Enrolment

A scholarship awards from the Graduate Research Fund, Prince of Songkla University

Royal Golden Jubilee Ph.D. Program, The Thailand Research Fund

List of Publication and Proceedings

Publication

Tunsagool, P., Roytrakul, S., Phaonakrop, N., Jaresitthikunchai, J. and Leelasuphakul, W. (2016) "Effect of Exogenous Salicylic Acid on Protein Synthesis in Tangerine (*Citrus reticulata* Blanco) Fruit under Stress". Agricultural Sci. J. 47: 3 (Suppl.) : 143-146.

Proceedings

Tunsagool, P., Roytrakul, S., Phaonakrop, N., Jaresitthikunchai, J. and Leelasuphakul, W. (2016) "Effect of Exogenous Salicylic Acid on Protein Synthesis in Tangerine (*Citrus reticulata* Blanco) Fruit under Stress". Agricultural Sci. J. 47: 3 (Suppl.) : 143-146. (The 2nd award of oral presentation in the 14th National Postharvest Technology Conference, June 2 – 3, 2016, at Wiang Inn hotel, Chiang Rai, Thailand).

Tunsagool, P., Roytrakul, S., Phaonakrop, N., Jaresitthikunchai, J. and Leelasuphakul, W. (2016) "Purification of Cyclic Lipopeptides from *Bacillus subtilis* ABS-S14 and Effect of Exogenous Salicylic Acid on *Citrus reticulata* Blanco Proteins Synthesis Inducing in Stress Responses". Abstracts of the 115th RGJ

Seminar Series, July 28 – 29, 2016, at BSc 3, Basic Science Buildings, Faculty of Science, PSU, Songkhla, Thailand.

Tunsagool, P., Phaonakrop, N., Jaresitthikunchai, J., Roytrakul, S. and Leelasuphakul, W. (2017) "Induction of plant defensive proteins in *Citrus reticulata* Blanco by *Bacillus subtilis* ABS-S14 cyclic lipopeptides and methyl jasmonate". Abstracts of the RGJ – Ph.D. Congress 18, June 8 – 10, 2017, at Richmond Stylish Convention Hotel, Nonthaburi, Thailand (The outstanding oral presentation in the RGJ – Ph.D. Congress 18).